This information product has been peer reviewed and approved for publication as a preprint by the U.S. Geological Survey. The final published information product will be published as a Scientific Investigation Report by the U.S. Geological Survey after editorial review, therefore the final version of this information product may have slightly different content and formatting. Feel free to contact the authors with any questions you may have.

Multiple-Well Monitoring Site Adjacent to the Midway-Sunset and Buena Vista Oil Fields, Kern County, California

By Rhett R. Everett[1,2], Janice M. Gillespie[1], Riley S. Gannon[1], Anthony A. Brown[1], and Andrew Y. Morita[1]

[1] U.S. Geological Survey, California Water Science Center

[2] reverett@usgs.gov

This information product has been peer reviewed and approved for publication as a preprint by the U.S. Geological Survey.

Multiple-Well Monitoring Site Adjacent to the Midway-Sunset and Buena Vista Oil Fields, Kern County, California

By Rhett R. Everett[1], Janice M. Gillespie[1], Riley S. Gannon[1], Anthony A. Brown[1], and Andrew Y. Morita[1]

[1]U.S. Geological Survey,California Water Science Center

Prepared in cooperation with the California State Water Resources Control Board

Acknowledgments

This study was funded by the California State Water Resources Control Boards' Oil and Gas Regional Monitoring Program and U.S. Geological Survey Cooperative Matching Funds. We also thank the California Department of Conservation Division of Geologic Energy Management (CalGEM) for providing information supporting the study.

We acknowledge the valuable assistance of U.S. Geological Survey staff MacKenzie M. Shepherd, Maryanne Bobbitt, Matthew K. Landon, and Gregory A. Smith. We also acknowledge the staff of the U.S.

Geological Survey Research Drilling Program Robert Leininger, Jack Hennagan, Ford Murphy, Edward Oliphant, Joshua Biter, Benjamin Sandoval, and Mathew Kinder.

Contents

Figures

Figure 3. Comparison of density porosity (DPHZ) and neutron porosity (NPHI) logs from the Midway-Sunset Buena Vista multiple-well monitoring site (MSBV), Kern County, California. Only values for saturated intervals were used for this graph. Data summarized from U.S. Geological Survey, 2024c.

Figure 4. Measured and calculated total dissolved solids (TDS) for selected depths at the Midway-Sunset Buena Vista multiple-well monitoring site (MSBV), Kern County, California (U.S. Geological Survey, 2024b, c). Calculated TDS values determined from geophysical logs using the equation from Bateman and Konen (1977). U.S. Geological Survey site numbers and well construction information is available in table 6.

Figure 5. Thin section from cores at the Midway-Sunset Buena Vista multiple-well monitoring site (MSBV), Kern County, California. Photo identifier, core name, and sample depth are listed above each photo. Full image of thin section with area of detail marked shown in upper right corner. Scale bar in lower right corner. (*A*) Authigenic (light gray) gypsum crystals growing in the spaces between grains. (*B*) detrital clasts of gypsum shown by white arrows. (*C*) Diatomite clast showing dissolution around its edges (blue epoxy denotes pore space). Upper arrow points to foraminifera fossil. Lower arrow points to mostly dissolved diatomite frustule. (*D*) Biogenic diatomite clasts with dissolution along the edge of the clasts and along fractures within the clasts. Blue epoxy denotes pore space (*E*) *Amnicola* sp. fragment. (*F*) Bone fragment.

Figure 6.X-ray diffraction results of subsamples from whole- and sidewall-cores collected from the Midway-Sunset Buena Vista multiple-well monitoring site (MSBV), Kern County, California. Data summarized from (U.S. Geological Survey, 2024c.

Figure 7. Scanning electron microscopy images at 250x, 3,000x, and 20,000x of a clast from 256.2 feet below land surface collected from core MSBV-6C-1 at the Midway-Sunset Buena Vista multiple-well monitoring site (MSBV), Kern County, California. Data summarized from (U.S. Geological Survey, 2024c.

Figure 8. Porosity estimated from geophysical logs and measured from core samples collected at the Midway-Sunset Buena Vista multiple-well monitoring site (MSBV), Kern County, California. Geophysical log data from U.S. Geological Survey (2024c).

Figure 9. Specific retention of core material at selected depths from the Midway-Sunset Buena Vista multiple-well monitoring site (MSBV), Kern County, California. Data summarized from U.S. Geological Survey, 2024c.

Table 11. Density, porosity and specific retention of subsamples from whole- and sidewall-cores collected from the Midway-Sunset Buena Vista multiple-well monitoring site (MSBV), Kern County, California. Data summarized from U.S. Geological Survey, 2024c.

Figure 10. Specific retention in relation to the percent opal-CT and total clay in the alluvium and Tulare Formations measured in samples collected at the Midway-Sunset Buena Vista multiple-well monitoring site (MSBV), Kern County, California. Data summarized from U.S. Geological Survey, 2024c.

Figure 11. Water level in relation to well depth at the Midway-Sunset Buena Vista multiple-well monitoring site (MSBV), Kern County, California. Water-level data from U.S. Geological Survey (2024b). Site identification and well construction information are available in table 6.

Figure 12. Changes in water levels relative to 12:00 p.m. Pacific Daylight Time on July 28, 2023, observed in wells at the Midway-Sunset Buena Vista multiple-well monitoring well site (MSBV), Kern County, California. Site identification and well construction information are available in table 6. Water-level data from U.S. Geological Survey (2024b).

Tables

Conversion Factors

U.S. customary units to International System of Units

Multiply	By	To obtain
	Length	
inch (in.)	2.54	centimeter (cm)
inch (in.)	25.4	millimeter (mm)
foot (ft)	0.3048	meter (m)
mile (mi)	1.609	kilometer (km)
	Area	
Acre	4,047	square meter (m^2)
Acre	0.4047	hectare (ha)
Acre	0.4047	square hectometer (hm^2)
Acre	0.004047	square kilometer (km^2)
square foot (ft^2)	929.0	square centimeter (cm^2)
square foot (ft^2)	0.09290	square meter (m^2)
square inch (in^2)	6.452	square centimeter (cm^2)
section (640 acres or 1 square mile)	259.0	square hectometer (hm^2)
square mile (mi^2)	259.0	hectare (ha)
square mile (mi^2)	2.590	square kilometer (km^2)
	Flow rate	
gallon per minute (gal/min)	0.06309	liter per second (L/s)
	Pressure	
pound per square inch (lb/in^2)	6.895	kilopascal (kPa)
	Density	
pound per cubic foot (lb/ft^3)	16.02	kilogram per cubic meter (kg/m^3)
pound per cubic foot (lb/ft^3)	0.01602	gram per cubic centimeter (g/cm^3)

International System of Units to U.S. customary units

Multiply	By	To obtain
	Length	
centimeter (cm)	0.3937	inch (in.)
microns (µm)	0.00004	inch (in.)
	Volume	
liter (L)	33.81402	ounce, fluid (fl. oz)
liter (L)	2.113	pint (pt)
liter (L)	1.057	quart (qt)
liter (L)	0.2642	gallon (gal)
	Mass	
kilogram (kg)	2.205	pound avoirdupois (lb)

Temperature in degrees Celsius (°C) may be converted to degrees Fahrenheit (°F) as follows:

°F = (1.8 × °C) + 32.

Temperature in degrees Fahrenheit (°F) may be converted to degrees Celsius (°C) as follows:

°C = (°F − 32) / 1.8.

Datums

Vertical coordinate information is referenced to the North American Vertical Datum of 1988 (NAVD 88).

Horizontal coordinate information is referenced to the North American Datum of 1983 (NAD 83).

Elevation, as used in this report, refers to distance above the vertical datum.

Supplemental Information

Specific conductance is given in microsiemens per centimeter at 25 degrees Celsius (µS/cm at 25 °C).

Concentrations of chemical constituents in water are given in either milligrams per liter (mg/L) or micrograms per liter (µg/L).

Abbreviations

A amorphous

API American Petroleum Institute

AT20 array induction two foot resistivity with 20-inch depth of investigation

AT90 array induction two foot resistivity with 90-inch depth of investigation

bls below land surface

BTEX benzene, toluene, ethylbenzene, and xylenes

C Christenson core system

C1 methane

C2 ethane

C3 propane

C4 butane

C5 pentane

CaCO3 calcium carbonate

CalGEM California Department of Conservation Geologic Energy Management Division

cm	centimeters
cm^3	cubic centimeters
CO	carbon monoxide
CO_2	carbon dioxide
CST	chronological sample taker
CT	cristobalite-tridymite
DECT	dual energy computerized tomography
DPHI	density porosity
DPHZ	standard resolution density porosity
EM	electromagnetic
EPA	U.S. Environmental Protection Agency
F	Fahrenheit
FID	flame ionization detector
ft	feet
ft^3	cubic feet
g	grams
g/cm^3	grams per cubic centimeter
gal	gallons
H_2S	hydrogen sulfide
HCAL	calibrated caliper
HGR	high resolution gamma ray
HI	hydrogen index
K	potassium

km/s kilometers per second

L liter

mg milligram

min minutes

MSBV Midway-Sunset Buena Vista multiple-well monitoring site

NAD 83 North American Datum of 1983

NAVD 88 North American Vertical Datum of 1988

NGVD 29 National Geodetic Vertical Datum of 1929

NPHI neutron porosity

NPHI* Thermal Neutron Porosity (original Ratio Method) in Selected Lithology

NTU nephelometric turbidity units

NWIS National Water Information System

pCi/L picocuries per liter

PEF photoelectric factor

PHI porosity

ppm parts per million

PR dynamic Poisson’s ratio

PVC polyvinyl chloride

QCI quartz crystallinity index

RDP research drilling program

RHOB bulk density

RHOZ standard resolution formation density

RIR reference intensity calibration ratios

RM resistivity of the mud

RMF resistivity of the mud filtrate

RMP Regional Monitoring Program

Ro electrical resistivity of a fully water saturated sedimentary rock

Rw resistivity of the formation water

SEM scanning electron microscope

SO_2 sulfur dioxide

SP spontaneous potential

SW sidewall core system

TDS total dissolved solids

UCS unconfined compressive strength

µsec/ft microseconds per foot

USGS U.S. Geological Survey

Vb bulk volume

Vp compression wave sonic velocity

Vs shear wave sonic velocity

XRD X-ray powder diffraction

YM dynamic Young's modulus

Zeff effective nuclear charge

° degrees

°C degrees Celsius

µg/L micrograms per liter

µm micrometer

μS/cm microsiemens per centimeter

Well-Numbering System

Wells are identified and numbered according to their location in the rectangular system for the subdivision of public lands. Identification consists of the township number, north or south; the range number, east or west; and the section number. Each section is divided into sixteen 40-acre tracts lettered consecutively (except I and O), beginning with “A” in the northeast corner of the section and progressing in a sinusoidal manner to “R” in the southeast corner. Within the 40-acre tract, wells are sequentially numbered in the order they are inventoried. The final letter refers to the base line and meridian. In California, there are three base lines and meridians; Humboldt (H), Mount Diablo (M), and San Bernardino (S). All wells in the study area are referenced to the San Bernardino base line and meridian (S). Well numbers consist of 15 characters and follow the format 003S002E07P002S. In this report, well numbers are abbreviated and written 3S/2E-7P2. Wells in the same township and range are referred to only by their section designation, 7P2.

Accessing Data

Site information, water-level data, and water quality results presented in this report can be accessed using the U.S. Geological Survey (USGS) National Water Information System (NWIS) at https://waterdata.usgs.gov/nwis/ (U.S. Geological Survey, 2024b). All discrete water-level measurements, the daily minimum depths to water, and daily maximum water-surface elevations for all continuously monitored wells presented in this report are available on NWIS. In digital copies of this report, the USGS site numbers (table 6) presented in the tables are hyperlinked directly to the data in NWIS. Any updates applied to data presented in this report after publication will be available on NWIS.

Geophysical logs can be accessed through the USGS GeoLog Locator portal (https://webapps.usgs.gov/GeoLogLocator; U.S. Geological Survey, 2024c), using the USGS site number for the deepest monitoring well MSBV #1 (USGS site number 350751119241101). Sites with available geophysical logs can be searched by the USGS site number (table 6) or can be located using the interactive map. Lithologic samples (shaker and sieve) collected during the drilling of the multiple-completion monitoring wells are archived at the USGS office in San Diego, California. Photographs of the shaker and sieve samples (along with the full descriptions and notes recorded by the site hydrologist), split whole core samples, and thin sections can be accessed through the USGS GeoLog Locator. Requests for access to samples, field notes, or bench notes can be directed to the USGS California Water Science Center.

Abstract

Groundwater quality in and around oil fields in the Southern San Joaquin Valley is of interest to many California residents that rely heavily on groundwater for domestic, commercial, and agricultural use. To help assess the effects of historical oil-field activities and natural geologic sources on groundwater near the southwest margins of the Kern County Groundwater Subbasin, a multiple-well monitoring site was installed near the administrative boundary between the Midway-Sunset and Buena Vista Oil Fields in Kern County, California. The installation of the Midway-Sunset Buena Vista multiple-well monitoring site (MSBV) supports regional analysis of the relations of oil and gas sources to groundwater quality by providing information about the geology, hydrology, geophysical properties, and water quality of the alluvial and upper Tulare aquifers in areas where groundwater data were limited. Data collected from the site included drill cuttings, whole core samples, sidewall core samples, mud-gas analysis, borehole geophysical logs, depth to water measurements, and water quality samples.

Whole cores were scanned using dual energy computed tomography. Subsamples of selected cores were analyzed for density, porosity, specific retention, and bulk minerology. Thin sections of the subsamples were prepared, photographed, and examined. Two samples were analyzed using scanning electron microscope technology to examine the microporosity of diatomite laden sediment. Instrumentation installed in the wells collect hourly depth to water measurements. Analysis of the data show there is 355 feet of alluvium overlying the Tulare Formation at the well site. The contact between the two formations is an aquitard resulting in a perched aquifer in the alluvium and unconfined aquifer in the Tulare Formation. The alluvium is more heterogenous and finer grained than the Tulare Formation resulting in markedly higher porosity in the alluvium compared to the Tulare Formation. Higher specific retention observed in the alluvium is attributed to the finer grained sediment and greater abundance of reworked diatomite (as represented by opal-CT [cristobalite-tridymite]) compared to the Tulare Formation. Total dissolved solids (TDS) approached or exceeded 10,000 milligrams per liter (mg/L) in the alluvium from approximately 176 to 242 feet below land surface and at the top of the Amnicola clay at approximately 670 feet below land surface within the Tulare Formation. Elevated TDS, chloride, and boron concentrations in the alluvium and on top of the Amnicola clay likely reflect groundwater that is mixed with oil-field water. Water chemistry and modern-aged groundwater in the alluvial monitoring well (MSBV #3) are consistent with the oil-field water in the alluvium being derived from documented historical surface disposal of oil-field water upslope (northwest) of the site. Water chemistry and pre-modern groundwater age in the deeper Tulare monitoring well (MSBV #1) on top of the Amnicola clay are consistent with oil-field fluids derived from upslope natural geologic sources or old oil wells that leak in the subsurface. Shallow groundwater in the Tulare (MSBV #2) is not affected by mixing with oil-field sources.

Introduction

The state of California passed Senate Bill 4 in 2013 which authorized the California State Water Resources Control Board (State Water Board) to monitor potential effects of oil and gas operations on groundwater. In response, the State Water Board established the Oil and Gas Regional Monitoring Program (RMP) to protect all waters designated for any beneficial use near oil and gas operations, while prioritizing the monitoring of groundwater that is or has the potential to be a source of drinking water (California State Water Resources Control Board, 2015, 2022b). The U.S. Geological Survey (USGS), serving as the technical lead for the Oil and Gas RMP, is evaluating groundwater resources near areas of oil and gas development in California, to determine (1) the location of groundwater resources near oil fields; (2) the proximity of oil and gas operations to groundwater resources, and the geologic materials between them; (3) the presence or absence of evidence of fluids from oil and gas sources in groundwater; and (4) the pathways or processes responsible when fluids from oil and gas sources are present in groundwater (U.S. Geological Survey, 2024a).

The Midway-Sunset and Buena Vista Oil Fields are two of the many fields selected for regional groundwater mapping and monitoring by the State Water Board as part of the Oil and Gas RMP (Davis and others, 2018). As part of this evaluation, the USGS installed a multiple-well monitoring site near the administrative boundary between the Midway-Sunset and Buena Vista Oil Fields in the southern San Joaquin Valley about 3 miles east of Taft, California (fig. 1, California Department of Conservation 2021). Data collected at the Midway-Sunset Buena Vista multiple-well monitoring site (MSBV) provides information about the geology, hydrology, geophysical properties, and water quality of the alluvial and upper Tulare aquifers to a depth of 730 feet (ft) below land surface (bls). These data enhance the understanding of relations between adjacent groundwater and the Midway-Sunset and Buena Vista Oil Fields in an area where groundwater data are limited, particularly at different depths in the alluvial and upper Tulare aquifers. This report presents construction information for the MSBV and initial geohydrologic data collected from the site. Similar sites installed near the Lost Hills, North and South Belridge, Poso Creek, and Elk Hills Oil Fields, were described by Everett and others (2020a, b, 2023a, b).

Figure 1. (A) Location of the Midway-Sunset and Buena Vista Oil Fields. (B) Location of the Midway-Sunset Buena Vista multiple-well monitoring site (MSBV), production and injection wells related to oil and gas development, and areas of known historical produced water surface disposal or storage and disposal injection in or near the Midway-Sunset and Buena Vista Oil Fields, Kern County, California.

Hydrogeologic setting

The study area is limited to the southeastern portion of the Midway Valley; a structural low located between the anticlinal structures of the Temblor Range to the southwest and Buena Vista Hills to the northeast that is drained by the ephemeral Sandy Creek (fig. 1). The MSBV is near the southeastern extent of the administrative boundary between the Midway-Sunset and Buena Vista Oil Fields, approximately 3 miles east of Taft, California in southwestern Kern County (fig. 1). Regionally, the MSBV is in the southwest quarter of the Kern County Groundwater Subbasin (subbasin number 5-022.14; California Department of Water Resources, 2020) in the San Joaquin Valley, which is on the southern end of the Tulare Lake Hydrologic Region (California Department of Water Resources, 2020; fig. 1).

Groundwater extraction from aquifers in the Tulare Lake Hydrologic Region accounts for approximately 43 percent (%) of California's average annual groundwater use (California

Department of Water Resources, 2020). The principal water-bearing units in the vicinity of the MSBV lie within the Pliocene to Pleistocene Tulare Formation, and the overlying Pleistocene to Holocene deposits that include the (1) older alluvium and terrace deposits, and (2) recent alluvial and river sediments (hereafter referred to as the alluvial aquifer; California Department of Water Resources, 2015). The Tulare aquifer consists of the water-bearing units within the Tulare Formation that are separated locally and regionally by several confining units. The alluvial aquifer, consisting of the sediments overlying the Tulare Formation, is a complex set of interbedded aquifers and aquitards that function regionally as a single water-yielding unit (Sneed, 2001).

Regionally, the Corcoran Clay member of the Tulare Formation generally marks the division between unconfined (upper) and confined (lower) aquifer conditions. Locally, on the southeastern end of the Midway Valley, a clay at the base of the alluvium similarly marks the division between unconfined and confined conditions. However, at the MSBV site, and to the northwest, the aquifer below the clay is unconfined resulting in a perched aquifer above the clay.

Regionally, groundwater generally flows to the east-northeast (California Department of Water Resources, 2023; Gillespie and others, 2022); however, regional groundwater flow models or elevation maps do not extend into the Midway Valley. Locally, the shallow groundwater (perched and unconfined) flows southeast through Midway Valley, following the path of Sandy Creek (Geomega Inc., 2008; Gannon and others, 2025b).

Most groundwater in the study area in the Tulare Formation and surface alluvium is brackish (3,000 to 10,000 milligrams per liter [mg/L] total dissolved solids [TDS]) or fresh (<3,000 mg/L TDS; Gannon and others, 2025a, Gannon and others, 2025b). Local sources of recharge are precipitation, percolation from ephemeral streams draining the Temblor Range, and municipal and domestic wastewater runoff (Wood and Dale, 1964; Bean and Logan, 1983). Other sources of recharge include historic and present-day oil field activities. Historic activities include disposal of produced water (water extracted with oil) in unlined channels and ponds while present-day activities include the injection of water into the subsurface, either into oil reservoirs for enhanced recovery, or into non-oil-producing formations for disposal (Bean and Logan, 1983; Davis and others, 2022; Gannon and others, 2025b).

Precipitation records for the Carrizo California station (National Weather Service identification number 044916; fig. 1), operated by the Bureau of Land Management 21 miles west of MSBV, indicate an average annual rainfall of 8.4 inches for the period from 2000 through 2023 (Western Regional Climate Center, 2024). Nearly 90 percent (7.4 inches) of annual precipitation occurred, on average, during November through April with more precipitation falling during the month of December (1.6 inches on average) than any other month. Rainfall was not measured during July or August from 2000 to 2023.

Midway Valley is drained by three named ephemeral streams, Buena Vista Creek, Broad Creek, and Sandy Creek (fig. 1). Buena Vista and Broad Creeks drain the northern half of Midway Valley and flow through Buena Vista Valley, while Sandy Creek drains a large portion of the southern part of the valley. Sandy Creek begins in the Temblor Range, transects the Midway Valley on the north side of Taft, then follows the base of the Buena Vista Hills and terminates near the Buena Vista Lake Bed (fig. 1). Sandy Creek drains approximately 35 square miles (mi^2), of which 23 mi^2 are within the administrative boundary of the Midway-Sunset and Buena Vista Oil Fields.

The major groundwater withdrawal in the greater area is for municipal, industrial, and agricultural use and mostly occurs east and north of the Buena Vista Lake Bed (Bean and Logan, 1983; California Department of Water Resources, 2023). Groundwater withdrawal within Midway-Sunset and Buena Vista Oil Fields is limited to a few wells used for oil field and industrial activities (California Department of Water Resources, 2025; California Department of Conservation, 2023).

Local conditions

The MSBV location was selected to provide better information regarding vertical and lateral changes in groundwater gradients and water quality of the alluvial and upper Tulare aquifers adjacent to the Midway-Sunset and Buena Vista Oil Fields. The MSBV is downgradient from these intensively developed oil fields and upgradient from local groundwater resources (Faunt, 2009; Gillespie and others, 2022). The monitoring site was designed to allow collection of geochemical, geophysical, and hydrologic data to evaluate if adjacent groundwater zones may be affected by (1) naturally existing oil and gas in aquifers in proximity to oil fields or (2) a range of historical and present-day oil- and gas- development activities. Several activities in developed oil fields could affect groundwater, including surface spills and historical surface disposal practices, leakage of produced water from disposal ponds, injection of produced water into the subsurface for enhanced recovery and disposal, and potential introduction of preferential pathways, such as leaky or improperly abandoned oil and gas wells or test holes (Davis and others, 2018; Gillespie and others, 2019a, 2019b, 2022; Gannon and others, 2025b).

There is an abundance of oil-production and disposal activities near MSBV. Activities within 2 miles of the MSBV include 795 oil or gas-production wells (560 that are plugged and 235 that are active, new, or idle); 7 water-disposal wells (5 plugged, 2 idle); 2 water flood wells (plugged), 1 gas storage well (plugged), and 11 areas (catch basins, ponds, sumps, or other surface sites) where produced water storage has occurred (California Department of

Conservation, 2021; California State Water Resources Control Board, 2022a; Davis and others, 2022). The MSBV is about 970 ft from the nearest water disposal well (American Petroleum Institute [API] 0402975577), 2,600 ft from the nearest idle well (API 0402945238), 0.8 miles from the nearest water flood well (API 0402907298), 0.9 miles from the nearest active oil well (API 0402919819), 1.1 miles from the nearest operational surface disposal facility, and 2.4 miles from the nearest active steam flood well (California Department of Conservation, 2021).

Prior to mid-1950s, disposal of produced water was accomplished through percolation and evaporation. In the Midway Valley produced water was discharged into percolation ponds or directly into portions of Sandy Creek, Broad Creek, and Buena Vista Creek (Rickett and Reaves, 1954; Bean and Logan, 1983; DiGiulio and others, 2021; Davis and others, 2022). Impoundments (dams) used to collect water, thus at least temporarily restricting flow to downstream areas) were constructed along the creeks allowing water to pool so residual oil could be skimmed and additional impoundments were constructed at the terminuses of the creeks to reduce the flow of produced water towards the area of the Buena Vista Lake Bed (fig. 1; Bean and Logan, 1983). In the mid-1950s many of the smaller percolation ponds were abandoned in favor of larger percolation facilities, several of which were located along the boundary between the Midway-Sunset and Buena Vista Oil Fields. The MSBV is about 260 ft south of a section of Sandy Creek where historically, produced water may have flowed (Rickett and Reaves, 1954). The closest area where produced water-storage occurred after the late 1950s is approximately 1.1 miles north-northwest of MSBV (California State Water Resources Control Board, 2022a; Davis and others, 2022).

Methods

The MSBV was completed by the USGS Research Drilling Program during May 2023. Samples and data collected during the process included drill cuttings, continuous mud-gas analysis and discrete mud-gas samples, whole and sidewall cores, geophysical logs, water quality samples, and time-series water levels. The methods used to drill, collect samples and data, install the monitoring wells, and analyze the data are explained in the following sections.

Site Selection

Because groundwater sample data are sparse in the Midway-Sunset/Buena Vista Oil Fields study area, interpretations of borehole geophysical logs collected when oil wells are drilled are the primary source of water quality information in the oil fields. Gillespie and others (2019a, 2019b, 2022) previously described results of water quality assessments in other western San Joaquin Valley oil fields to the north of the Midway-Sunset and Buena Vista Oil Fields study area.

Higher porosity and specific retention in the alluvium could affect movement of saline oil-field water from surface disposal sites and could affect interpretation of borehole geophysical logs to estimate TDS in groundwater. The MSBV site was selected in an area that allowed for the collection of geophysical logs, cores, and water quality samples from the alluvium and upper Tulare Formation to evaluate if the alluvium contained higher percentages of clay and detrital diatomite, resulting in higher porosity and specific retention, than the underlying Tulare Formation.

The cores and resulting textural, mineralogical, and geochemical analyses of the core samples described below were used to provide data supporting a regional effort in progress to apply the methods of Gillespie and others (2019a, 2019b, 2022) to analyze water quality in the Midway-Sunset and Buena Vista Oil Fields study area.

Drilling

The MSBV pilot borehole, with a diameter ranging from 8 $^{3}/_{4}$ to 7 $^{7}/_{8}$ inches, was drilled to a depth of 730 ft bls using direct mud-rotary drilling. The process involves pumping a bentonite slurry (drill mud) down the borehole through the drill pipe. The drill mud exits the drill pipe at the drill bit, mixes with the drill cuttings, then flows up the borehole annulus to the surface. At the surface, the sediment-laden drill mud is pumped to a shaker tank and passed over vibrating screens (mesh size 70) to remove the sediment particles larger than fine sand. The partially filtered drill mud is then pumped through multiple centrifugal cones that separate out the remaining finer-grained sediment. The cleaned drill mud is then reused downhole.

To reduce the possibility of introducing contamination to the surrounding groundwater, only water-well safe drill mud and additives, and potable water were used to make the slurry. A sample of the drill mud was analyzed by a third-party laboratory for quality control purposes. The drill mud was routinely monitored throughout the drilling process for weight, viscosity, electrical-conductance, and pH. Newly mixed drill mud was frequently added to the slurry as the volume of the borehole increased.

Drilling was completed in 20-foot intervals. The start and end time of each drilled interval was recorded to determine the average rate of penetration. After each 20-foot interval the borehole was wiped (running the drill bit up and down the hole while still rotating the bit) multiple times to remove all cuttings and increase the likelihood of producing a smooth borehole wall. Sufficient time was allowed to insure all the cuttings were circulated out of the hole before the next interval was drilled.

The time required for the drill cuttings to be brought to the surface after being drilled (circulation time), increases with depth and varies depending on borehole diameter and pump rates. The circulation time is important to determine the time when sediments from a given depth will be present at the surface on the shaker screen and can be collected or, conversely, determine from what depth drill cuttings were produced when distinct changes were observed. The circulation time was routinely calculated using the rice test method. This test involves adding uncooked white rice to the drill mud inside the pipe immediately before an interval is drilled. The time required for the rice to be observed on the shaker screen was used for the circulation time. Due to the large difference between the small internal diameter of the drill pipe and the large diameter of the drilled borehole, the fluid velocity inside the drill pipe is much greater than in the borehole; therefore, the travel time of the rice from the surface to the bit is considered negligible in comparison and not counted as a two-way travel time.

Routine data collection and analysis activities during the drilling included the collection and analysis of drill cuttings, continuous monitoring of the drill mud for hydrocarbon and select hazardous gases, and the collection of core samples. After reaching total depth, the entire borehole was wiped again to increase the likelihood of producing a smooth borehole wall thereby allowing for the collection of higher quality geophysical logs. Finally, a suite of geophysical logs was collected in the open borehole. A detailed description of these activities is provided in the following sections.

Drill Cutting Collection and Analysis

Drill cuttings were collected throughout the drilling process and analyzed (along with notes from the on-site geologist) to summarize the lithology. Drill cuttings, denoted as “shaker drill cuttings,” were collected at 10-foot intervals from vibrating #70 screens on the shaker. Additional shaker cuttings were collected where lithologic changes were observed during drilling. Drill cuttings, denoted as “sieve drill cuttings,” were composited over 20-foot intervals by routinely collecting and filtering drill mud from the borehole through a #120 sieve. The circulation times were used to determine the appropriate delay between drilling a given interval and collecting the sample at the surface. Due to mechanical separation and differences between the two collection methods, the shaker samples are slightly biased towards the coarser grained and the sieve samples are slightly biased towards the finer grained.

The unwashed cuttings collected during test drilling were described (grain size and color) in the field. The textures of drill cuttings and core material, where provided, were determined by using a method developed by Folk (1954), and the particle-size distributions were described by using the National Research Council (1947) classification. This approach allows general grain-size descriptions (such as sand) to be correlated to size limits in millimeters or inches. Color, determined on moist, unwashed cuttings, was described according to numerical designations in the Munsell Soil Color Chart (Munsell Color, 1994). The cuttings are archived at the USGS office in San Diego, California. Photographs of the cuttings are available through the USGS GeoLog Locator (U.S. Geological Survey, 2024c). Generalized lithologic logs were compiled from descriptions of drill cuttings, core material, and observations recorded during drilling in the field and in the office (fig. 2).

Figure 2. Well construction, summary lithology, and geophysical log data from the Midway-Sunset Buena Vista multiple-well monitoring site (MSBV), Kern County, California. Water-level data from U.S. Geological Survey (2024b), geophysical log data from U.S. Geological Survey (2024c), and U.S. Geological Survey site numbers can be found in table 6. All geophysical logs, except caliper, were measured by SLB (formerly Schlumberger). Caliper logs were measured by USGS. Methane and oil show were measured by Horizon Well Logging Inc. Yellow shading between formation density and neutron porosity indicates unsaturated sediment. (Abbreviations: API, American Petroleum Institute units; AT20, array induction two foot resistivity with 20-inch depth of investigation; AT90, array induction two foot resistivity with 90-inch depth of investigation; g/cm^3, grams per cubic centimeter; ft^3/ft^3, cubic foot per cubic foot; MSBV, Midway-Sunset Buena Vista multiple-well monitoring site).

The most reliable test for hydrocarbons in drill cuttings is the cut fluorescence, or wet cut test, which utilizes an organic solvent to dissolve the oil (cut) and an ultraviolet light to observe the fluorescence of the resulting cut (Swanson, 1981). Samples were collected every 10 ft, rinsed lightly with acetone, and inspected under an ultraviolet light for fluorescence (Wyman and Castano, 1974; Swanson, 1981). Fluorescence was not observed in any of the analyzed samples indicating that there were no oil shows in the sediments throughout the depth of the completed borehole (730 ft bls).

Mud-Gas Collection and Analysis

Continuous mud gas logging of the drill mud stream was performed by Horizon Well Logging Inc. during the drilling of the pilot hole. Mud gas logging, also known as hydrocarbon well logging or gas logging, entails gathering qualitative and semi-quantitative data from hydrocarbon gas detectors that record the concentrations of natural gas brought up in the drilling mud (Crain, 2024). Total gas detected in the drilling mud does not represent the actual quantity of oil or gas in the reservoir, but the apparent relative concentrations of gas in the drilling mud with respect to depth; when combined with oil-field gas chromatograph analysis to determine the individual gas components (methane [C1], ethane [C2], propane [C3], butane [C4], and pentane [C5]), mud gas logging can assist in locating zones of oil or gas as they are penetrated (Crain, 2024).

To record the highest quality data possible, a mud-gas separator was placed in the drill mud stream within a few ft of the borehole and the mud logging lab was placed as close to the rig as possible (within 50 ft). This allowed the least amount of time for degassing of the drill mud before sample collection and the shortest offset in time from sample collection to analyses. Gas samples were continuously analyzed with a Shenkai 3Q06 high-speed (normal pentane elutes in less than 30 seconds; Shenkai Petroleum & Chemical Equipment Co., Ltd., Shanghai, China) flame ionization detector (FID) chromatography with columns specific to light alkanes and a sensitivity of 1 part per million.

In addition to continuous analysis of C1–C5 gases, the mud logging unit was equipped with an IsoTube Gas Sampling System (Isotech Laboratories, Inc., Champaign, IL; Isotech, 2024a) to collect gas samples. Gas samples were collected based on predetermined depths and detection levels. Predetermined samples included 130 ft (just below the perched water table), at 100-foot intervals starting at 200 ft bls, 355 ft bls (just below the basal clay), 455 ft bls (assumed water table), and at the total depth of the borehole (fig. 2). Additionally, samples were planned to be collected if the apparent methane concentrations exceeded 20 parts per million (ppm), but there was not an opportunity to collect a sample at the single depth of 220 ft bls where high methane was observed. A total of 10 samples were collected for laboratory analysis of C1–C5 gas concentrations and carbon and hydrogen isotope compositions of methane and ethane at

Isotech Laboratories, Inc. to examine potential hydrocarbon gas sources (table 1). Six of the mud-gas samples collected were selected for laboratory analysis of hydrocarbon gases, with samples analyzed at least every 100 feet and at depths where the mud-gas log showed higher concentrations of methane (table 1).

Table 1. Mud-gas samples collected from the Midway-Sunset Buena Vista multiple-well monitoring site (MSBV), Kern County, California. Data summarized from U.S. Geological Survey, 2024b.

In addition to monitoring hydrocarbon gases, the drill mud stream was monitored for select hazardous gas exposure. Monitored gases included sulfur dioxide (SO_2), hydrogen sulfide (H_2S), carbon monoxide (CO), and carbon dioxide (CO_2). No detections of these gases were observed during the drilling of the pilot hole.

Core Collection and Analysis

Core samples (whole [vertical] and sidewall [horizontal]) were collected from selected depths to obtain intact sediment samples of the alluvium and upper Tulare Formation. Whole core samples were collected from 230 to 290 ft bls (table 2). This interval was selected to collect sediments within the alluvium where resistivity anomalies were observed in nearby wells. A total of 43 ft of whole core material was recovered from the alluvium. Attempts to obtain whole cores from the underlying Tulare Formation were unsuccessful. Sidewall cores were collected at 30 selected depths throughout the entire borehole (table 3). Eleven sidewall samples were obtained from the alluvium—including six from within the whole core interval for comparison—and 19 sidewall samples were recovered from the Tulare Formation.

Table 2. Whole cores collected from the Midway-Sunset Buena Vista multiple-well monitoring site (MSBV), Kern County, California. Data summarized from U.S. Geological Survey, 2024c.

Table 3. Sidewall cores collected from the Midway-Sunset Buena Vista multiple-well monitoring site (MSBV), Kern County, California. Data summarized from U.S. Geological Survey, 2024c.

Whole Core Collection

Whole-core samples were collected using the Christensen (Boart Longyear, Sal Lake City, Utah) 94-millimeter core barrel wireline drilling and coring system. The wireline system consists of two parts, an inner and outer core barrel assembly. The outer core barrel assembly consists of multiple subs (hollow pipe with specialized notches, grooves, and rings) and a drag bit with an open center at the bottom. The inner barrel consists of multiple latching devices, a core sleeve, and a shoe (hardened steel point with an open center). A 2.4-inch diameter by 5-foot-long Lexan liner (Lexan, Miami, Florida) was inserted into the inner core barrel assembly and held in place by the shoe. The inner core barrel assembly was then lowered through the center of the drill pipe using a wireline system. At the bottom of the drill pipe, the inner core barrel assembly latches into the subs of the outer core barrel assembly. The shoe typically extends past the teeth on the drill bit by about an inch. As drilling proceeds, the shoe was pushed down over the sediment which slides through the center of the shoe and into the core liner while the drill bit cuts away the sediment on the outside opening the borehole to allow room for the drill pipe. After the interval was cored, a retrieving mechanism was lowered down through the drill pipe using a wireline system to retrieve the inner barrel which was then brought to the surface.

At the surface, the core liner was removed from the inner barrel for processing. The core shoe was separated from the liner, placed in a press, and the sediment in the shoe (hereafter referred to as the shoe sample) was extracted into a sealable bag. The top of the core liner was then cut flush with the top of the core sediment. A cap was placed on the bottom and top of the core liner and sealed with electrical tape, effectively preventing the core material from disaggregating. The length of the core and shoe and the general lithology at the top and bottom of the core was recorded. Finally, the top of the core was marked, and the core was labeled with the core identifier which consists of the site abbreviation, the sequential core number, a code representing the collection method ("C" for Christenson core system), and the section number and the depth interval cored (for example MSBV-3C-1 240' to 245').

In most cases, the length of the core material recovered was less than the length of the cored interval. In these cases, the depth of the top of the core was registered to the top of the cored interval. For example, 3.5 ft of core material was recovered from MSBV-1C-3 (240 ft to 245 ft); therefore, the sediment in this core was assumed to represent the stratigraphy from the depths 240–243.5 ft bls (table 2). The recovered core length was less than the total recovery because the shoe sample was not analyzed like the core sample, because the unconsolidated sediment of the shoe sample typically fell apart before analysis (table 2).

Sidewall Core Collection

Thirty sidewall cores were collected by SLB (formerly Schlumberger) Wireline Services using the chronological sample taker (CST) tool (SLB, Houston, Texas; SLB, 2024a). Sidewall cores were identified using a similar system to the whole cores except that "SW" (for sidewall) was used for the collection method and only one depth was provided (for example MSBV-3SW-1 at 668.99 ft). Sidewall cores were collected from the bottom of the hole upward (deepest sidewall core is #1), therefore the sequential numbers were reversed from the whole core samples.

Selection of the depths of the sidewall cores was an iterative process. The overall approach was to examine drill cuttings, drilling notes, and geophysical logs and collect sidewall samples of sediment that: 1) likely contained diatomite, 2) represented the different lithology types observed throughout the borehole, 3) was adjacent to a change in lithology, or 4) could potentially be within the screened interval of one of the monitoring wells. After selecting several depths matching the criteria, the process was repeated until the depths of 30 sidewall cores (maximum capability of the CST) were selected.

Core Analysis

Whole cores were selected for further analysis based on lithology (top of the core, shoe sample, and visual inspection of the material through the semitransparent semi-flexible core liner) and geophysical logs. Whole cores (MSBV-1C, -3C, -5C, -6C, -7C, -8C, -9C, and -10C) were identified as containing mostly course-grained materials and were processed for laboratory analysis including porosity and specific retention, X-ray diffraction, thin section preparation, and inspection by Scanning Electron Microscope (SEM). Cores that appeared to contain mostly fine-grained material (MSBV-2C, -4C, -11C, and -12C) were processed for archival.

Core Handling

Selected whole core samples were delivered to the Core Laboratories (https://www.corelab.com) facility in Bakersfield, California within 72 hours of collection. The cores were stored horizontally on dry ice and prepared for shipping. To allow the cores to fit in specialized shipping containers, the cores were cut into 3-foot lengths, measuring from the top down, the bottom sections of the cut cores were given a new section number (for example the bottom of MSBV-3C-1 was labeled MSBV-3C-2). The cores were shipped overnight on dry ice to the Core Laboratories facility in Midland, Texas for analysis. The cores were stored on dry ice until they were split.

Sidewall core samples were extracted from the CST, prepped, and shipped by SLB staff to the Core Laboratories facility in Midland, Texas. Once delivered, the sidewall core samples were stored on dry ice until they were analyzed. Core Laboratories staff assigned a core quality index to each sidewall cores considering the quality of the specific retention, X-ray diffraction, and thin section samples that could be obtained (table 3).

Core Scanning

The whole core samples were scanned using dual energy computerized tomography (DECT) methods (Appendix 1). The scan provided a three-dimensional visualization of the unsplit core including preliminary lithological description, high resolution bulk density, effective nuclear charge (Zeff), photoelectric factor (PEF), porosity (PHI), unconfined compressive strength (UCS), compression wave sonic velocity (Vp), shear wave sonic velocity (Vs), dynamic Poisson's ratio (PR), and dynamic Young's modulus (YM; Appendix 1). The data collected from the scans were used to select the intervals of the whole cores that would be subsampled for additional analysis.

Subsample Selection

Core material (subsampled whole core and sidewall cores) from 19 depths were selected for subsampling and analysis (table 4). Analysis included porosity and specific retention, X-ray diffraction, thin section preparation, and inspection by SEM. Sample depths were selected based on analysis of the drill cuttings, geophysical logs, and core scans. Sample depths were selected throughout the entire range of available samples with an attempt to characterize the different types of sediment encountered and to locate sediment that might contain diatomite.

Table 4. Analysis of subsamples from whole- and sidewall-cores collected from the Midway-Sunset Buena Vista multiple-well monitoring site (MSBV), Kern County, California. Data summarized from U.S. Geological Survey, 2024c.

Porosity and Specific Retention

Total porosity is defined as the ratio of the total pore volume to the total volume of a material. Effective porosity is defined as the ratio of the volume of interconnected pore spaces to the total volume (of a sediment/core sample). Specific retention is defined as the ratio of the volume of the water retained in the pore space after drainage and the total sample volume. The porosity of selected core subsamples was measured, and specific retention was calculated by Core Laboratories.

The effective (drainage) porosity was measured using American Society of Testing and Materials (ASTM) method D425 (ASTM International, 2008). This method was selected because it is relatively simple, has widespread usage, and provides a conservative value for effective porosity (specific yield) and specific retention (irreducible water). Effective porosity was determined by saturating the core sample with water, confining it in a temperature-controlled centrifuge (proprietary to Core Laboratories) at sufficient stress to prevent deformation, and centrifuging with an applied force of 1,000 times gravity for 1 hour (ASTM International, 2008). The water forced out of the core during the drainage process was collected in calibrated tubes and the weight measured at the end of the test. The core sample tested also was weighed before and after saturation, and dry. Effective porosity is determined by dividing the volume of water drained from the core sample by the total volume of the saturated core sample. The specific retention was calculated using the following equation:

[(weight of water drained from centrifuge − dry weight) / effective porosity] x 100 (1)

X-Ray Diffraction

X-ray powder diffraction (XRD) is used to identify minerals and other crystalline materials in a sample (Dulong and Jackson, 1997). When a focused X-ray beam interacts with atoms, a portion of the beam is either transmitted, absorbed by the sample, refracted and scattered, or diffracted (Dulong and Jackson, 1997). Core Laboratories performed XRD analysis on all 19 selected subsamples (table 4).

Sample Preparation

Samples submitted for whole-rock and clay-fraction XRD mineral analyses were first disaggregated in a mortar and pestle. Approximately five grams (g) of each sample were transferred to reagent-grade isopropyl alcohol and ground using a McCrone micronizing mill (The MaCrone Group, Inc Westmont, Illinois) for five minutes. The resultant powders were dried, disaggregated, and homogenized, then back-loaded into aluminum sample holders to produce random whole-rock powder mounts. A separate aliquot of the initial hand-ground sample was dispersed in a dilute sodium phosphate solution using a sonic probe. The suspensions were then centrifugally size-fractionated to isolate clay-size (<4 micrometers [μm] equivalent spherical diameter) materials for a concurrent clay-focused XRD analysis. The suspensions were then vacuum deposited on silver membrane filters to produce oriented clay mineral aggregates.

Membrane mounts were attached to stainless steel slugs and exposed to ethylene glycol vapor for a minimum of 24 hours.

Analytical Procedures

XRD analyses of the samples were performed using a Scintag Pad X automated powder diffractometer (Scintag, San Jose, California) equipped with a copper source (40 kilovolts, 30-40 milliamps) and a solid-state or proprietary detection system. The whole rock samples were analyzed over an angular range of 2-70 degrees (°) 2θ (two-theta) at a scan rate of one degree/minute and a step size of 0.02°2θ. The glycol-solvated clay fraction mounts were analyzed over an angular range of 2-40° 2θ at a scan rate of 1.5 degrees/minute and a step size of 0.03° 2θ. Phase identification was done utilizing the computer-assisted search/match algorithm in MDI Jade 9.3 XRD software (MDI, 2025) and the International Centre for Diffraction Data database (International Centre for Diffraction Data, 2025) for minerals and inorganic compounds.

Semi-quantitative determinations of whole-rock and phyllosilicate mineral amounts are completed using integrated peak areas (derived from peak-decomposition / profile-fitting methods) and empirical reference intensity calibration ratios (RIR) determined specifically for the diffractometer used in data collection. The total clay mineral (including mica) abundance of each sample is determined from the whole-rock XRD patterns using combined {00l} and {hkl} clay mineral reflections and suitable empirical RIR factors.

XRD patterns from glycol-solvated clay-fraction samples are analyzed using techniques similar to those described above. Determinations of mixed-layer clay ordering and expandability are completed by comparing experimental diffraction data from the glycol-solvated clay mineral aggregates with Core Laboratories proprietary database of simulated one-dimensional diffraction profiles.

Quartz crystallinity index (QCI) is a semi-quantitative method for determining the level of crystallinity of quartz (Murata and Norman, 1976). Murata and Norman (1976) proposed a QCI scale (0–10) based on the intensity of the (212) X-ray diffraction peak. The QCI can provide insight on the source of the quartz grains and the degree of diagenetic alteration. Low QCI indicates poor crystalline quarts, such as biogenic quartz (opal-CT [cristobalite-tridymite]), while high QCI indicates more crystalline quartz. Quartz crystallinity index was determined by Core Laboratories following the published work by Murata and Norman (1976).

Petrographic Thin Sections

A petrographic thin section is a thin slice (typically 30 µm thick) of polished material (typically mineral, rock, or sediment) mounted to a glass slide and coated with epoxy. The slice is thin enough that light can pass through the material. Therefore, the material can be examined with a polarizing petrographic microscope to determine the minerals that are present in the sample.

Core Laboratories prepared thin sections of the 19 subsamples that were analyzed with XRD (table 5). To prepare the thin section, a plug collected from the core was impregnated at 800 pounds per square inch with an epoxy resin to solidify the sediment allowing it to be cut and to prevent loss of material during grinding. The epoxy was stained blue to highlight the pore spaces in the finished thin-section. The sample was then mounted on a frosted glass slide, cut, and ground in a lubricant (water or oil if water sensitive minerals such as halite or large amounts of smectite were suspected) to a thickness of 30 µm. Once the thin section was prepared it was stained with (1) alizarin red and K-ferricyanide to assist in differentiating carbonate minerals and (2) sodium cobaltinitrite to assist in differentiating quartz, potassium feldspar, and plagioclase feldspar.

Table 5. Thin section subsamples from whole- and sidewall-cores collected from the Midway-Sunset Buena Vista multiple-well monitoring site (MSBV), Kern County, California. Data summarized from U.S. Geological Survey, 2024c.

High resolution photographs of the thin sections were obtained utilizing specialized software from Core Laboratories. Low resolution photos of the thin sections are available through the USGS GeoLog Locator (U.S. Geological Survey, 2024c).

Scanning Electron Microscope

A SEM utilizes a focused beam of electrons to scan a sample resulting in an image of the surface at greater magnification and resolution than is possible using regular optical methods. Two subsamples were collected, processed, and scanned using a SEM to help confirm the presence of reworked clasts of diatomite rich sediment and better understand their porosity.

A reworked diatomite clast from 256.2 ft bls (Core MSBV-1C-5) was collected, subsampled, processed, and scanned using SEM. Multiple images were collected at increasing magnification focusing on different structures within the clast (Appendix 3). The first scan provided an image at a magnification of 250x (fig. 3.1A and 3.2E). A scan with a magnification of 3,000x focused on a moldic pore (secondary porosity created through dissolution of a preexisting part of a sediment; fig. 3.1B) and two scans, one with a magnification of 18,000x (fig. 3.1C) and one with a magnification of 20,000x (fig. 3.1D), focused on pore wall and clast matrix observed in Figure 3.1B. Another set of scans with magnifications of 1,600x (fig. 3.2F), 7,000x (fig. 3.2G) and 25,000x (fig. 3.2H) focused on skeletal fragments of diatoms, an albite grain, and the poorly developed lepispheres in the matrix.

Core Photography

After subsampling was complete the cores were split longitudinally by Core Laboratories. Low resolution photos of the cores are available in Appendix 4 and through the USGS GeoLog Locator.

Geophysical Logging and Analysis

To assist in the identification of lithologic and stratigraphic units, geophysical logging of the borehole was completed using standard wireline methods (Keys and MacCary, 1971; Shuter and Teasdale, 1989; Keys, 1990; Kenyon and others, 1995). Geophysical logs completed at the site by USGS staff include caliper, natural gamma, normal resistivity (16- and 64-inch normal; not shown in fig. 2), spontaneous potential (SP), electromagnetic (EM) induction (expressed and discussed as resistivity), borehole fluid temperature, and full wave sonic (sonic porosity; selected logs shown in fig. 2; U.S. Geological Survey, 2024c). Geophysical logs completed at the site by SLB Wireline Services included the Platform Express tool (SLB, Houston, Texas), which measures borehole diameter, spontaneous potential, natural gamma, array induction, bulk density, and neutron porosity (selected logs shown in fig. 2; SLB, 2024b, c, d). Logging was completed in the small-diameter pilot hole because higher-quality logs could be collected compared with logs from larger-diameter holes. Prior to logging the resistivity of the mud (RM) was 12.95 ohm-meters at 62.3 degrees Fahrenheit and the resistivity of the mud filtrate (RMF) was 10.99 ohm-meters at 62.3 degrees Fahrenheit.

Caliper logs measure the diameter of the borehole (Century Geophysical, LLC, 2024a; SLB, 2024b). In unconsolidated sediments the caliper log can be used to identify the depth intervals of consolidated layers, washed-out sand, or the presence of swelling clay. Changes in borehole diameter can affect the measurements of geophysical logs by reducing the quality or making zones of similar lithology appear different; therefore, analysis of the caliper log is a critical part of interpreting the geophysical logs and when making calculations with the data. Caliper logs are also useful during the well construction process by providing accurate borehole-volume calculations for placement of sand filter packs and environmental sealing materials.

Natural-gamma logs measure the intensity of gamma-rays emitted from the natural decay of potassium-40 and of the daughter products of uranium and thorium (Century Geophysical, LLC, 2024b; Schlumberger, 1972; SLB, 2024c). Generally, increases in gamma-ray emissions are observed in clay, feldspar-rich sand and gravel, and granite. Natural gamma logs are used primarily to define lithology indicators, depth correction of multiple geophysical logs collected in the same borehole, and correlation of geologic units among boreholes within the same region.

The SP log measures the difference in electrical potentials, as a voltage, that develops at the contacts between different formations, such as shale or clay beds and a sand aquifer (Century Geophysical, LLC, 2024b; SLB, 2024c). SP is a function of the chemical activities of fluids in the borehole and adjacent rocks, the temperature, and the type and quantity of clay present; therefore, SP logs are directly influenced by the drilling fluid in undeveloped water wells. If the drilling fluid in the borehole is fresher than the formation water, there is a negative SP opposite sand beds—this is the so-called standard response. If the salinities are reversed, the SP response is positive opposite the sands (Keys and MacCary, 1971). SP logs are not directly related to porosity or permeability.

Resistivity tools measure the apparent resistivity of a volume of material surrounding the borehole under the direct application of an electric current (Keys and MacCary, 1971). These logs are used to determine formation and fluid resistivity. In general, low resistivity indicates water with higher concentrations of dissolved solids or fine-grained deposits such as silt, clay, and shale; high resistivity indicates water with lower concentrations of dissolved solids or coarser material, such as sand or gravel. The short normal resistivity probe measures the apparent resistivity of material surrounding the borehole that was most likely invaded with drilling fluid while the long normal resistivity probe measures the apparent resistivity at a greater radius, which is considered to be representative of material that is saturated with formation water beyond the invaded zone (Century Geophysical, LLC, 2024b). Comparison of the two logs is a useful indicator of aquifer zones with relatively high TDS. The short and long normal resistivity curves collected by USGS are not discussed but are available from U.S. Geological Survey (2024c).

EM induction and array induction logs yield detailed information about the vertical electrical conductivity of the formation and pore water (McNeill, 1986; Century Geophysical, LLC, 2024c; SLB, 2024c). Electrical conductivity is affected by the porosity, permeability, clay and silt content of the sand-and-gravel aquifers, and the dissolved-solids concentration of the groundwater in the aquifer. EM induction logs can help identify water-bearing units to determine optimum depths for the placement of monitoring well screens and can help identify temporal changes in water quality through sequential logging (Williams and others, 1993). While EM logs measure conductivity, it is more useful to present the data as resistivity; therefore, resistivity was calculated during logging from the inverse of the conductivity. In this report, the array induction two foot resistivity with 20-inch depth of investigation (AT20) and array induction two foot resistivity with 90-inch depth of investigation (AT90) resistivity curves collected by SLB Wireline Services are presented in figure 2 and discussed. Additional resistivity curves are available from U.S. Geological Survey (2024c).

An acoustic (sonic) log measures the time it takes for a pulsed compressional sound wave to travel from a downhole transmitter to downhole receivers. The sonic tool used has two receivers, near and far, that recorded the arrival time of the compressional sound wave (Century Geophysical, LLC, 2024d). In unconsolidated material, sonic logs can be used to identify the water table and contacts between lithologic units that were penetrated by the borehole. The difference in arrival times between the receivers, or delta t, can be related to the physical properties of the adjacent material, primarily porosity. The standard method (Wyllie Time Average) of calculating porosity overestimates porosity in unconsolidated sediments; therefore, porosity was calculated using the Raymer-Hunt formula (Century Geophysical, LLC, 2024d; Raymer, and others, 1980).

Raymer-Hunt Formula for porosity:

$$\text{Sonic Porosity} = 63 \times [1 - (\text{tMatrix}/\text{tLog})] \qquad (2)$$

where

tLog = is the reading on the sonic log in microseconds/foot (µsec/ft).

tMatrix = is the transit time of the formation matrix in usec/ft.

Bulk density tools emit medium-energy gamma rays into a borehole wall where they collide with electrons in the formation, lose energy, and scatter after successive collisions (SLB, 2024d). Some gamma rays return to detectors in the logging tool where they are counted and their energy levels are measured. The number of collisions is related to the electron density, which for most minerals and fluids encountered in oil and gas wells is directly proportional to the bulk density (SLB, 2024d). The bulk density measured by the tool results from the combined effects of the fluid filling the pore space and the rock/sediment matrix. The bulk density can be used to estimate density porosity (DPHI) by applying a matrix coefficient for either sandstone, limestone, or dolomite. A sandstone matrix coefficient was applied to this density log collected in the MSBV borehole.

DPHI is calculated using the following equation:

$$DPHI = (\rho_{ma} - \rho_b)/(\rho_{ma} - \rho_f) \qquad (3)$$

where

ρ_{ma} is the density of the rock matrix (in this case, sandstone with ρ_{ma} = 2.65 g/cm^3),

ρ_f is fluid density (in this case, water with ρ_f = 1.0 g/ cm^3), and

ρ_b is bulk density which is read directly from the log.

If gas or air is present within a zone, the assumption that the fluid density equals that of water is incorrect and the density curve will record abnormally high porosity in these intervals.

Neutron porosity tools emit high-energy fast neutrons which lose energy when they collide with nuclei in the formation materials until they achieve a low energy state and are then referred to as thermal neutrons (SLB, 2024d). The neutron porosity tool counts the returning thermal neutrons at known distances from the source; these counts are converted into a hydrogen index (HI) measurement, which is used to compute neutron porosity. The energy loss is related to the relative mass of the particles with which the neutron collides. Hydrogen, the most effective element for reducing the energy of fast neutrons, is associated with the liquids (oil or water) that fill the pore space in the surrounding formation (SLB, 2024d). Neutron porosity (NPHI) is read directly from the log curve.

In clean sands (sands with little fine-grained sediments such as clay or silt) filled with water or oil, the DPHI and NPHI logs should overlie each other if the correct lithology input is applied. When shale or gas is present or the formation is unsaturated, a separation between the DHPI and NPHI curves is observed. When shale is present the neutrons are slowed by hydroxide ion (OH^-) groups attached to the mineral lattice of the clays. The tool interprets the H ion in the OH^- group as porosity so that the NPHI log will read higher than the DPHI log in clay-rich zones. Therefore, the separation between the curves increases in clay-rich zones and the NPHI log plots to the left (high porosity) of the DPHI curve (SLB, 2024d). This behavior is useful for determining clay volume within an interval. Hydrogen atoms are sparse in intervals where gas or air is present in the pore spaces, thus the NPHI curve notes abnormally low porosity in these zones. Because the DPHI curve records these intervals as abnormally high porosity, a large separation is also observed but, in this case, the NPHI plots on the right (low porosity) and DPHI plots on the left (high porosity)—a phenomenon known as crossover.

SLB geophysical log files report values under multiple channels. In some cases, different methods are used to measure or calculate the same parameter. For example, there are 3 different channels for natural gamma data: standard gamma labeled as GR, environmentally corrected gamma labeled as ECGR, and high-resolution gamma labeled as HGR. In this report the following data channels are used for the different parameters: caliper, calibrated caliper labeled as HCAL; natural gamma, high resolution gamma ray labeled as HGR; SP, spontaneous potential labeled as SP; shallow induction, Array Induction Two Foot Resistivity A20 labeled as AT20; deep induction, Array Induction Two Foot Resistivity A90 labeled as AT90; formation density, standard resolution formation density labeled as RHOZ ; density porosity, standard resolution density porosity labeled as DPHZ); neutron porosity, Thermal Neutron Porosity (original Ratio Method) in Selected Lithology) labeled as NPHI* (SLB, 2024e).

Well Installation and Development

Well-screen and filter-pack intervals were selected based on the geophysical and lithologic data. After these intervals were selected, the pilot hole was reamed to increase the borehole diameter to allow for the construction of the three-well monitoring site.

The monitoring wells were constructed with flush-threaded schedule 80 polyvinyl chloride (PVC) casing. The screened interval for each monitoring well consisted of a 20-foot section of slotted (2 x 0.020 inch) PVC at the bottom. The deepest well (MSBV #1) was constructed with 2.5-inch-diameter (nominal) PVC casing to allow for future geophysical logging, and the two shallow wells were constructed with 2-inch-diameter (nominal) PVC casing. Once the well was lowered to the desired depth, a filter pack of No. 3 Monterey sand (Cemex, S.A.B. de C.V., San Pedro, Mexico; granules) was tremied around the screened interval, typically from about 20 ft below to 20 ft above the screen (fig. 2). A low-permeability bentonite grout was then tremied in place above filter pack to seal the borehole and effectively isolate the screened interval of the monitoring well. The process was repeated for each successive well. The wells were installed with screened intervals from 650 to 670 (MSBV #1), 460 to 480 (MSBV #2), and 220 to 240 (MSBV #3) ft bls (fig. 2; table 6).

Table 6. Identification and construction information from the Midway-Sunset Buena Vista multiple-well monitoring site (MSBV), Kern County, California (U.S. Geological Survey, 2024b, c).

After construction was completed, the wells were developed by airlifting and using a surging technique with compressed air to remove drilling fluid and develop the filter pack surrounding each monitoring well. Field parameters (specific conductance, pH, water temperature, apparent color, and turbidity) were recorded during the process. Well development continued until drilling mud was not evident and field parameters stabilized (five readings, 5 minutes apart, vary less than 5 percent). The average flow rate for each day and development time was used to estimate the discharge. The estimated total discharge was calculated by adding the daily discharge estimated for each day during the development period (table 7). After well development, turbidities of all wells were equal to or below 10 nephelometric turbidity units (NTU; table 7).

Table 7. Well-development and water-level data from the Midway-Sunset Buena Vista multiple-well monitoring site (MSBV), Kern County, California. Data summarized from U.S. Geological Survey, 2024b, c.

Water Level Monitoring

Groundwater levels, measured as depth to water below land-surface datum, were routinely measured in all three monitoring wells and include both periodic discrete (manual) measurements and hourly data recorded by downhole pressure transducers. Data collection and calibration followed methods described by Cunningham and Schalk (2011). The first discrete water level measurement for each well was measured on July 28, 2023, when transducers were installed in MSBV #2 and #3. A transducer was installed in MSBV #1 on December 22, 2023.

Discrete water levels were measured in each well and the transducer data was downloaded every 3 to 4 months.

Discrete water levels were measured and recorded to within 0.01 ft using a calibrated electric tape. The time-series data collected by the transducers was calibrated to match the discrete measurements. Both the discrete and time-series data are available on using the USGS National Water Information System (NWIS) at https://waterdata.usgs.gov/nwis/ (U.S. Geological Survey, 2024b).

Multiple-well groundwater monitoring sites provide water level data in different formations and/or at different depths within the same formation at one location. These data can be used to provide insight into the vertical differences in water levels. The vertical component of the water-level gradients at the site were calculated from the discrete water level measurements made on July 28, 2023, following methods outlined by the U.S. Environmental Protection Agency (2023). The vertical component of the water-level gradient indicates the potential for groundwater flow in the vertical direction but is only one of many factors influencing groundwater flow.

Water Quality Collection and Analysis

To delineate the chemical characteristics and source of the groundwater, samples were collected from each well in accordance with the protocols established by the USGS National Field Manual (U.S. Geological Survey, variously dated) and analyzed for (1) major-ion chemistry, (2) minor and trace elements, (3) nutrients, (4) radium isotopes, (5) dissolved-organic carbon and organic-carbon characteristics, (6) volatile organic compounds, (7) concentrations and isotopic values of light hydrocarbon gases, (8) the stable isotopes of hydrogen (deuterium) and oxygen (oxygen-18) in water, (9) boron and strontium isotopes, (10) carbon (carbon-13) stable isotopes, (11) noble and atmospheric gases, and (12) groundwater-age tracers tritium and carbon-14 activities in dissolved inorganic carbon. The collection and analysis procedures are further described by Gannon and others (2025a, 2025b). The three monitoring wells (MSBV #1–3) were sampled during November 14–15, 2023 and November 12–13, 2024.

Water quality samples were quality-assured using data checks (such as ion-balance calculations and sample rerun requests from analyzing laboratories) and quality-control data collected for this study and other studies conducted during a similar period, following methods discussed in Gannon and others (2025a, 2025b). Quality-control data include field and source-solution blanks to assess positive bias as a result of contamination during sample handling or analysis. Quality-control data also include surrogate compounds added in the laboratory to samples analyzed for volatile organic compounds to identify general problems that may arise during laboratory sample analysis and could affect the results for all compounds in that sample. Though replicates were not collected, each well has similar results between samples in 2023 and 2024 suggesting low variability within an analyte. Ion charge balance errors were below 5 percent for all samples. All results discussed in this report passed these quality-control tests.

While direct sampling and chemical analysis is the gold standard for determining TDS in aquifers, the distribution of wells that can be sampled is limited and indirect methods of estimating TDS can help fill in data gaps. In this study, a variation of the Archie Equation (Archie, 1942) and an algorithm developed by Bateman and Konen (1977) were used to estimate salinity in clean sand intervals between 146 and 665 ft bls. This effort was part of regional efforts to estimate salinity of clean sand intervals in aquifers overlying and adjacent to oil fields in the western San Joaquin Valley described by Gillespie and others (2019a, 2019b, 2022).

Archie (1942) related the in situ electrical resistivity of a fully water saturated sedimentary rock (Ro) to its porosity (ϕ), nondimensional factors related to matrix properties (the cementation factor [m], and the tortuosity factor [a]), and the resistivity of the formation water (Rw) as shown in equation 4.

$$Rw = Ro *((\phi^{m})/a) \qquad (4)$$

To solve for Rw, several assumptions were made. The deep resistivity (AT90) from the geophysical log was assumed to be the most representative of the formation resistivity. The cementation factor (m) was assumed to be 1.8 and the tortuosity factor (a) was assumed to be 1.0. Methods for estimating porosity for use in Archie's equation vary. Anyaehie and Olanrewaju (2010) note that a good estimate of porosity can be derived from the density log if the fluid and matrix density are known. This approach of using only the density porosity is used in calculations for water resistivity by California Resources Corporation (2016) in their aquifer exemption application for the nearby Elk Hills Oil Field. Others, such as Asquith and Gibson (1982), weight the density and neutron porosity equally to derive an average porosity. In this evaluation, the average porosity (ϕ, avg PHI) was determined from the geophysical logs by weighting density porosity (DPHI) twice as much as neutron porosity (NPHI; Gillespie and others, 2022) using the following equation:

$$(NPHI+(2*DPHI))/3 \qquad (5)$$

where

NPHI is the neutron density from the geophysical log (NPHI* data channel)

DPHI is the porosity density from the geophysical log (DPHZ data channel)

Rw was then converted to mg/L NaCl equivalent at formation temperature using equations from Bateman and Konen (1977).

The amount of mixing of two different sources of groundwater can be estimated assuming the geochemical composition is a binary mixture of the two sources using the following equation.

$$x = (qM - qG)/(qP - qG) \qquad (6)$$

where

x is the fraction of oil-field water

qP is the concentration of constituent in average oil-field water

qG is the concentration of constituent in ambient groundwater sample (MSBV #2)

qM is the concentration of constituent in mixed water sample (MSBV #1)

Geochemical mixing of the groundwater at MSBV was calculated. These mixtures were calculated by comparing sample values (MSBV #1 and MSBV #3) with presumed ambient groundwater values (MSBV #2) and average oil-field water values for the conservative geochemical tracers of TDS, chloride, boron, oxygen-18, and deuterium (Weddle, 1967; Seitz and others, 2024). A simple binary mixing equation was used, where the fraction of oil-field water (x) equals the difference between the sample (qM) and ambient groundwater (qG) divided by the difference between average oil-field water (qP) and ambient groundwater (qG), or $x = (qM - qG)/(qP - qG)$. For a given well (MSBV #1 or MSBV #3), a mixing fraction was calculated for each constituent for both 2023 and 2024, and then all resultant values were combined to obtain the average oil-field water mixing fraction and 1-sigma standard deviation at the well.

Results and Interpretation

Mud-Gas Results

Methane concentrations above the approximate baseline concentration of 10 ppm were most apparent at depth intervals from 217 and 230 ft bls. The highest mud gas methane concentration of 29 ppm occurred at a depth of 219 ft bls. There were no detections of sulfur dioxide (SO_2), hydrogen sulfide (H_2S), carbon monoxide (CO), or carbon dioxide (CO_2) in the drill mud during drilling. Six of the 10 mud-gas samples collected were analyzed for the hydrocarbon gases (table 8; Isotech Laboratories, Inc. 2024b). There were no detections of gases in the discrete samples.

Table 8. Analysis of mud-gas samples collected from the Midway-Sunset Buena Vista multiple-well monitoring site (MSBV), Kern County, California. Data summarized from U.S. Geological Survey, 2024b.

Geophysical Log Results

Geophysical logs show the contact between the Tulare Formation and the overlying alluvium at 355 ft bls. Plots of depth versus neutron porosity (NPHI* data channel) and density (DPHZ data channel) show that the contact is marked by a sharp change in porosity at approximately 355 ft bls (fig. 3). Only liquid bearing intervals were used in this plot to remove the crossover effect in unsaturated zones. Both density and neutron porosity are markedly higher (10 percent and 14 percent, respectively) in the alluvium compared to the Tulare Formation. In addition, there is a larger spread in density and neutron porosity values in the alluvium than in the Tulare Formation with the neutron values being higher than the density. This suggests that clay content is higher in the alluvium and the Tulare Formation contains more clean sand intervals. Resistivity is also lower, by about 6 ohmmeters on average, in the alluvium than in the underlying Tulare Formation which is indicative of the presence of finer-grained deposits, or water with higher concentrations of dissolved solids, or both.

Figure 3. Comparison of density porosity (DPHZ) and neutron porosity (NPHI) logs from the Midway-Sunset Buena Vista multiple-well monitoring site (MSBV), Kern County, California. Only values for saturated intervals were used for this graph. Data summarized from U.S. Geological Survey, 2024c.

The density neutron logs also indicate the presence of at least two distinct water tables within the logged interval. The base of cross over (shaded yellow in fig. 2) in the alluvium is at approximately 110 ft bls and marks the depth of the water table within the alluvium. The base of cross over (depth to top of water table) in the Tulare Formation is at approximately 378 ft. This shows that the logged interval contains two distinct saturated layers, a perched aquifer in the alluvium and a regional aquifer in the Tulare Formation.

Only the upper part of the Tulare Formation was penetrated by the well. The boundary between the upper and lower parts of the Tulare Formation is a regional clay layer known as the Amnicola clay. The top of the Amnicola clay at the MSBV site is marked by a sharp increase in the natural gamma (increase in radioactivity) log, a negative shift on the SP log and a separation between the density and neutron curves in which the neutron curve reads a much higher porosity than the density curve (fig. 2). Because the neutron curve measures porosity by measuring the hydrogen concentration within a formation (hydrogen is usually found in water or oil present in the pore space) it records erroneously high porosities in clays such as the Amnicola due to the attached OH^- groups in the clay lattice (Zaydoon, 2025). Normally, the Amnicola clay would also display lower resistivity than the overlying sands in the upper Tulare Formation but, in this well, a thin layer of saline water lies above the clay within the sand of the upper Tulare

Formation. Therefore, the base of the upper Tulare Formation sands also has very low resistivity at the MSBV site.

TDS calculated from the geophysical logs in the alluvium ranged from about 3,500 to almost 20,000 mg/L and were higher than 10,000 mg/L between 176 and 242 ft bls (table 9; fig. 4). TDS measured in groundwater samples (see “Water Quality Results” section) collected from the monitoring wells confirmed that the calculated estimates from the geophysical logs were reasonable (fig. 4). The TDS values are consistent with groundwater in the alluvium being affected by the infiltration of saline oil-field water (Gannon and others, 2025b). The underlying Tulare Formation contains water with an average TDS of about 3,900 mg/L except just above the Amnicola clay, where the TDS values in the Tulare Formation increase to over 11,000 mg/L between 652 and 665 ft bls (table 9; fig. 4; see “Water Quality Results” section).

Table 9. Estimates of total dissolved solids in groundwater at selected depths at the Midway-Sunset Buena Vista multiple-well monitoring site (MSBV), Kern County, California (U.S. Geological Survey, 2024c).

Figure 4. Measured and calculated total dissolved solids (TDS) for selected depths at the Midway-Sunset Buena Vista multiple-well monitoring site (MSBV), Kern County, California (U.S. Geological Survey, 2024b, c). Calculated TDS values determined from geophysical logs using the equation from Bateman and Konen (1977). U.S. Geological Survey site numbers and well construction information is available in table 6.

Core Results

Core Scanning Results

DECT scans of the whole core in the alluvium revealed a sequence of thin (a few inches to 2 ft thick) heterogeneous beds composed of laminated clays, sands, and angular to subrounded clasts up to 2 centimeters (cm) in diameter (Appendix 1). The larger clasts are concentrated in thin layers approximately 3 cm thick, but the smaller clasts appear to float within a sandy matrix. Most clasts have very low sphericity with the long axis approximately 3–4 times longer than the short axis. DECT data were not available from the Tulare Formation because no vertical cores were collected—only sidewall core that were not scanned.

Petrographic Thin Sections Results

Sand sized grains within the alluvium are mainly angular to sub-angular and consist of quartz, feldspar, and lithics. Minor biotite is also present. Both orthoclase and plagioclase feldspar are present and albitization is common in many of the potassium feldspars. Lithic grains appear to be primarily sedimentary. The sample from 300 ft (table 5, MSBV-23SW-1) is filled with authigenic evaporite which occludes most of the pore space (fig. 5*A*, table 5). Crystalline evaporites are also present in the sample at 267 ft (table 5, MSBV-23SW-1) but the evaporites in this sample have more discrete grain boundaries and appear to be detrital rather than authigenic (fig. 5B, table 5).

Figure 5. Thin section from cores at the Midway-Sunset Buena Vista multiple-well monitoring site (MSBV), Kern County, California. Photo identifier, core name, and sample depth are listed above each photo. Full image of thin section with area of detail marked shown in upper right corner. Scale bar in lower right corner. (*A*) Authigenic (light gray) gypsum crystals growing in the spaces between grains. (*B*) detrital clasts of gypsum shown by white arrows. (*C*) Diatomite clast showing dissolution around its edges (blue epoxy denotes pore space). Upper arrow points to foraminifera fossil. Lower arrow points to mostly dissolved diatomite frustule. (*D*) Biogenic diatomite clasts with dissolution along the edge of the clasts and along fractures within the clasts. Blue epoxy denotes pore space (*E*) *Amnicola* sp. fragment. (*F*) Bone fragment.

Clasts in the alluvium are subangular to subround and consist mainly of sedimentary lithics—primarily diatomite, carbonates, siltstones and claystones. Foraminifera and diatoms are abundant in the diatomite and carbonate clasts (fig. 5*C*). The diatomite was probably derived from erosion of the Monterey diatomites (Belridge diatomite) exposed in the adjacent Temblor Range (Dibblee, 2005a, 2005b, 2005c). Many of the diatomite frustules exhibit partial to nearly full dissolution (fig. 5*C*). The thin sections were impregnated with blue epoxy for analysis, and many diatomite clasts show dissolution features along their margins and along fractures within the clasts (fig. 5*D*).

The texture and composition of sand sized grains within the Tulare Formation are similar to those observed in the overlying alluvium. However, the Tulare Formation contains far fewer biogenic lithic clasts such as diatomite. Siltstone and claystone clasts are more common as are volcanic and metamorphic clasts. Few microfossils were observed in thin section. Fossils observed consisted mainly of *Amnicola* sp. fragments and a bone fragment (figs. 5*E*, 5*F*).

X-Ray Diffraction Results

Nineteen samples from both whole core and sidewall cores were analyzed for bulk mineralogy using XRD (table 10, fig. 6). The Tulare Formation is more arkosic than the alluvium. Diatomite is present, as represented by opal-CT, in each of the samples from the alluvium but only four samples of the Tulare Formation and at much smaller quantities (table 10). XRD of diatomite clasts collected from core MSBV-6C-1 (approximately 256.2 ft bls) contained 56.5 percent opal-CT by weight indicating that the diatomite is opal-CT phase.

Table 10. X-ray diffraction results of subsamples from whole- and sidewall-cores collected from the Midway-Sunset Buena Vista multiple-well monitoring site (MSBV), Kern County, California. Data summarized from (U.S. Geological Survey, 2024c.

Figure 6. X-ray diffraction results of subsamples from whole- and sidewall-cores collected from the Midway-Sunset Buena Vista multiple-well monitoring site (MSBV), Kern County, California. Data summarized from (U.S. Geological Survey, 2024c.

Scanning Electron Microscope Results

SEM photographs of a diatomite clast from 256.2 ft bls (core MSBV-6C-1) show that diatom frustules are completely or partially dissolved and replaced by lepispheres (microcrystalline, blade shaped crystals of a metastable variety of quartz) of opal-CT (fig. 7). The transformation of opal-A (amorphous) to opal-CT takes place at burial ranges of approximately 0.3 to 1.2 miles (Pisciotto, 1981; Keller and Isaacs, 1985). The alluvium lies at depths much shallower than this. Therefore, the source of the diatomite clasts is most likely the Monterey Formation which, after burial of 0.3 to 1.2 miles, was uplifted in the adjacent Temblor Range, from which Sandy Creek drains (fig. 1).

Figure 7. Scanning electron microscopy images at 250x, 3,000x, and 20,000x of a clast from 256.2 feet below land surface collected from core MSBV-6C-1 at the Midway-Sunset Buena Vista multiple-well monitoring site (MSBV), Kern County, California. Data summarized from (U.S. Geological Survey, 2024c.

Porosity and Specific Retention Results

Porosity of the sediment was estimated from the geophysical logs (neutron porosity, density porosity, sonic porosity) and measured from core subsamples. Analysis of the geophysical logs shows a variation in the different methods (fig. 8). Throughout most of the logged interval the density porosity was slightly lower than the neutron porosity while the sonic porosity was consistently higher, by about 30 percent in the alluvium and 50 percent in the Tulare Formation (table 9). Deviations between the neutron porosity and the density porosity are most apparent in the unsaturated sediments and in the Amnicola clay. The density porosity was higher than the neutron porosity in the unsaturated sediments and lower in the Amnicola clay. Total porosity measurements of the core subsamples were close in value (within 5 percent) to the neutron log, with three exceptions (MSBV-8C-1, 8.5 percent higher; MSBV-9C-1, 9.8 percent higher, and MSBV-15SW-1, 5.5 percent lower), suggesting the neutron density log is most representative of the porosity at this site (fig. 8). Porosity estimated using neutron logs, density logs, and core samples are all subject to uncertainties, the latter due to potential compaction or disruption of sediment structure as part of the coring and sample handling process, so there is no single porosity estimation method that is ideal for all textures and settings.

Figure 8. Porosity estimated from geophysical logs and measured from core samples collected at the Midway-Sunset Buena Vista multiple-well monitoring site (MSBV), Kern County, California. Geophysical log data from U.S. Geological Survey (2024c).

Specific retention is the ratio of the amount of water a rock can retain against gravity to the total volume of the rock. Molecular attraction and capillary forces keep the water from being removed from the pore spaces by drainage. Specific retention is important to determine the rate at which fluids such as infiltrated produced water will move through the subsurface within the aquifer. Twelve samples from cores in both the Tulare Formation (4 samples) and the alluvium (8 samples) were chosen for specific retention measurements. The specific retention is reported as a percentage of the pore space in these analyses. Plots of specific retention vs depth show that specific retention is highest within the alluvial aquifer (fig. 9). Therefore, water is expected to travel more slowly through unsaturated parts of the alluvial aquifer than unsaturated parts of the Tulare Formation.

Figure 9. Specific retention of core material at selected depths from the Midway-Sunset Buena Vista multiple-well monitoring site (MSBV), Kern County, California. Data summarized from U.S. Geological Survey, 2024c.

XRD analysis shows that the alluvial aquifer contains more diatomite (as opal-CT) and clay compared to the Tulare Formation—both of which can hold large amounts of water against gravity drainage due to their small pore sizes, cohesiveness, and hydrophilic (in the case of diatomite) properties (table 11). Plots of opal-CT and total clay vs specific retention indicate that specific retention increases along with an increase in the fraction of both of these mineral facies (fig. 10).

Table 11. Density, porosity and specific retention of subsamples from whole- and sidewall-cores collected from the Midway-Sunset Buena Vista multiple-well monitoring site (MSBV), Kern County, California. Data summarized from U.S. Geological Survey, 2024c.

Figure 10. Specific retention in relation to the percent opal-CT and total clay in the alluvium and Tulare Formations measured in samples collected at the Midway-Sunset Buena Vista multiple-well monitoring site (MSBV), Kern County, California. Data summarized from U.S. Geological Survey, 2024c.

Groundwater Levels

Analysis of the discrete water levels measured on July 28, 2023, show the water level in the shallowest well (MSBV #3) was 109 ft bls which was 268 ft higher than the water level of about 377 ft bls in the deeper wells (MSBV #2, MSBV #1, fig. 11). However, MSBV #3 is in the perched shallow aquifer in the alluvium, which is hydraulically separated at the MSBV site from the regional aquifer system in the upper Tulare Formation by an unsaturated zone in the upper Tulare Formation, cemented sand in the upper Tulare Formation, and clay-rich sediments in the lower part of the alluvium. Previous work in the area has indicated that the unsaturated zone in the upper Tulare Formation is not present everywhere southeast of Taft, so there could be saturated hydraulic connection between aquifer layers in the alluvium and the upper Tulare Formation at other locations within a few miles of MSBV (Geomega Inc., 2008; Gannon and others, 2025b). The thickness and properties of the basal clay-rich sediments and cemented sands in the upper Tulare Formation are also spatially variable, so groundwater flow from the alluvium toward the Tulare Formation could occur in places. There is essentially no vertical component of the water-level gradient (−0.002 ft/ft) between MSBV #2 and #1 within the Tulare Formation above the Amnicola clay. There is no water level data below the Amnicola clay at the MSBV site.

Figure 11. Water level in relation to well depth at the Midway-Sunset Buena Vista multiple-well monitoring site (MSBV), Kern County, California. Water-level data from U.S. Geological Survey (2024b). Site identification and well construction information are available in table 6.

Water-level changes through time were used to help determine the degree of hydraulic interaction between aquifer layers. The change in water level for each well relative to 12:00 p.m. Pacific Daylight Time on July 28, 2023, at the beginning of the period when hourly data were recorded, was calculated through November 20, 2025 (fig. 12). Water levels remained relatively static, varying by less than 1 ft. Daily to weekly fluctuations are apparent in the water level data. Over the period of record (July 2023 to November 2025) a slight decline was observed in the deep well (MSBV #1), no change was observed in the middle well (MSBV #2) and a slight rise was observed in the shallow well (MSBV #3).

Figure 12. Changes in water levels relative to 12:00 p.m. Pacific Daylight Time on July 28, 2023, observed in wells at the Midway-Sunset Buena Vista multiple-well monitoring well site (MSBV), Kern County, California. Site identification and well construction information are available in table 6. Water-level data from U.S. Geological Survey (2024b).

Water Quality Results

Selected water quality data is discussed here and presented in table 12 while the entirety of the data is available in NWIS (U.S. Geological Survey, 2024b). Concentrations of TDS in water samples collected from the three MSBV wells in 2023 ranged from 4,010 mg/L at MSBV #2 to 24,600 mg/L at MSBV #3 (fig. 4; table 12). Water quality data collected in 2024 had similar results to 2023 for all parameters (table 12).

Table 12. Water-quality indicators (field parameters), total dissolved solids, and selected results in samples collected from the Midway-Sunset Buena Vista multiple-well monitoring site (MSBV), Kern County, California (U.S. Geological Survey, 2024b).

The elevated TDS (24,600 mg/L), chloride (12,900 mg/L), and boron (32,500 micrograms per liter [µg/L]) at MSBV #3 in 2023 likely reflect groundwater that is mixed with oil-field water based on regional analysis in the Midway-Sunset and Buena Vista Oil Field study area by Gannon and others (2025b). The sample from MSBV #3 has the petroleum hydrocarbon compounds benzene, toluene, ethylbenzene, and xylenes (BTEX) present (table 12) with an elevated benzene concentration of 145 µg/L which, along with the presence of propane, indicates the likelihood of groundwater mixed with some oil-field fluids (Schoell, 1980; Whiticar, 1999; Taylor and others, 2000; Gannon and others, 2025b). The hydrogen and oxygen stable isotope values at MSBV #3 are much more positive than unaffected water in the area (for example

MSBV #2) and trend toward oil-field water values, further indicating the likelihood of mixing (Gannon and others, 2025b). Surface disposal of oil-field water northwest of the drill site (fig. 1; Geomega Inc., 2008) is a likely source of mixing based on two primary lines of evidence: (1) the presence of low but detectable tritium which indicates the presence of groundwater that recharged in 1953 or later (Lindsey and others, 2019); and (2) the detection of trihalomethanes (for example trichloromethane concentration of 0.1431 µg/L) and other halogenated organic compounds, which are representative of chlorinated municipal wastewater effluent (Carter and others, 2012) discharged to the surface near Taft.

MSBV #1, completed in the Tulare Formation, is also likely mixed with oil-field fluids based on the detections of the indicator compounds BTEX (benzene of 39.1 µg/L) and propane (Gannon and others, 2025b). MSBV #1 has old, premodern water (4.6 percent modern carbon, no detectable tritium) and no detections of surface-source compounds like trihalomethanes in MSBV #3, suggesting a subsurface source of mixing for MSBV #1. Subsurface sources in the area include naturally occurring seepage to relatively shallow depths overlying oil-producing reservoirs or oil-well infrastructure (Gannon and others, 2025b). Recent work by Molofsky and others (2025) suggests that very low hydrocarbon gas alkane ratios (that is, the concentration of methane divided by the summed concentrations of ethane and propane) are typically representative of raw reservoir gases while higher ratios are typically representative of hydrocarbon gases that have naturally migrated via faults and fractures. The study by Molofsky and others (2025) showed that no samples of naturally migrated gas had alkane ratios below 10 ($n = 193$), while 60 percent of reservoir gas samples were less than 25 ($n = 2{,}925$). Thus, the alkane ratio of 0.6 in MSBV #1 may indicate reservoir gas and not natural seepage, suggesting a direct conduit from the reservoir to the sample via aging oil-field infrastructure. There are over

50 oil wells within 0.75 miles of MSBV, and two shallow water disposal wells less than 0.2 miles from MSBV (California Department of Conservation, 2023). In addition, analysis by Gannon and others (2025b) of mud gas and oil show data in the Midway-Sunset and Buena Vista Oil Fields indicate naturally occurring hydrocarbons at depths shallower than developed oil reservoirs are present in places that could be a potential source of hydrocarbons detected in MSBV #1, although the available data within 2 miles of the MSBV are limited.

MSBV #2, which is also completed in the Tulare Formation, shows no signs of mixing with oil-field fluids and likely represents ambient Tulare Formation groundwater. This allows for an estimation of the amount of mixing at MSBV #1 assuming the geochemical composition of MSBV #1 is a binary mixture of oil-field water and ambient groundwater similar to MSBV #2. The mixing fraction is obtained by comparing the excess salinity, ion, and stable isotope concentrations at MSBV #1 above ambient groundwater values at MSBV #2 with average oil-field water values. Oil-field water in proximal production zones Top Oil, Wilhelm, Gusher, and Calitroleum have, on average, TDS of 35,000 mg/L, chloride of 20,000 mg/L, and boron of 50,000 µg/L (Weddle, 1967) as well as −30 per mil deuterium and 0 per mil oxygen-18 (Seitz and others, 2024). Compared to MSBV #2, MSBV #1 has approximately 2,500 mg/L higher TDS, 1,500 mg/L higher chloride, and 11,000 µg/L higher boron concentrations, as well as 2 per mil higher oxygen-18 and 6 per mil higher deuterium (table 12).

Geochemical mixing calculations resulted in MSBV #1 having an oil-field water fraction of 14 ± 6 percent, and MSBV #3 having an oil-field water fraction of 68 ± 7 percent. These calculations suggest that the samples from MSBV #1 contain a conservative estimate of 10 percent oil-field water. The amount of mixing at MSBV #3 can similarly be estimated by assuming its results (table 12) represent a binary mixture between MSBV #2 and average oil-field water. The results at MSBV #3 are somewhat less precise than at MSBV #1 because ambient groundwater at MSBV #3 may have a different composition than that represented by MSBV #2, and because the presumed surface source for mixing at MSBV #3 is likely more variable than the subsurface source for MSBV #1. Calculations suggest that the samples from MSBV #3 contain a conservative estimate of two-thirds oil-field water.

Summary

The Midway-Sunset Buena Vista multiple-well monitoring site (MSBV) in Kern County, California included about 355 feet (ft) of alluvium overlying Tulare Formation to the bottom of the hole at 730 ft. Clay rich sediments at the base of the alluvium and cemented sand near the top of the Tulare Formation contribute to hydrologic separation between the alluvium and the Tulare Formation. Groundwater levels in the perched alluvial aquifer layer were about 267 ft higher than those in the upper Tulare Formation. Porosity was markedly higher in the alluvium, perhaps reflecting more clay and the presence of porous detrital diatomite in the alluvium, compared to the predominantly sandy upper Tulare Formation. Underlying the upper Tulare Formation, the Amnicola clay was present from 670 ft below land surface (bls) to the bottom of the hole at 730 ft bls and likely serves as a confining unit between the upper and lower Tulare Formation.

Porosity logs and water-levels in monitoring wells completed in the alluvial and Tulare Formation indicated two distinct saturated layers, a perched aquifer in the alluvium and a regional aquifer in the Tulare Formation. The alluvial perched aquifer had a depth to water of about 109 ft and the upper Tulare Formation has a depth to water of about 377 ft, with an approximately 30 ft thick unsaturated zone in the upper Tulare below the base of the alluvium.

Calculations from geophysical logs and analysis of water quality samples from the monitoring wells indicated that total dissolved solids (TDS) in the alluvium ranged from 3,540 to 24,600 milligrams per liter (mg/L) in the alluvium and was higher than 10,000 mg/L between 176 and 242 ft bls. These TDS values are consistent with groundwater in the alluvium being affected by the infiltration of relatively more saline oil-field water from a surface source (Gannon and others, 2025b). The underlying Tulare Formation contains groundwater with lower TDS of 3,500 to 4,500 mg/L, except immediately above the Amnicola clay, where the TDS was higher than 10,000 mg/L around 665 ft bls. The saline groundwater on top of the Amnicola clay could be related to oil and gas development or natural geologic sources and pathways in the subsurface.

Vertical core samples in the alluvium and sidewall core samples in the alluvium and Tulare Formation were collected and selected core samples were analyzed for a variety of physical, mineralogical, and chemical analyses.

Dual energy computerized tomography (DECT) scans of core samples indicated that the alluvial sediments are highly heterogeneous in texture.

Thin sections showed diatomite clasts were present in the alluvium that included dissolution features. The diatomite clasts were much less abundant in the underlying Tulare Formation. Scanning electron microscope photos showed that the diatomite clasts are partially or completely dissolved and replaced by opal-CT (cristobalite-tridymite). X-ray diffraction analysis confirmed that all samples from the alluvium and half the samples from the Tulare formation contained opal-CT (diatomite) and the abundances were higher in the alluvium. The transformation of opal-A to opal-CT takes place at burial ranges of about 0.3 to 1.2 miles. The alluvium lies at depths much shallower than this. Therefore, the source of the diatomite clasts is most likely erosion of the Monterey Formation which, after burial of 0.3 to 1.2 miles, was uplifted in the adjacent upslope Temblor Range.

Analysis of core samples indicated that specific retention was higher in the alluvial sediments than in the Tulare Formation, indicating that water is likely to move more slowly through unsaturated parts of the alluvial sediments than unsaturated parts of the Tulare Formation. The higher specific retention in the alluvium reflects that the sediment is finer textured and more heterogenous compared to the sediment in the Tulare Formation. The higher specific retention in the alluvium is also a result of the larger abundance of detrital highly porous diatomite clasts.

Multiple lines of geochemical and isotopic evidence in groundwater samples collected from the MSBV wells indicate that the shallowest well in the alluvium (MSBV #3) contains oil-field fluids and modern groundwater age tracers consistent with effects of a surface disposal source; the results at MSBV #3 are consistent with effects of historical surface disposal sources on some groundwater at other locations near the MSBV site and elsewhere in the Midway-Sunset and Buena Vista Oil Fields study described by Gannon and others (2025b). The deepest well (MSBV #1) on top of the Amnicola clay has lower concentrations than MSBV #3, in the alluvium, but also shows multiple indicators of mixing with oil-field fluids. However, the depth and pre-modern groundwater age of groundwater from this well indicates this well has been affected by a subsurface source, which could include leaky oil-well infrastructure or natural geologic sources of oil-field fluids. The intermediate depth well (MSBV#2) shows no indications of mixing with oil-field fluids and likely represents ambient groundwater from the upper Tulare Formation. Profiles of TDS determined from analysis of the geophysical logs and groundwater samples in 2023 were consistent with these interpretations, with the highest TDS of up to 24,600 mg/L (MSBV #3, 2023) in the alluvium, lowest and relatively uniform values of 4,010 mg/L (MSBV #2, 2023) through most the upper Tulare Formation, and intermediate TDS values just above the Amnicola clay of 6,580 mg/L (MSBV #1, 2023).

References Cited

Anyaehie, J.C., and Olanrewaju, O., 2010, Hydrocarbon effect correction on porosity calculation from density neutron logs using volume of shale in Niger Delta: Nigeria Annual International Conference and Exhibition, Tinapa - Calabar, Nigeria, July 2010, accessed at https://doi.org/10.2118/140618-MS.

Archie, G.E., 1942, The electrical resistivity log as an aid in determining some reservoir characteristics: Transactions of the AIME, v. 146, p. 54–62.

ASTM International, 2008, ASTM D425 standard test method for centrifuge moisture equivalent of soils: West Conshohocken, PA, accessed September 24, 2023, at https://www.astm.org/d0425-17.html.

Asquith, G.B., and Gibson, C.R., 1982, Basic Well Log Analysis for Geologists: American Association of Petroleum Geologists, Tulsa, OK. 1982, p. 216.

Bateman, R.M., and Konen, C.E., 1977, The log analyst and the programmable pocket calculator: Society of Petrophysicists and Well Log Analysts, v. 18, no. 5, p. 3–10.

Bean, R.T., and Logan, J., 1983, Lower Westside water quality investigation, Kern County—Prepared for California State Water Resources Control Board under contract No. 2-096-158-0, p. 128.

California Department of Conservation, 2021, Online data: California Department of Conservation, Geologic Energy Management Division (CalGEM), accessed May 31, 2021, at https://www.conservation.ca.gov/calgem/Online_Data/Pages/Index.aspx.

California Department of Conservation, 2023, Oil and gas online data: Geologic Energy Management Division, accessed September 14, 2023, at https://www.conservation.ca.gov/calgem/Pages/WellFinder.aspx.

California Department of Water Resources, 2015, California's groundwater update 2013—A compilation of enhanced content for California water plan: California Department of Water Resources, accessed November 26, 2022, at https://data.cnra.ca.gov/dataset/california-water-plan-groundwater-update-2013.

California Department of Water Resources, 2020, California's groundwater (bulletin 118): California Department of Water Resources, accessed December 12, 2022, at https://water.ca.gov/Programs/Groundwater-Management/Bulletin-118.

California Department of Water Resources, 2023, SGMA data viewer: accessed April 23, 2023, at https://sgma.water.ca.gov/webgis/?appid=SGMADataViewer#gwlevels.

California Department of Water Resources, 2025, Well completion report map application: accessed January 9, 2025, at https://dwr.maps.arcgis.com/apps/webappviewer/index.html?id=181078580a214c0986e2da28f8623b37.

California Resources Corporation, 2016, Elk Hills Oilfield Phase 1 Area Tulare Formation Aquifer Exemption Application June 2, 2016, accessed 2021 May 11, 2021, at https://www.conservation.ca.gov/calgem/Pages/Aquifer-Exemptions-Status.aspx#elkhillsp1.

California State Water Resources Control Board, 2015, Model criteria for groundwater monitoring in areas of oil and gas well stimulation: California State Water Resources Control Board, 39 p., accessed September 2, 2019, at https://www.waterboards.ca.gov/water_issues/programs/groundwater/sb4/docs/model_criteria_final_070715.pdf.

California State Water Resources Control Board, 2022a, Water quality in areas of oil and gas production—Produced water ponds: California State Water Resources Control Board, accessed April 23, 2022, at https://www.waterboards.ca.gov/water_issues/programs/groundwater/sb4/oil_field_produced/produced_water_ponds/.

California State Water Resources Control Board, 2022b, Regional groundwater monitoring: California State Water Resource Control Board, accessed March 3, 2022, at https://www.waterboards.ca.gov/water_issues/programs/groundwater/sb4/regional_monitoring.

California State Water Resources Control Board, 2022c, Secondary Drinking Water Standards, accessed December 12, 2022, at https://www.waterboards.ca.gov/drinking_water/certlic/drinkingwater/documents/ddw_secondary_standards.pdf.

Carter, J.M., Moran, M.J., Zogorski, J.S., and Price, C.V., 2012, Factors associated with sources, transport, and fate of chloroform and three other trihalomethanes in untreated groundwater used for drinking water: Environmental Science and Technology, v. 46, no. 15, p. 8189–8197, accessed August 30, 2023, at https://doi.org/10.1021/es301839p.

Century Geophysical, LLC, 2024a, Three arm caliper logging tool—9074 tool specifications: Century Geophysical Corporation, accessed March 3, 2024, at https://www.century-geo.com/9074.

Century Geophysical, LLC, 2024b, Series E logging tool—9144 tool specifications: Century Geophysical Corporation, accessed March 3, 2024, at https://www.century-geo.com/9144.

Century Geophysical, LLC, 2024c, Slim hole induction logging tool—9512 tool specifications: Century Geophysical Corporation, accessed March 3, 2024, at https://www.century-geo.com/9512.

Century Geophysical, LLC, 2024d, 9320 Series full wave sonic tool specifications: Century Geophysical Corporation, accessed March 3, 2024, at https://www.century-geo.com/9320.

Crain, E.R., 2024, Crain's petrophysical handbook—Mud logging and mud gas logging: Accessible Petrophysics Ltd., accessed January 12, 2024, at https://www.spec2000.net/08-mud.htm.

Cunningham, W.L., and Schalk, C.W., comps., 2011, Groundwater technical procedures of the U.S. Geological Survey: U.S. Geological Survey Techniques and Methods book 1, chap. A1, 154 p., accessed March 12, 2015, at https://doi.org/10.3133/tm1A1.

Davis, T.A., Landon, M.K., and Bennett, G.L., 2018, Prioritization of oil and gas fields for regional groundwater monitoring based on a preliminary assessment of petroleum resource development and proximity to California's groundwater resources: U.S. Geological Survey Scientific Investigations Report 2018–5065, 115 p., accessed February 8, 2019, at https://doi.org/10.3133/sir20185065.

Davis, T.A., Gannon, R.S., Warden, J.G., Rodriguez, O., Gillespie, J.M., Ball, L.B., Qi, S.L., and Metzger, L.F., 2022, Produced water disposal at percolation and evaporation ponds in and near oil fields in the southwestern San Joaquin Valley, California (ver. 2.0, October 2024): U.S. Geological Survey data release, https://doi.org/10.5066/P999XIP9.

Dibblee, T. W., Jr, 2005a, Geologic map of the Fellows Quadrangle: Dibblee Geology Center Map #DF-56, Santa Barbara Museum of Nat. Hist., Santa Barbara, CA.

Dibblee, T. W., Jr, 2005b, Geologic map of the Elkhorn Hills Quadrangle: Dibblee Geology Center Map #DF-108, Santa Barbara Museum of Nat. Hist., Santa Barbara, CA.

Dibblee, T. W., Jr, 2005c, Geologic map of the Maricopa and Pendtland Quadrangles: Dibblee Geology Center Map #DF-94, Santa Barbara Museum of Nat. Hist., Santa Barbara, CA.

DiGiulio, D.C., Rossi, R.J., Jaeger, J.M., Shonkoff, S.B.C., and Ryan, J.N., 2021, Vulnerability of groundwater resources underlying unlined produced water ponds in the Tulare Basin of the San Joaquin Valley, California: Environmental Science and Technology, v. 55, no. 21, p. 14782–14794, accessed August 30, 2023, at https://doi.org/10.1021/acs.est.1c02056.

Dulong, F.T., and Jackson, J.C., 1997, X-ray powder diffraction: U.S. Geological Survey Information Handout, 2 p., accessed September 2, 2024, at https://doi.org/10.3133/70220360.

Everett, R.R., Brown, A.A., Gillespie, J.M., Kjos, A., and Fenton, N.C., 2020a, Multiple-well monitoring site adjacent to the North and South Belridge Oil Fields, Kern County, California: U.S. Geological Survey Open-File Report 2020–1116, 10 p., accessed November 26, 2020, at https://doi.org/10.3133/ofr20201116.

Everett, R.R., Kjos, A., Brown, A.A., Gillespie, J.M., and McMahon, P.B., 2020b, Multiple-well monitoring site adjacent to the Lost Hills Oil Field, Kern County, California: U.S. Geological Survey Open-File Report 2019–1114, 8 p., accessed February 21, 2020, at https://doi.org/10.3133/ofr20191114.

Everett, R.R., McMahon, P.B., Stephens, M.J., Gillespie, J.M., Shepherd, M.M., and Fenton, N.C., 2023a, Multiple-well monitoring site within the Poso Creek Oil Field, Kern County, California: U.S. Geological Survey Open-File Report 2023–1047, 11 p., accessed July 12, 2023, at https://doi.org/10.3133/ofr20231047.

Everett, R.R., Gillespie, J.M., Shepherd, M.M., Morita, A.Y., Bobbitt, M., Kohel, C.A., and Warden, J.G., 2023b, Multiple-well monitoring site adjacent to the Elk Hills Oil Field, Kern County, California: U.S. Geological Survey Open-File Report 2023–1073, 11 p., accessed October 26, 2023, at https://doi.org/10.3133/ofr20231073.

Faunt, C.C., ed., 2009, Groundwater availability of the Central Valley Aquifer, California: U.S. Geological Survey Professional Paper 1766, 227 p., accessed December 11, 2018, at https://doi.org/10.3133/pp1766.

Folk, R.L., 1954, The distinction between grain size and mineral composition in sedimentary rock nomenclature: The Journal of Geology, v. 62, no. 4, p. 344–359, https://doi.org/10.1086/626171.

Gannon, R.S., Kulongoski, J.T., and Marcusa, J.A., 2025a, Water chemistry data for samples collected at groundwater sites in the Midway-Sunset and Buena Vista Oil Fields study area, March 2018–April 2019, Kern County, California: U.S. Geological Survey data release, https://doi.org/10.5066/P148AZKG.

Gannon, R.S., Landon, M.K., Kulongoski, J.T., Stephens, M.J., Ball, L.B., Warden, J.G., Davis, T.A., Gillespie, J.M., and Cozzarelli, I.M., 2025b, Relations of groundwater quality to long-term surface disposal of produced water near the Midway-Sunset and Buena Vista Oil Fields, California, USA: Science of the Total Environment, v. 987, p. 179637, accessed July 25, 2025, at https://doi.org/10.1016/j.scitotenv.2025.179637.

Geomega Inc., 2008, Phase II groundwater investigation report Valley Waste Disposal Company Midway Valley-Southeast Taft Area: Boulder, CO.

Gillespie, J.M., Davis, T.A., Ball, L.B., Herrera, P.J., Wolpe, Z., Medrano, V., Bobbitt, M., and Stephens, M.J., 2019a, Geological, geochemical, and geophysical data from the Lost Hills and Belridge Oil Fields: U.S. Geological Survey data release, accessed August 21, 2019, at https://doi.org/10.5066/P90QH6CI.

Gillespie, J.M., Davis, T.A., Stephens, M.J., Ball, L.B., and Landon, M.K., 2019b, Groundwater salinity and the effects of produced water disposal in the Lost Hills-Belridge Oil Fields, Kern County, California: Environmental Geoscience, v. 26, no. 3, p. 73–96, accessed August 21, 2019, at https://doi.org/10.1306/eg.02271918009.

Gillespie, J.M., Stephens, M.J., Chang, W., and Warden, J., 2022, Mapping aquifer salinity gradients and effects of oil field produced water disposal using geophysical logs—Elk Hills, Buena Vista and Coles Levee Oil Fields, San Joaquin Valley, California: PLoS One, v. 17, no. 3, p. e0263477, accessed November 9, 2022, at https://doi.org/10.1371/journal.pone.0263477.

International Centre for Diffraction Data, 2025, Powder Diffraction File, https://www.icdd.com/.

Isotech Laboratories, Inc., 2024a, Sampling Products > IsoTube, accessed June 14, 2024, at https://isotechlabs.com/products/isotubes/.

Isotech Laboratories, Inc., 2024b, Analytical Services > View by Sample Type > Gas > Mudgas > MG-2, accessed June 14, 2024, at https://isotechlabs.com/analytical/sampletype/gas/mudgas/mg2.html.

Keller, M.A., and Isaacs, C.M., 1985, An evaluation of temperature scales for silica diagenesis in diatomaceous sequences including a new approach based on the Miocene Monterey Formation, California: Geo-Marine Letters, v. 5, no. 1, p. 31–35. [Available at https://doi.org/10.1007/BF02629794.]

Kenyon, B., Kleinberg, R., Straley, C., Gubelin, G., and Morriss, C., 1995, Nuclear magnetic resonance imaging—Technology for the 21st century: Oilfield Review, v. 7, p. 19–33.

Keys, W.S., 1990, Borehole geophysics applied to ground-water investigations: U.S. Geological Survey Techniques of Water-Resources Investigations, book 2, chap. E2, 150 p., accessed March 22, 2019, at https://doi.org/10.3133/twri02E2.

Keys, W.S., and MacCary, L.M., 1971, Application of borehole geophysics to water-resources investigations: U.S. Geological Survey Techniques of Water-Resources Investigations, book 2, chap. E1, 126 p., accessed January 29, 2009, at https://doi.org/10.3133/twri02E1.

Lindsey, B.D., Jurgens, B.C., and Belitz, K., 2019, Tritium as an indicator of modern, mixed, and premodern groundwater age: U.S. Geological Survey Scientific Investigations Report 2019–5090, 18 p., accessed at https://doi.org/10.3133/sir20195090.

McNeill, J.D., 1986, Geonics EM39 borehole conductivity meter-theory of operation: Mississauga, Ontario, Geonics Ltd., Technical Note 20, 11 p.

MDI, 2025, Materials Data JADE, Livermore California, https://materialsdata.com/prodjd.html.

Molofsky, L.J., Etiope, G., Segal, D.C., and Engle, M.A., 2025, Methane-rich gas emissions from natural geologic seeps can be chemically distinguished from anthropogenic leaks: Communications Earth & Environment, v. 6, article no. 11, accessed January 7, 2025, at https://doi.org/10.1038/s43247-024-01990-8.

Munsell Color, 1994, Munsell soil color charts: Baltimore, Md., Munsell Color, Inc.

Murata, K.J., and Norman, M.B., 1976, An index of crystallinity for quartz: American Journal of Science, v. 276, no. 9, p. 1120–1130. [Available at https://doi.org/10.2475/ajs.276.9.1120.]

National Research Council, 1947, Report of the subcommittee on sediment terminology: Transactions - American Geophysical Union, v. 28, no. 6, p. 936–938. [Available at https://doi.org/10.1029/TR028i006p00936.]

Pisciotto, K. A., 1981, Diagenetic trends in the siliceous facies of the Monterey Shale in the Santa Maria region, California. Sedimentology, 28:547-571.

Raymer, L., Hunt, E., and Gardner, J.S., 1980, An improved sonic transit time-to-porosity transform: Proceedings of Society of Petrophysicists and Well-Log Analysts, Houston, p. 1–13.

Rickett, W., and Reaves, J., 1954, Midway-Sunset District, report of oil field waste water production, quality, and disposal, summer and fall of 1953. Obtained from the Central Valley Regional Water Quality Control Board, p. 64.

Schoell, M., 1980, The hydrogen and carbon isotopic composition of methane from natural gases of various origins: Geochimica et Cosmochimica Acta, v. 44, no. 5, p. 649–661, accessed September 14, 2023, at https://doi.org/10.1016/0016-7037(80)90155-6.

Schlumberger, 1972, Log interpretation, volume I—principles: New York, Schlumberger Limited, 113 p.

Seitz, N.O., Cozzarelli, I.M., Gannon, R.S., Jaeschke, J.B., Kulongoski, J.T., Lorah, M.M., Marcusa, J.A., and McMahon, P.B., 2024, Produced water chemistry data collected from the Poso Creek, Midway-Sunset, and Buena Vista Oil Fields, 2019–2021, Kern County, California: U.S. Geological Survey data release, at https://doi.org/10.5066/P97P2NAN.

Shuter, E., and Teasdale, W.E., 1989, Application of drilling, coring, and sampling techniques to test holes and wells: U.S. Geological Survey Techniques of Water-Resources Investigations, book 2, chap. F1, 97 p., accessed July 8, 1999, at https://doi.org/10.3133/twri02F1.

SLB, 2024a, CST chronological sample taker: March 3, 2024, at https://www.slb.com/-/media/files/fe/product-sheet/cst-ps.ashx.

SLB, 2024b, Caliper: accessed March 3, 2024, at https://www.slb.com/-/media/files/fe/product-sheet/ppc-ps.ashx?la=ja-jp.

SLB, 2024c, Platform express: accessed March 3, 2024, at https://www.slb.com/-/media/files/fe/brochure/platform-express-br.ashx.

SLB, 2024d, The defining series—Measuring porosity downhole: accessed March 3, 2024, at https://www.slb.com/resource-library/oilfield-review/defining-series/defining-porosity.

SLB, 2024e, Schlumberger curve mnemonic dictionary: accessed March 3, 2024, at https://www.apps.slb.com/cmd/.

Sneed, M., 2001, Hydraulic and mechanical properties affecting ground-water flow and aquifer-system compaction, San Joaquin Valley, California: U.S. Geological Survey Open-File Report 2001–35, 26 p., accessed September 26, 2019, at https://doi.org/10.3133/ofr0135.

Swanson, R.G., 1981, Sample examination manual: Tulsa Oklahoma, American Association of Petroleum Geologists, 54 p., accessed October 24, 2019, at https://doi.org/10.1306/Mth1413.

Taylor, S.W., Sherwood Lollar, B., and Wassenaar, I., 2000, Bacteriogenic ethane in near-surface aquifers—Implications for leaking hydrocarbon well bores: Environmental Science and Technology, v. 34, no. 22, p. 4727–4732, accessed August 30, 2023, at https://doi.org/10.1021/es001066x.

U.S. Environmental Protection Agency, 2022, Secondary Drinking Water Standards: Guidance for Nuisance Chemicals, accessed December 12, 2022, at https://www.epa.gov/sdwa/secondary-drinking-water-standards-guidance-nuisance-chemicals.

U.S. Environmental Protection Agency, 2023, EPA on-line tools for site assessment calculation—Vertical gradient calculator: U.S. Environmental Protection Agency, accessed September 24, 2023, at https://www3.epa.gov/ceampubl/learn2model/part-two/onsite/vgradient.html.

U.S. Geological Survey, 2024a, California oil, gas, and groundwater (COGG) program: California Water Science Center, U.S. Geological Survey website, accessed January 10, 2024, at https://webapps.usgs.gov/cogg/.

U.S. Geological Survey, 2024b, USGS water data for the nation—National water information system: U.S. Geological Survey website, accessed November 26, 2024, at https://doi.org/10.5066/F7P55KJN.

U.S. Geological Survey, 2024c, USGS GeoLog Locator: U.S. Geological Survey website: accessed December 8, 2023, at https://doi.org/10.5066/F7X63KT0.

Weddle, J.R., 1967, Oilfield waters in southwestern San Joaquin Valley Kern County, California: Division of Oil and Gas, Summary of Operations-California Oil Fields, v. 53, no. 1.

Western Regional Climate Center, 2024, RAWS USA climate archive: Western Regional Climate Center website, accessed January 12, 2024, at https://wrcc.dri.edu/cgi-bin/rawMAIN.pl?caCCAR.

Whiticar, M.J., 1999, Carbon and hydrogen isotope systematics of bacterial formation and oxidation of methane: Chemical Geology, v. 161, no. 1–3, p. 291–314, accessed August 30, 2023, at https://doi.org/10.1016/S0009-2541(99)00092-3.

Williams, J.H., Lapham, W.W., and Barringer, T.H., 1993, Application of electromagnetic logging to contamination investigations in glacial sand-and-gravel aquifers: Ground Water

Monitoring and Remediation, v. 13, no. 3, p. 129–138. [Available at https://doi.org/10.1111/j.1745-6592.1993.tb00082.x.]

Wood, P.R., and Dale, R.H., 1964, Geology and ground-water features of the Edison-Maricopa area, Kern County, California: U.S. Geological Survey Water Supply Paper 1656, p. 108. [Available at https://doi.org/10.3133/wsp1656.]

Wyman, R.E., and Castano, J.R., 1974, Show descriptions from core, sidewall and ditch samples: Society of Petrophysicists and Well-Log Analysts, 15th Annual Logging Symposium, June 2–5, 1974, accessed October 24, 2019, at https://onepetro.org/SPWLAALS/proceedings-abstract/SPWLA-1974/All-SPWLA-1974/SPWLA-1974-W/19976.

Zaydoon, A.-H., 2025, Tishk International University, Well Logging-II, Neutron Log, accessed September, 21, 2025, at https://lecture-notes.tiu.edu.iq/wp-content/uploads/2025/02/3-Neutron-Log.pdf.

For more information concerning the research in this report, contact the

Director, California Water Science Center

U.S. Geological Survey

6000 J Street, Placer Hall

Sacramento, California 95819

https://www.usgs.gov/centers/california-water-science-center

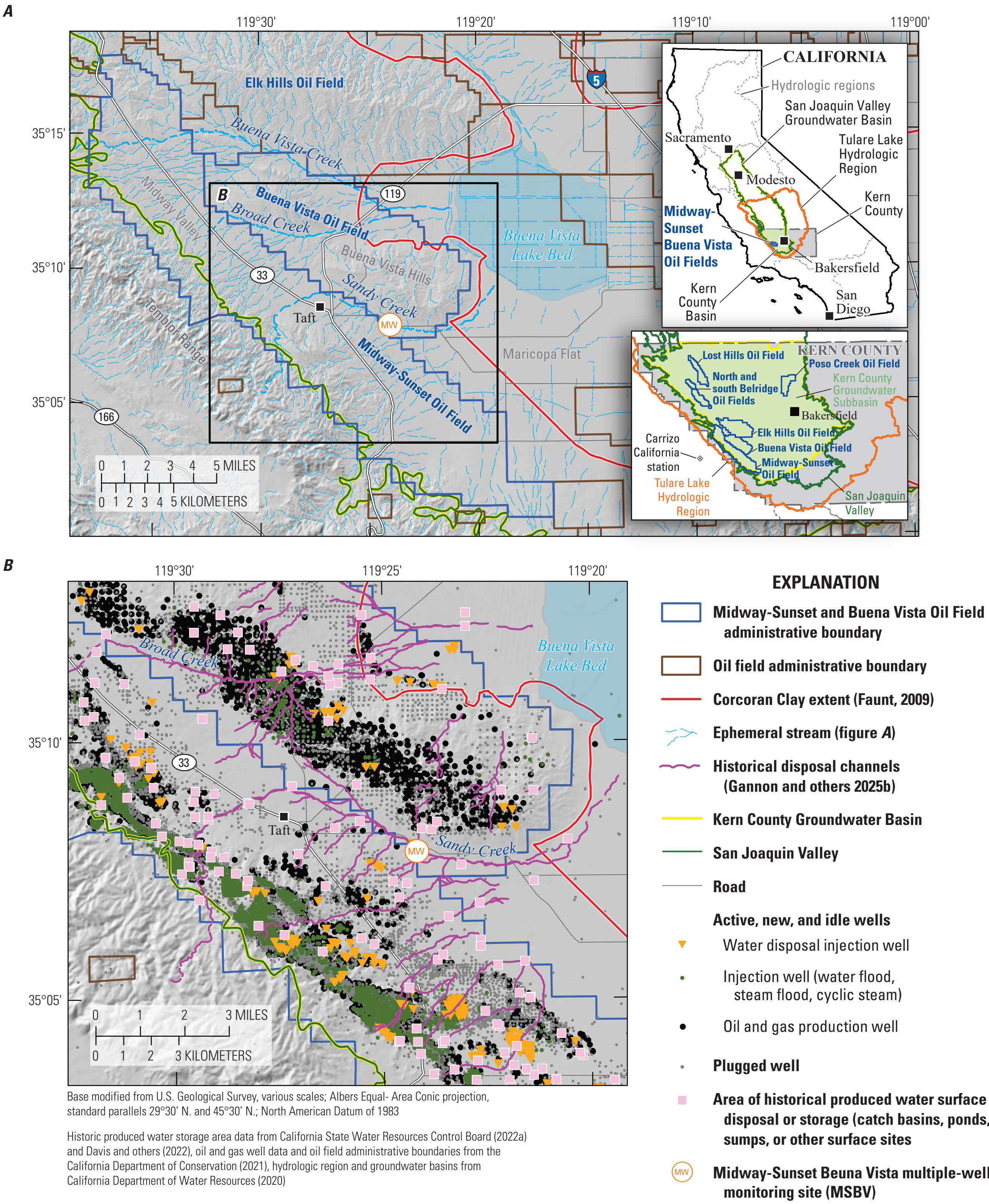

Base modified from U.S. Geological Survey, various scales; Albers Equal- Area Conic projection, standard parallels 29°30′ N. and 45°30′ N.; North American Datum of 1983

Historic produced water storage area data from California State Water Resources Control Board (2022a) and Davis and others (2022), oil and gas well data and oil field administrative boundaries from the California Department of Conservation (2021), hydrologic region and groundwater basins from California Department of Water Resources (2020)

Figure 1. (A) Location of the Midway-Sunset and Buena Vista Oil Fields. (B) Location of the Midway-Sunset Buena Vista multiple-well monitoring site (MSBV), production and injection wells related to oil and gas development, and areas of known historical produced water surface disposal or storage and disposal injection in or near the Midway-Sunset and Buena Vista Oil Fields, Kern County, California.

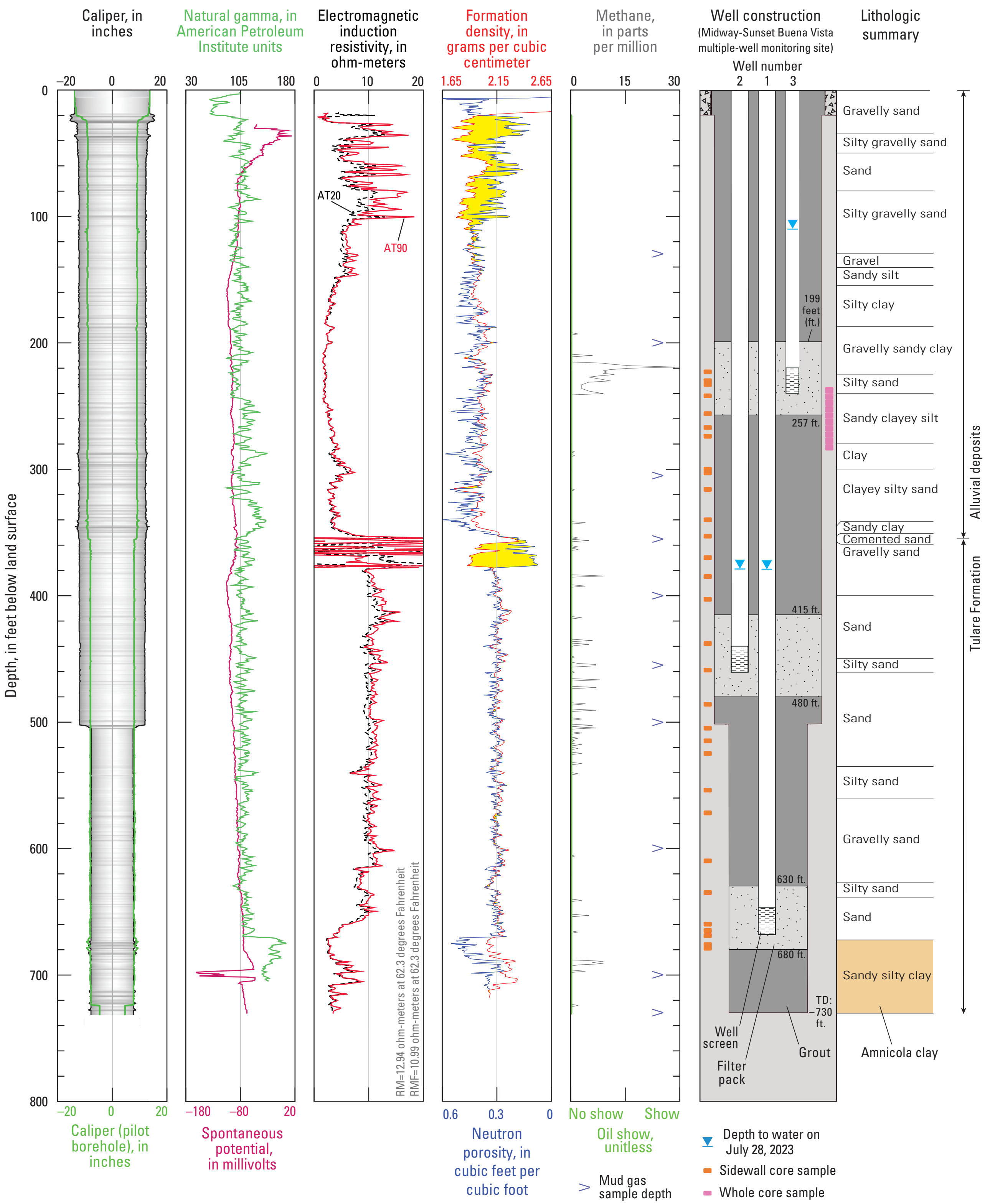

Figure 2. Well construction, summary lithology, and geophysical log data from the Midway-Sunset Buena Vista multiple-well monitoring site (MSBV), Kern County, California. Water-level data from U.S. Geological Survey (2024b), geophysical log data from U.S. Geological Survey (2024c), and U.S. Geological Survey site numbers can be found in table 6. All geophysical logs, except caliper, were measured by SLB (formerly Schlumberger). Caliper logs were measured by USGS. Methane and oil show were measured by Horizon Well Logging Inc. Yellow shading between formation density and neutron porosity indicates unsaturated sediment. (Abbreviations: AT20, array induction two foot resistivity with 20-inch depth of investigation; AT90, array induction two foot resistivity with 90-inch depth of investigation).

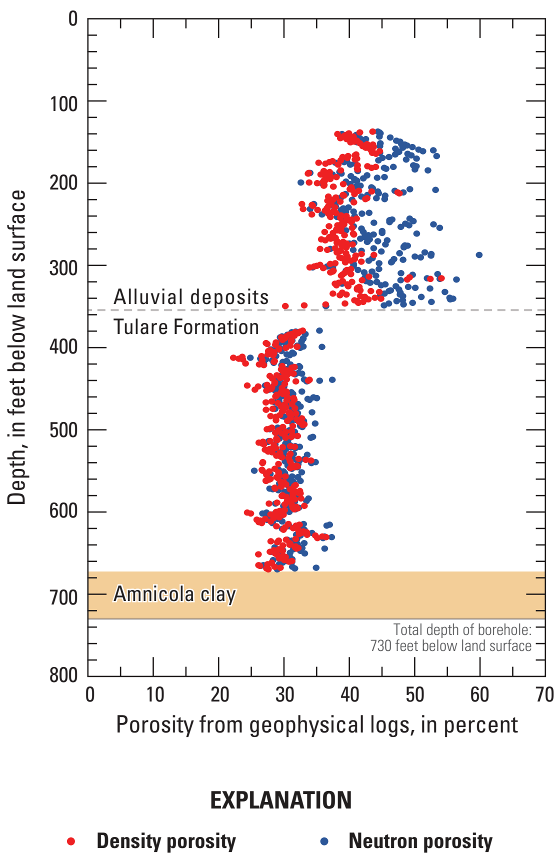

Figure 3. Comparison of density porosity (DPHZ) and neutron porosity (NPHI) logs from the Midway-Sunset Buena Vista multiple-well monitoring site (MSBV), Kern County, California. Only values for saturated intervals were used for this graph. Data summarized from U.S. Geological Survey, 2024c.

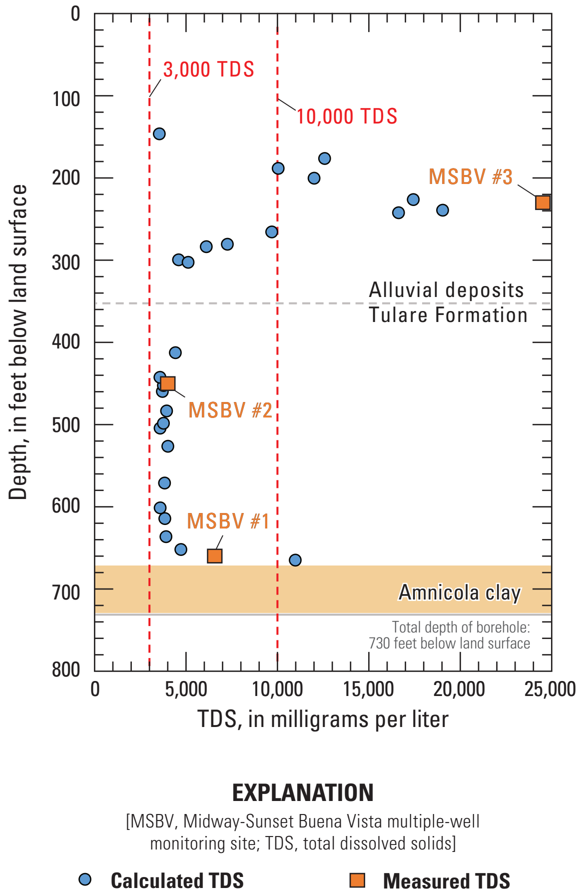

Figure 4. Measured and calculated total dissolved solids (TDS) for selected depths at the Midway-Sunset Buena Vista multiple-well monitoring site (MSBV), Kern County, California (U.S. Geological Survey, 2024b, c). Calculated TDS values determined from geophysical logs using the equation from Bateman and Konen (1977). U.S. Geological Survey site numbers and well construction information is available in table 6.

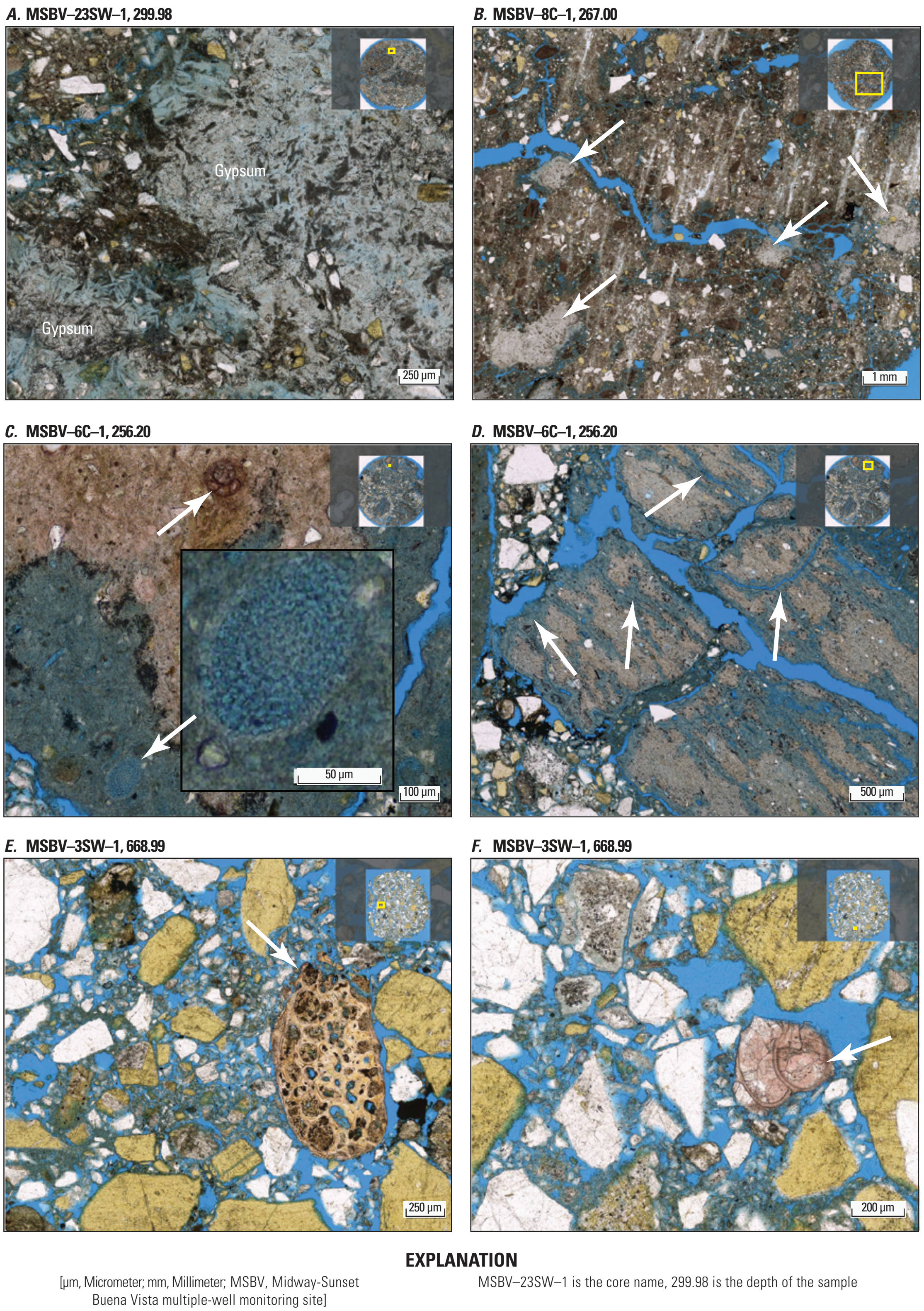

Figure 5. Thin section from cores at the Midway-Sunset Buena Vista multiple-well monitoring site (MSBV), Kern County, California. Photo identifier, core name, and sample depth are listed above each photo. Full image of thin section with area of detail marked shown in upper right corner. Scale bar in lower right corner. (A) Authigenic (light gray) gypsum crystals growing in the spaces between grains. (B) detrital clasts of gypsum shown by white arrows. (C) Diatomite clast showing dissolution around its edges (blue epoxy denotes pore space). Upper arrow points to foraminifera fossil. Lower arrow points to mostly dissolved diatomite frustule. (D) Biogenic diatomite clasts with dissolution along the edge of the clasts and along fractures within the clasts. Blue epoxy denotes pore space (E) Amnicola sp. fragment. (F) Bone fragment.

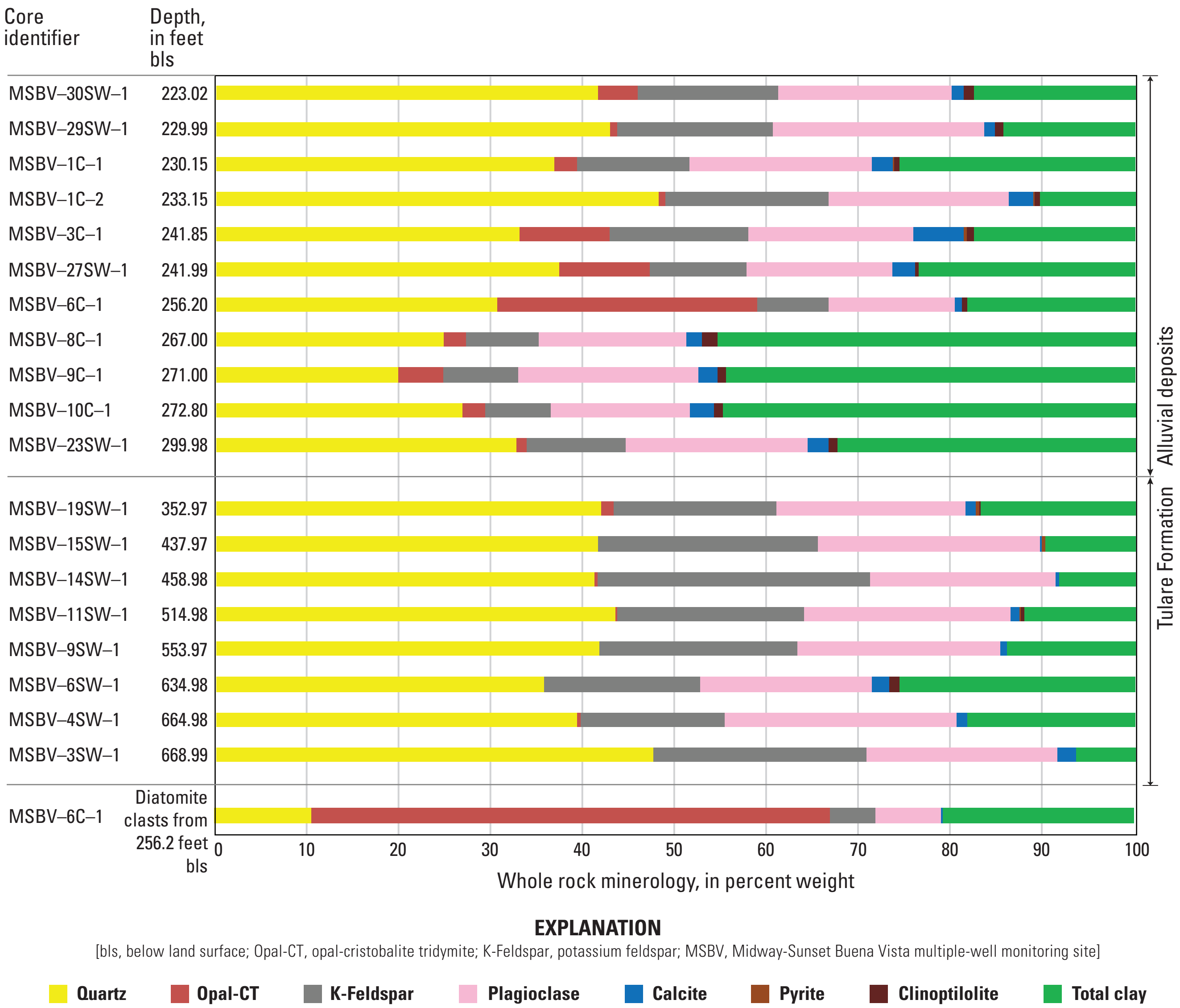

Figure 6. X-ray diffraction results of subsamples from whole- and sidewall-cores collected from the Midway-Sunset Buena Vista multiple-well monitoring site (MSBV), Kern County, California. Data summarized from (U.S. Geological Survey, 2024c.

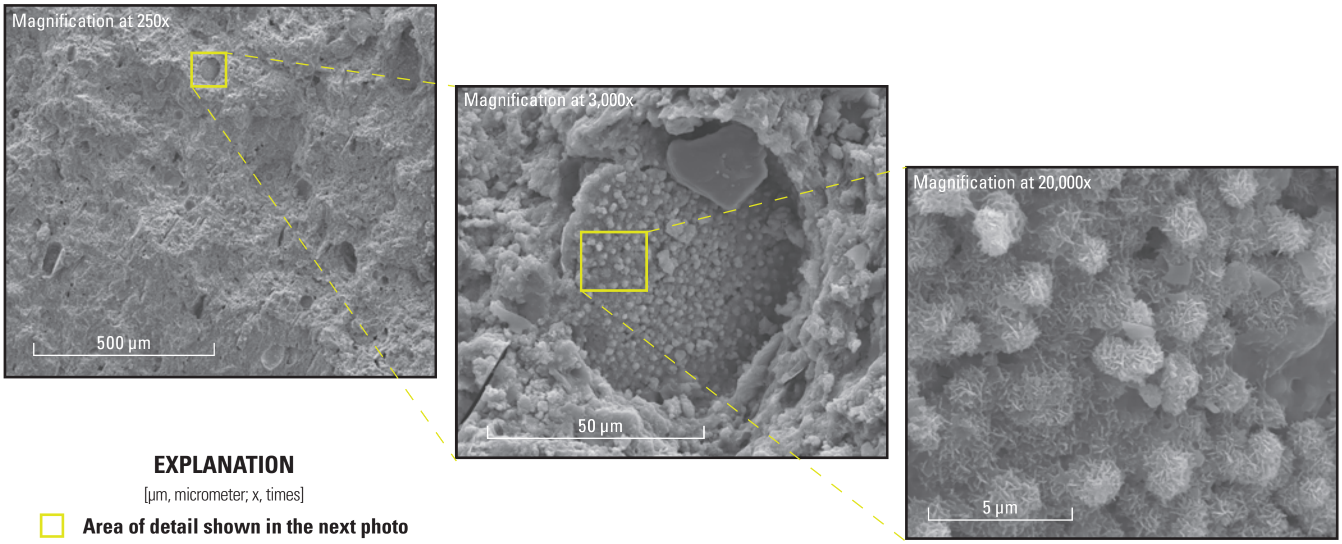

Figure 7. Scanning electron microscopy images at 250x, 3,000x, and 20,000x of a clast from 256.2 feet below land surface collected from core MSBV-6C-1 at the Midway-Sunset Buena Vista multiple-well monitoring site (MSBV), Kern County, California. Data summarized from (U.S. Geological Survey, 2024c.

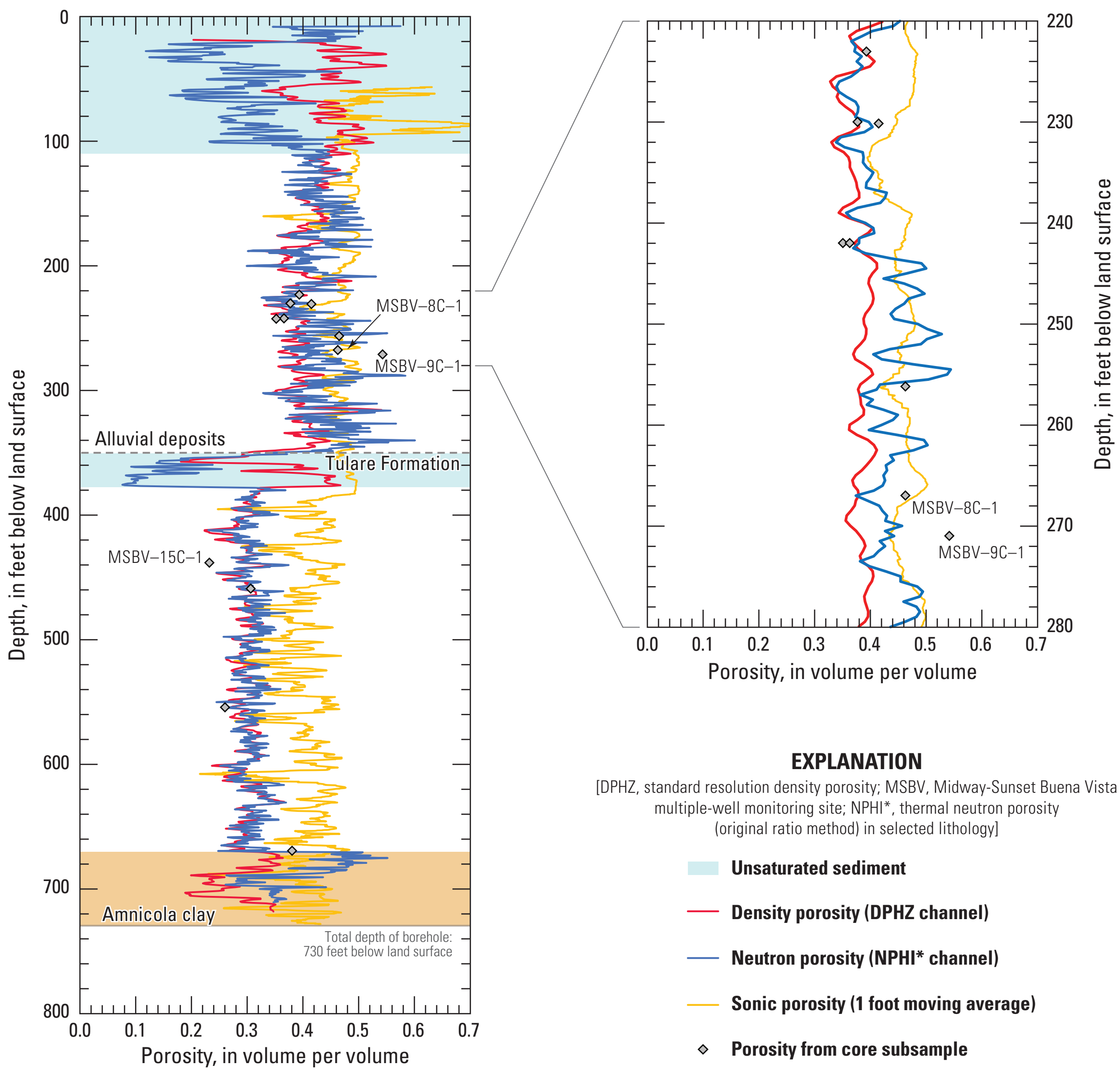

Figure 8. Porosity estimated from geophysical logs and measured from core samples collected at the Midway-Sunset Buena Vista multiple-well monitoring site (MSBV), Kern County, California. Geophysical log data from U.S. Geological Survey (2024c).

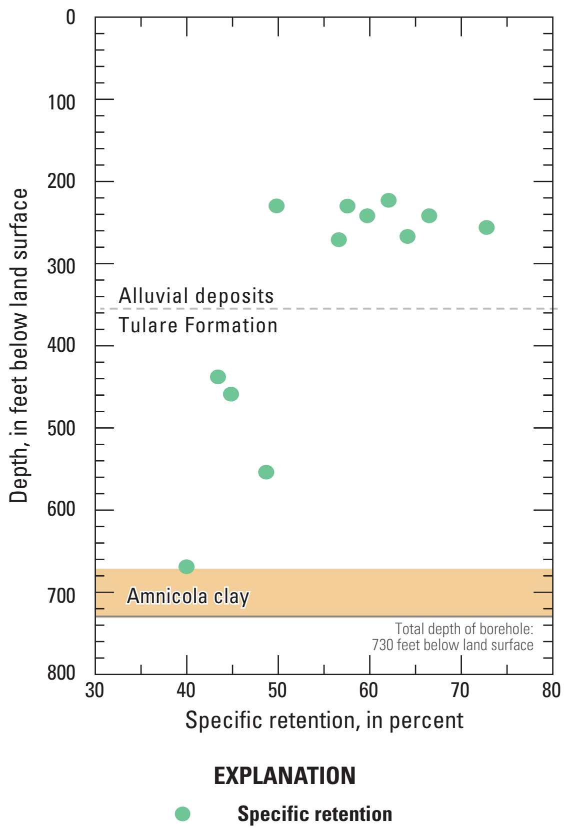

Figure 9. Specific retention of core material at selected depths from the Midway-Sunset Buena Vista multiple-well monitoring site (MSBV), Kern County, California. Data summarized from U.S. Geological Survey, 2024c.

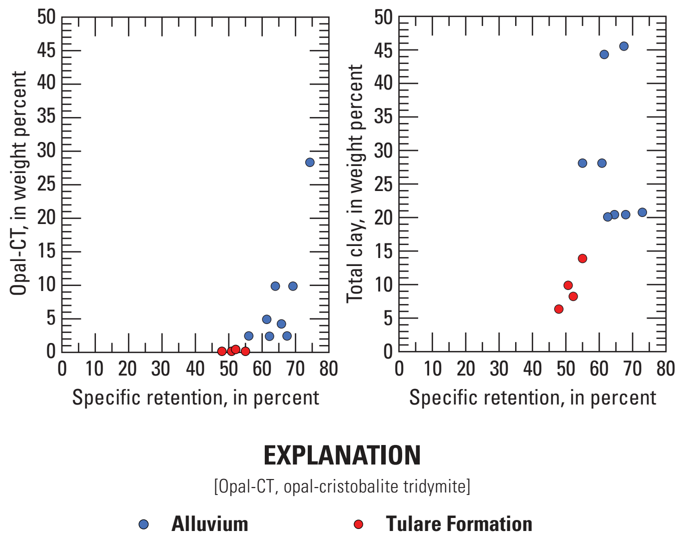

Figure 10. Specific retention in relation to the percent opal-CT and total clay in the alluvium and Tulare Formations measured in samples collected at the Midway-Sunset Buena Vista multiple-well monitoring site (MSBV), Kern County, California. Data summarized from U.S. Geological Survey, 2024c.

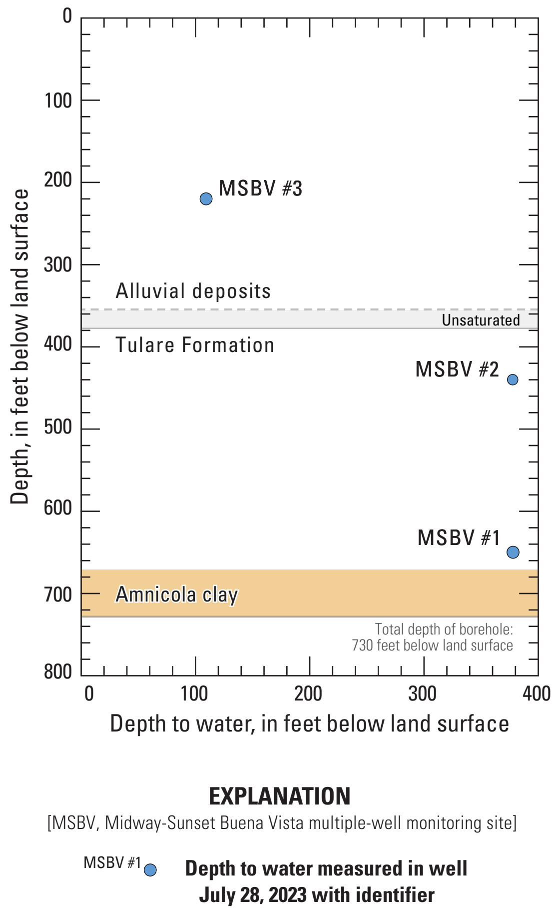

Figure 11. Water level in relation to well depth at the Midway-Sunset Buena Vista multiple-well monitoring site (MSBV), Kern County, California. Water-level data from U.S. Geological Survey (2024b). Site identification and well construction information are available in table 6.

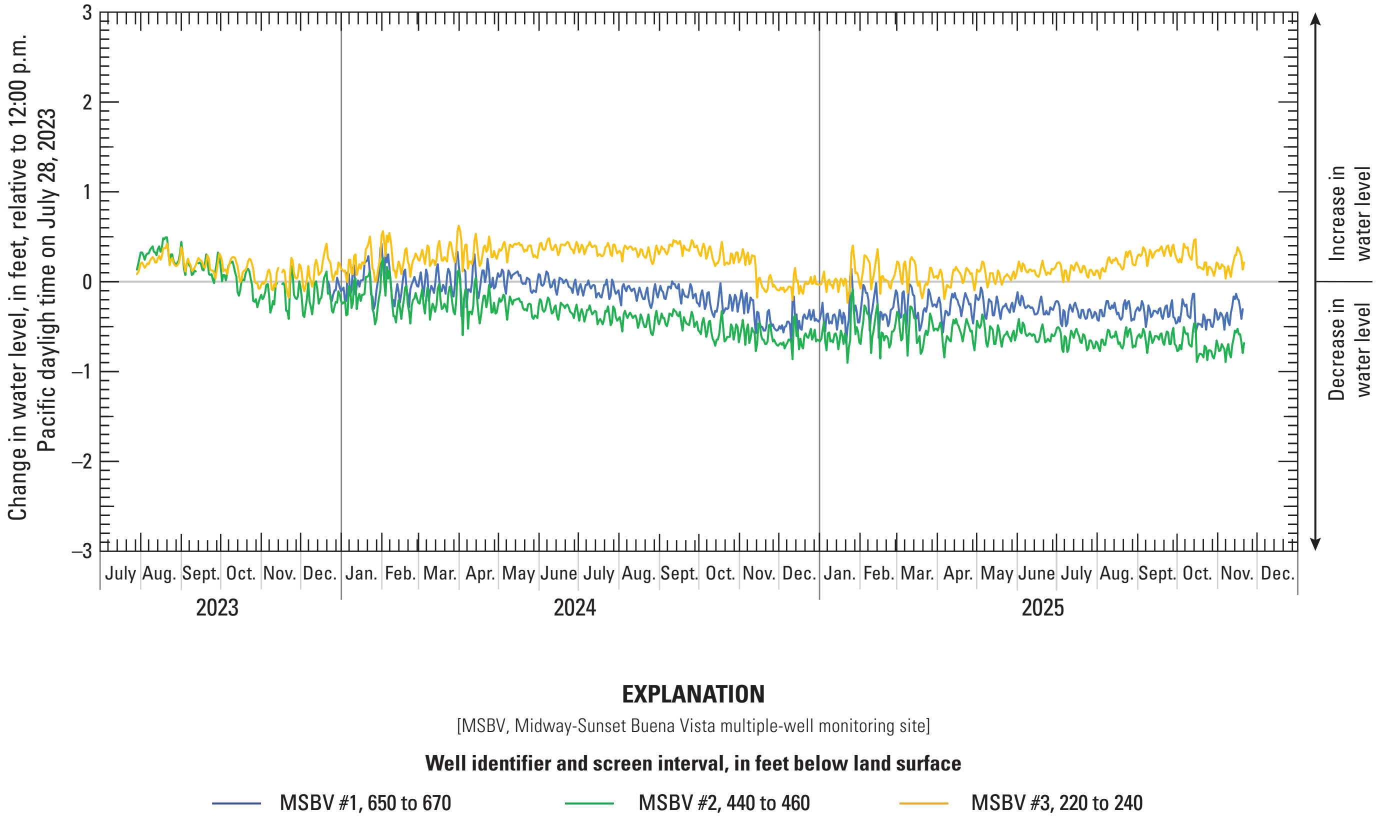

Figure 12. Changes in water levels relative to 12:00 p.m. Pacific Daylight Time on July 28, 2023, observed in wells at the Midway-Sunset Buena Vista multiple-well monitoring well site (MSBV), Kern County, California. Site identification and well construction information are available in table 6. Water-level data from U.S. Geological Survey (2024b).

Table 1. Mud-gas samples collected from the Midway-Sunset Buena Vista multiple-well monitoring site (MSBV), Kern County, California.

[ft bls, feet below land surface; H2, hydrogen; hh:mm, hour:minute; MG-2, Isotech (2024b) Level 2 mud gas analysis; mm/dd/yyyy, month/day/year; —, sample not analyzed]

Sample identification	sample depth (ft bls)	Sample date (mm/dd/yyyy)	Sample time (hh:mm)	Laboratory analysis
Alluvium				
MSBV-130	130	5/7/2023	14:15	—
MSBV-200	200	5/9/2023	15:00	MG-2 plus delta H2 of methane
MSBV-305	305	5/11/2023	10:35	—
Tulare Formation				
MSBV-355	355	5/11/2023	15:55	MG-2 plus delta H2 of methane
MSBV-400	400	5/13/2023	11:35	—
MSBV-455	455	5/14/2023	09:45	MG-2 plus delta H2 of methane
MSBV-500	500	5/14/2023	14:50	MG-2 plus delta H2 of methane
MSBV-600	600	5/16/2023	12:55	MG-2 plus delta H2 of methane
MSBV-700	700	5/17/2023	13:18	MG-2 plus delta H2 of methane
MSBV-730	730	5/17/2023	15:10	—

Table 2. Whole cores collected from the Midway-Sunset Buena Vista multiple-well monitoring site (MSBV), Kern County, California.

[bls, below land surface; ft, feet; m, medium; mm/dd/yyyy, month/day/year; vc, very coarse; vf, very fine]

Core identifier	Sample date (mm/dd/yyyy)	Cored interval (ft bls)		Recovery (ft)		Total recovery (ft)	Recovery (percentage)	Depth of recovered core (ft bls)		General lithology	
		From	To	Core	Shoe			Top	Bottom	Top of core	Bottom of core
Alluvium											
MSBV-1C-1	05/09/2023	230	235	4.1	0.3	4.4	88	230	234.1	Silty sand (vf-vc)	Silty sand (vf-vc)
MSBV-2C-1	05/09/2023	235	240	2.3	0.3	2.6	52	235	237.3	Silty sand (vf-vc)	Silty sand (vf-vc)
MSBV-3C-1	05/10/2023	240	245	3.5	0.3	3.8	75	240	243.5	Clayey sandy (vf-m) silt	Clayey silt
MSBV-4C-1	05/10/2023	245	250	2.3	0.4	2.7	54	245	247.3	Clayey silt	Clayey silt
MSBV-5C-1	05/10/2023	250	255	2.5	0.3	2.8	55	250	252.5	Clayey silt	Clayey silt
MSBV-6C-1	05/10/2023	255	260	4.0	0.4	4.3	87	255	259.0	Sandy (vf-vc) silt	Silty sand (vf-m)
MSBV-7C-1	05/10/2023	260	265	3.6	0.3	3.9	78	260	263.6	Clayey silt	Clayey silt
MSBV-8C-1	05/10/2023	265	270	3.5	0.2	3.7	75	265	268.5	Clayey silt	Clayey silt
MSBV-9C-1	05/10/2023	270	275	4.9	0.3	5.3	105	270	274.9	Sandy (vf-m) silt	Sandy (vf-m) silt
MSBV-10C-1	05/10/2023	275	280	2.4	0.3	2.8	55	275	277.4	Sandy (vf-m) silt	Sand (vf-vc)
MSBV-11C-1	05/10/2023	280	285	3.0	0.3	3.3	67	280	283.0	Clay	Clay
MSBV-12C-1	05/10/2023	285	290	3.1	0.3	3.4	68	285	288.1	Clay	Clay

Table 3. Sidewall cores collected from the Midway-Sunset Buena Vista multiple-well monitoring site (MSBV), Kern County, California.

[A, excellent; B, good; C, fair; D, poor; F, testing not possible; ft bls, below land surface; mm/dd/yyyy, month/day/year; —, no comment]

Core identifier	Sample date (mm/dd/yyyy)	Sample depth (ft bls)	Core quality index[1]	Core quality comment
Alluvium				
MSBV-30SW-1	05/18/2023	223.02	A	—
MSBV-29SW-1	05/18/2023	229.99	A	—
MSBV-28SW-1	05/18/2023	232.98	D	Not enough material
MSBV-27SW-1	05/18/2023	241.99	F	Not enough material
MSBV-26SW-1	05/18/2023	256.04	F	Not enough material
MSBV-25SW-1	05/18/2023	266.98	C	—
MSBV-24SW-1	05/18/2023	273.96	F	Not enough material
MSBV-23SW-1	05/18/2023	299.98	D	Short, needs trimmed
MSBV-22SW-1	05/18/2023	303.04	B	—
MSBV-21SW-1	05/18/2023	315.99	F	Not enough material
MSBV-20SW-1	05/18/2023	340.01	C	Short
Tulare Formation				
MSBV-19SW-1	05/18/2023	352.97	F	Not enough material
MSBV-18SW-1	05/18/2023	369.97	C	—
MSBV-17SW-1	05/18/2023	384.99	D	Fractured in middle
MSBV-16SW-1	05/18/2023	402.98	B	—
MSBV-15SW-1	05/18/2023	437.97	F	Not enough material
MSBV-14SW-1	05/18/2023	458.98	D	Not enough material
MSBV-13SW-1	05/18/2023	485.98	C	Short, needs trimmed
MSBV-12SW-1	05/18/2023	504.97	B	—
MSBV-11SW-1	05/18/2023	514.98	C	Signs of fracturing
MSBV-10SW-1	05/18/2023	524.97	F	Not enough material
MSBV-9SW-1	05/18/2023	553.97	F	Not enough material
MSBV-8SW-1	05/18/2023	571.96	D	Signs of fracturing
MSBV-7SW-1	05/18/2023	609.98	F	—
MSBV-6SW-1	05/18/2023	634.98	D	Not cylindrical
MSBV-5SW-1	05/18/2023	659.97	D	Not cylindrical
MSBV-4SW-1	05/18/2023	664.98	B	—
MSBV-3SW-1	05/18/2023	668.99	D	Not cylindrical
MSBV-2SW-1	05/18/2023	675.98	B	—
MSBV-1SW-1	05/18/2023	678.97	A	—

[1]The sidewall core sample was rated considering the quality of the specific retention, x-ray diffraction, and thin section samples that could be obtained.

Table 4. Analysis of subsamples from whole- and sidewall-cores collected from the Midway-Sunset Buena Vista multiple-well monitoring site (MSBV), Kern County, California.

[ft bls, feet below land surface; SEM, scanning electron microscope; —, sample not analyzed]

Core identifier	Sample depth (ft bls)	Laboratory analysis			
		Porosity and specific retention	X-ray diffraction	Thin section	SEM
Alluvium					
MSBV-30SW-1	223.02	yes	yes	yes	—
MSBV-29SW-1	229.99	yes	yes	yes	—
MSBV-1C-1	230.15	yes	yes	yes	—
MSBV-1C-2	233.15	—	yes	yes	—
MSBV-3C-1	241.85	yes	yes	yes	—
MSBV-27SW-1	241.99	yes	yes	yes	—
MSBV-6C-1	256.20	yes	yes	yes	yes
MSBV-8C-1	267.00	yes	yes	yes	—
MSBV-9C-1	271.00	yes	yes	yes	—
MSBV-9C-1	272.80	—	yes	yes	—
MSBV-23SW-1	299.98	—	yes	yes	—
Tulare Formation					
MSBV-19SW-1	352.97	—	yes	yes	—
MSBV-15SW-1	437.97	yes	yes	yes	—
MSBV-14SW-1	458.98	yes	yes	yes	—
MSBV-11SW-1	514.98	—	yes	yes	—
MSBV-9SW-1	553.97	yes	yes	yes	—
MSBV-6SW-1	634.98	—	yes	yes	—
MSBV-4SW-1	664.98	—	yes	yes	—
MSBV-3SW-1	668.99	—	yes	yes	—

Table 5. Thin section subsamples from whole- and sidewall-cores collected from the Midway-Sunset Buena Vista multiple-well monitoring site (MSBV), Kern County, California.

[png, portable network graphics]

Core identifier	Sample depth (ft bls)	Sample orientation	Image file name
		Alluvium	
MSBV-30SW-1	223.02	horizontal	ThinSection_223.02.png
MSBV-29SW-1	229.99	horizontal	ThinSection_229.99.png
MSBV-1C-1	230.15	horizontal	ThinSection_230.15.png
MSBV-1C-2	233.15	horizontal	ThinSection_233.15.png
MSBV-3C-1	241.85	horizontal	ThinSection_241.85.png
MSBV-27SW-1	241.99	horizontal	ThinSection_241.99.png
MSBV-6C-1	256.20	horizontal	ThinSection_256.20.png
MSBV-8C-1	267.00	horizontal	ThinSection_267.00.png
MSBV-9C-1	271.00	horizontal	ThinSection_271.00.png
MSBV-9C-1	272.80	horizontal	ThinSection_272.80.png
MSBV-23SW-1	299.98	horizontal	ThinSection_299.98.png
		Tulare Formation	
MSBV-19SW-1	352.97	horizontal	ThinSection_352.97.png
MSBV-15SW-1	437.97	horizontal	ThinSection_437.97.png
MSBV-14SW-1	458.98	horizontal	ThinSection_458.98.png
MSBV-11SW-1	514.98	horizontal	ThinSection_514.98.png
MSBV-9SW-1	553.97	horizontal	ThinSection_553.97.png
MSBV-6SW-1	634.98	horizontal	ThinSection_634.98.png
MSBV-4SW-1	664.98	horizontal	ThinSection_664.98.png
MSBV-3SW-1	668.99	horizontal	ThinSection_668.99.png

Table 6. Identification and construction information from the Midway-Sunset Buena Vista multiple-well monitoring site (MSBV), Kern County, California.

[See figure 1 for well locations. Wells ordered from shallowest to deepest. The 15-digit U.S. Geological Survey (USGS) site number is used to uniquely identify the well. The common name is used throughout the report for quick reference. Land-surface datum (LSD) is a datum plane that is approximately at land surface at each well. The elevation of the LSD is described in feet above the North American Vertical Datum of 1988 (NAVD 88). **Abbreviations**: NWIS, ft bls, feet below land surface; na, not applicable; NWIS, National Water Information System]

Common well name	USGS Site identification number (hyperlinked to NWIS)	USGS Site name	Borehole Depth (ft bls)	Elevation of LSD (ft above NAVD 88)	Well diameter (inside, inches)	Depth to bottom of well (ft bls)	Depth to top of perforations (ft bls)	Depth to bottom of perforations (ft bls)
MSBV #3	350751119241103	032S024E21F001M	730	619.83	1.94	240	220	240
MSBV #2	350751119241102	032S024E21F002M	730	619.83	1.94	460	440	460
MSBV #1	350751119241101	032S024E21F003M	730	619.83	2.323	670	650	670
MSBV Borehole	350751119241104	032S024E21F MSBV Test Hole	730	619.83	na	na	na	na

Table 7. Well-development and water-level data from the Midway-Sunset Buena Vista multiple-well monitoring site (MSBV), Kern County, California.

[Wells are ordered from shallowest to deepest. Pre- and post-development depth-to-water and turbidity measurements may not represent true static water levels and are not available on the U.S. Geological Survey (USGS) National Water Information System (NWIS; U.S. Geological Survey, 2024b). Post-development turbidity measurements were collected for reference and are not available in NWIS. Estimated total discharge was calculated by adding daily estimated discharge during the entire development period. **Abbreviations**: ft bls, feet below land surface; gal, gallon; gal/min, gallons per minute; NTU, nephelometric turbidity units; v/v, volume per volume]

Common well name[1]	Pre-development depth to water (ft bls) (05/27/2023)	Post-development depth to water (ft bls) (06/09/2023)	Depth to water[2] (ft bls) (07/28/2023)	Final flow rate (gal/min)	Hours of development	Estimated total discharge (gal)	Purge per casing volume (v/v)	Purge per filter pack volume (v/v)	Post-development turbidity (NTU)
MSBV #3	108.96	109.31	109.31	6	32	9,570	476	36	1.9
MSBV #2	377.33	377.65	377.52	1.25	70	4,300	339	16	10.0
MSBV #1	377.86	378.09	377.87	10	8	4,800	74	44	2.0

[1]The USGS site numbers associated with these common names are shown in table 6.

[2]The vertical component of the water-level gradients at the site were calculated (U.S. Environmental Protection Agency, 2023) from multiple discrete water-level measurements collected on July 28, 2023 (fig. 2).

Table 8. Analysis of mud-gas samples collected from the Midway-Sunset Buena Vista multiple-well monitoring site (MSBV), Kern County, California.

[The five-digit U.S. Geological Survey (USGS) parameter code below the constituent name is used to uniquely identify a specific constituent or property. **Abbreviations:** abs, absolute; Btu, British thermal unit; calc, calculated; deg F, degrees Farenheight; ft bls, feet below land surface; ft^3, cubic foot; psi, pounds per square inch; <, less than; %, percent]

USGS Site identification number	Sample depth (feet below land surface)	Methane (C1) mole ratio, air, recovery (mole %) (54569)	Ethane (C2) mole ratio, air, recovery (mole %) (54570)	Ethene mole ratio, air, recovery (mole %) (54571)	Propane (C3) mole ratio, air, recovery (mole %) (54572)	Propene mole ratio, air, recovery (mole %) (54573)	n-Butane (C4) mole ratio, air, recovery (mole %) (54575)	n-Pentane (C5) mole ratio, air, recovery (mole %) (54577)	C6 and higher-molecular-weight hydrocarbons mole ratio, air, recovery (mole %) (54578)	2-Methylbutane mole ratio, air, recovery (mole %) (54576)	2-Methylpropane mole ratio, air, recovery (mole %) (54574)	Carbon dioxide mole ratio, air, recovery (mole %) (54566)	Carbon monoxide mole ratio, air, recovery (mole %) (54568)	Dinitrogen mole ratio, air, recovery (mole %) (54567)	Gross heating value of hydrocarbons, dry, calc, 60 deg F, 14.73 psi abs (Btu/ft3) (85588)	Hydrogen mole ratio, air, recovery (mole %) (54563)	Specific gravity (unitless) (72013)
Alluvium																	
350751119241104	200	< 0.0002	< 0.0001	< 0.0001	< 0.0001	< 0.0001	< 0.0001	< 0.0001	< 0.0001	< 0.0001	< 0.0001	0.048	< 0.01	78.61	0	<0.01	0.997
Tulare Formation																	
350751119241104	355	< 0.0002	< 0.0001	< 0.0001	< 0.0001	< 0.0001	< 0.0001	< 0.0001	< 0.0001	< 0.0001	< 0.0001	0.055	< 0.01	78.66	0	<0.01	0.997
350751119241104	455	< 0.0002	< 0.0001	< 0.0001	< 0.0001	< 0.0001	< 0.0001	< 0.0001	< 0.0001	< 0.0001	< 0.0001	0.13	< 0.01	79.07	0	<0.01	0.997
350751119241104	500	< 0.0002	< 0.0001	< 0.0001	< 0.0001	< 0.0001	< 0.0001	< 0.0001	< 0.0001	< 0.0001	< 0.0001	0.092	< 0.01	78.78	0	<0.01	0.997
350751119241104	600	< 0.0002	< 0.0001	< 0.0001	< 0.0001	< 0.0001	< 0.0001	< 0.0001	< 0.0001	< 0.0001	< 0.0001	0.07	< 0.01	78.85	0	<0.01	0.997
350751119241104	700	< 0.0002	< 0.0001	< 0.0001	< 0.0001	< 0.0001	< 0.0001	< 0.0001	< 0.0001	< 0.0001	< 0.0001	0.085	< 0.01	78.82	0	<0.01	0.997

Table 9. Estimates of total dissolved solids in groundwater at selected depths at the Midway-Sunset Buena Vista multiple-well monitoring site (MSBV), Kern County, California (U.S. Geological Survey, 2024c).

[The common name MSBV is used throughout the report for quick reference. **Abbreviations:** AT90, Array Induction Two Foot Resistivity A90; DPHZ, Standard Resolution Density Porosity; ft bls, feet below land surface; ft3/ft3, cubic feet per cubic feet; mg/L, milligrams per liter; NPHI, Thermal Neutron Porosity (original Ratio Method) in selected lithology; OHMM, ohm meter; Rw, resistivity of the formation water; °F, degrees Fahrenheit]

Common site name	Depth (ft bls)	Tortuosity factor [a] (unitless)	Cementation factor [m] (unitless)	Neutron porosity from NPHI[1] (ft^3/ft^3)	Density porosity from DPHZ[1] (ft^3/ft^3)	Average porosity[2] (ft^3/ft^3)	Sonic porosity[3] (ft^3/ft^3)	Deep resistivity from AT90 (OHMM)	Rw (OHMM)	Surface temperature (°F)	Bottom hole temperature4 (°F)[4]	Zone temperature (°F)	Rw at 75°F (OHMM)	Estimated total dissolved solids (mg/L)[5]
							Alluvium							
MSBV	146	1.0	1.8	0.42	0.39	0.40	0.50	8.1	1.6	65	94.2	70.8	1.5	3,540
MSBV	176	1.0	1.8	0.38	0.35	0.36	0.50	2.9	0.5	65	94.2	72.0	0.5	11,390
MSBV	188	1.0	1.8	0.34	0.34	0.34	0.47	3.8	0.5	65	94.2	72.5	0.5	11,390
MSBV	200	1.0	1.8	0.33	0.34	0.34	0.47	3.4	0.5	65	94.2	72.9	0.5	11,390
MSBV	226	1.0	1.8	0.35	0.33	0.34	0.52	2.4	0.3	65	94.2	74.0	0.3	19,790
MSBV	239	1.0	1.8	0.36	0.34	0.35	0.49	2.0	0.3	65	94.2	74.5	0.3	19,790
MSBV	242	1.0	1.8	0.38	0.37	0.37	0.47	2.1	0.4	65	94.2	74.6	0.4	14,480
MSBV	266	1.0	1.8	0.42	0.37	0.39	0.51	3.2	0.6	65	94.2	75.6	0.6	9,370
MSBV	281	1.0	1.8	0.37	0.36	0.36	0.47	4.4	0.7	65	94.2	76.1	0.7	7,950
MSBV	284	1.0	1.8	0.45	0.38	0.40	0.51	4.5	0.9	65	94.2	76.3	0.9	6,080
MSBV	300	1.0	1.8	0.38	0.36	0.37	0.48	6.8	1.1	65	94.2	76.9	1.1	4,920
MSBV	303	1.0	1.8	0.34	0.34	0.34	0.43	7.1	1.0	65	94.2	77.0	1.0	5,440
							Tulare Formation							
MSBV	413	1.0	1.8	0.25	0.22	0.23	0.46	15.7	1.1	65	94.2	81.4	1.2	4,480
MSBV	443	1.0	1.8	0.29	0.29	0.29	0.49	12.2	1.3	65	94.2	82.6	1.4	3,810
MSBV	453	1.0	1.8	0.29	0.26	0.27	0.46	13.5	1.3	65	94.2	83.0	1.4	3,810
MSBV	460	1.0	1.8	0.30	0.29	0.29	0.47	11.8	1.3	65	94.2	83.2	1.4	3,810
MSBV	484	1.0	1.8	0.30	0.28	0.29	0.34	11.3	1.2	65	94.2	84.2	1.3	4,120
MSBV	499	1.0	1.8	0.30	0.28	0.29	0.34	12.5	1.3	65	94.2	84.8	1.5	3,540
MSBV	505	1.0	1.8	0.29	0.30	0.30	0.31	11.5	1.3	65	94.2	85.0	1.5	3,540
MSBV	527	1.0	1.8	0.29	0.28	0.28	0.37	11.4	1.2	65	94.2	85.9	1.4	3,810
MSBV	571	1.0	1.8	0.29	0.29	0.29	0.41	11.1	1.2	65	94.2	87.7	1.4	3,810
MSBV	601	1.0	1.8	0.27	0.25	0.25	0.35	14.4	1.2	65	94.2	88.8	1.4	3,810
MSBV	614	1.0	1.8	0.28	0.27	0.27	0.46	11.9	1.1	65	94.2	89.4	1.3	4,120
MSBV	636	1.0	1.8	0.31	0.28	0.29	0.40	10.9	1.2	65	94.2	90.2	1.4	3,810
MSBV	652	1.0	1.8	0.30	0.26	0.27	0.46	10.0	0.9	65	94.2	90.9	1.1	4,920
MSBV	665	1.0	1.8	0.27	0.26	0.26	0.46	4.7	0.4	65	94.2	91.4	0.5	11,390

[1] NPHI and DPHZ from USGS_MSBV_R1B_AIT-TLD-HGNS_Main_Customer_18-May-2023-GenericV12.las (U.S Geological Survey, 2024c)

[2] Calculated using a weighted average where DPHZ is weighed twice as much as NPHI.

[3] Sonic porosity from MSBV_05-19-23_09-16_9320C2_.10_-0.80_733.20_PROC.LAS (U.S. Geological Survey, 2024c)

[4] Bottom hole temperature from USGS_MSBV_R1B_AIT-TLD-HGNS_TCOM_18-May-2023.pdf (U.S. Geological Survey, 2024c)

[5] Calculations made following methods defined by Bateman and Konen (1977).

Table 10. X-ray diffraction results of subsamples from whole- and sidewall-cores collected from the Midway-Sunset Buena Vista multiple-well monitoring site (MSBV), Kern County, California.

[Opal-CT represents the diatomite content in the cores. **Abbreviations:** A, amorphous; CT, cristobalite-tridymite; ft bls, feet below land surface; K, potassium; %, percent]

Core identifier	Sample depth (ft bls)	Whole rock mineralogy (weight %)									D-spacing {101} Opal-CT[1]	Quartz crystallinity index[2]	% Gypsum removed
		Quartz	Opal-A	Opal-CT	K-Feldspar	Plagioclase	Calcite	Pyrite	Clinoptilolite	Total clay			
Alluvium													
MSBV-30SW-1	223.02	41.6	0	4.3	15.4	18.9	1.2	0	1.1	17.6	4.1	8.5	0.9
MSBV-29SW-1	229.99	43.0	0	0.7	17.0	23.0	1.2	0	0.8	14.3	4.1	7.9	0.1
MSBV-1C-1	230.15	37.0	0	2.4	12.3	19.8	2.2	0.2	0.6	25.5	4.1	8.5	1.6
MSBV-1C-2	233.15	48.2	0	0.8	17.7	19.7	2.5	0.2	0.7	10.1	4.1	8.9	1.4
MSBV-3C-1	241.85	33.2	0	9.8	15.1	17.9	5.5	0.3	0.7	17.5	4.1	7.6	13.9
MSBV-27SW-1	241.99	37.5	0	9.9	10.5	15.8	2.5	0	0.4	23.5	4.1	7.1	0
MSBV-6C-1	256.2	30.7	0	28.3	7.7	13.8	0.7	0	0.7	18.0	4.1	7.1	0.9
MSBV-8C-1	267.0	24.8	0	2.5	7.9	16.1	1.6	0	1.8	45.4	4.1	6.4	1.1
MSBV-9C-1	271.0	19.9	0	4.9	8.1	19.6	2.1	0	1.0	44.3	4.1	4.6	1.8
MSBV-9C-1	272.8	26.9	0	2.5	7.1	15.2	2.5	0	1.0	44.9	4.1	7.3	0.6
MSBV-23SW-1	299.98	32.8	0	1.2	10.6	19.8	2.4	0	0.9	32.2	0	7.0	7.8
Average alluvuim		34.1	0	6.1	11.8	18.1	2.2	0.1	0.9	26.7	3.7	7.4	2.7
Tulare Formation													
MSBV-19SW-1	352.97	42.1	0	1.3	17.7	20.6	1.1	0.3	0.3	16.6	0	8.2	0
MSBV-15SW-1	437.97	41.6	0	0	24.1	24.1	0.2	0.3	0	9.8	0	9.2	0
MSBV-14SW-1	458.98	41.3	0	0.3	29.7	20.2	0.3	0	0	8.2	0	6.7	0
MSBV-11SW-1	514.98	43.6	0	0.2	20.3	22.5	0.8	0.3	0.4	11.9	0	8.3	0
MSBV-9SW-1	553.97	41.9	0	0	21.4	22.1	0.7	0	0	14.0	0	8.5	0
MSBV-6SW-1	634.98	35.9	0	0	16.9	18.7	1.9	0	1.1	25.5	4.1	10.7	0
MSBV-4SW-1	664.98	39.4	0	0.3	15.8	25.2	1.2	0	0	18.1	4.1	8.5	0
MSBV-3SW-1	668.99	47.7	0	0	23.1	20.9	2.0	0	0	6.3	0	8.2	0
Average Tulare Formation		40.0	0	0.9	19.1	21.2	1.3	0.1	0.4	16.9	1.2	8.3	1.1
MSBV-6C-1	diatomite clasts from 256.2 ft bls	10.5	0	56.5	4.9	7.3	0.2	0	0	20.7	4.1	8.4	0.2

[1]D-spacing of opal-CT in angstroms (Å)

[2]Quartz crystallinity index. Based on Murata and Norman (1976)

Table 11. Density, porosity, and specific retention results of subsamples from whole- and sidewall-cores collected from the Midway-Sunset Buena Vista multiple-well monitoring site (MSBV), Kern County, California.

[ft bls, below land surface; g/cm^3, grams per cubic centimeter; Vb, bulk volume; % percent]

Core identifier	Sample depth (ft bls)	Sample orientation	Density		Porosity		
			Bulk (g/cm^3)	Grain (g/cm^3)	Total[1] (%Vb)	Effective[2] (%Vb)	Specific retention (%)
MSBV-30SW-1	223.02	horizontal	1.58	2.59	39.3	14.9	65.7
MSBV-29SW-1	229.99	horizontal	1.64	2.64	37.7	18.1	55.9
MSBV-1C-1	230.15	horizontal	1.55	2.65	41.5	16.2	62.1
MSBV-3C-1	241.85	horizontal	1.69	2.63	35.5	11.4	69.2
MSBV-27SW-1	241.99	horizontal	1.71	2.69	36.3	14.3	63.8
MSBV-6C-1	256.20	horizontal	1.31	2.44	46.3	14.0	74.2
MSBV-8C-1	267.00	horizontal	1.41	2.61	46.1	18.2	67.3
MSBV-9C-1	271.00	horizontal	1.20	2.62	54.2	17.0	61.3
MSBV-15SW-1	437.97	horizontal	2.02	2.63	23.2	15.4	50.8
MSBV-14SW-1	458.98	horizontal	1.82	2.62	30.6	16.0	51.9
MSBV-9SW-1	553.97	horizontal	1.94	2.62	26.0	14.2	55.0
MSBV-3SW-1	668.99	horizontal	1.62	2.61	38.0	18.0	48.0

[1]Total Porosity = no pore fluids in place; all interconnected pore channels

[2]Effective Porosity = drainage porosity

Table 12. Water-quality indicators (field parameters), total dissolved solids, and selected results in samples collected from the Midway-Sunset Buena Vista multiple-well monitoring site (MSBV), Kern County, California (U.S. Geological Survey, 2024b).

[Wells are ordered from shallowest to deepest. The five-digit U.S. Geological Survey (USGS) parameter code below the constituent name is used to uniquely identify a specific constituent or property. Threshold type: MCL-CA, California State Water Resources Control Board maximum contaminant level; SMCL-CA, California State Water Resources Control Board secondary maximum contaminant level; SMCL-US, U.S. Environmental Protection Agency secondary maximum contaminant level. **Abbreviations:** $CaCO_3$, calcium carbonate; mg/L, milligrams per liter; mm/dd/yyyy, month/day/year; na, not analyzed; pCi/L, picocuries per liter; R, result rejected; µg/L, microgram per liter; µS/cm, microsiemens per centimeter; %, percent; *, value above or below threshold level; <, less than; °C, degrees Celsius]

Common well name[1]	Depth to top and bottom of perforations (ft bls)	Sample date	Dissolved oxygen, field (mg/L) (00300)	pH, field (standard units) (00400)	Water temperature, field (°C) (00010)	Specific conductance, field (µS/cm at 25°C) (00095)	Alkalinity, field (mg/L as $CaCO_3$) (39086)	Total dissolved solids (mg/L) (70300)	Benzene (µg/L) (34030)	Toluene (µg/L) (34010)	Ethylbenzene (µg/L) (34371)	m-Xylene + p-xylene (µg/L) (85795)	o-Xylene (µg/L) (77135)	Trichloromethane (µg/L) (32106)
Threshold type	na	na	na	SMCL-US	na	SMCL-CA	na	SMCL-CA	MCL-CA	MCL-CA	MCL-CA	MCL-CA	MCL-CA	na
Threshold level	na	na	na	6.5–8.5	na	900 (1,600)[2]	na	500 (1,000)[2]	1	150	300	1,750	1,750	na
Alluvium														
MSBV #3	220 - 240	11/15/2023	0.095	6.4*	25.4	35,000*	217	24,600*	145*	0.29	0.075	1.42	4.90	0.1431
MSBV #3	220 - 240	11/12/2024	0.0660	6.3*	24.0	35,400*	222	25,200*	na	na	na	na	na	na
Tulare Formation														
MSBV #2	440 - 460	11/14/2023	R	7.7	26.3	4,720*	129	4,010*	<0.026	<0.20	<0.036	<0.08	<0.032	<0.03
MSBV #2	440 - 460	11/13/2024	0.330	7.2	25.1	5,210*	108	4,080*	na	na	na	na	na	na
MSBV #1	650 - 670	11/15/2023	0.105	7.1	27.4	9,130*	114	6,580*	39.1*	<0.20	<0.036	0.12	0.942	<0.03
MSBV #1	650 - 670	11/12/2024	<1.0	7.1	26.5	9,000*	118	6,410*	na	na	na	na	na	na

Common well name[1]	Depth to top and bottom of perforations (ft bls)	Sample date	Methane (C1) mole ratio (mole %) (68823)	Ethane (C2) mole ratio (mole %) (68824)	Propane (C3) mole ratio (mole %) (68826)	Alkane ratio (ratio) (calculated as C1/(C2+C3))	Chloride (mg/L) (00940)	Boron (µg/L) (01020)	delta C-13/C-12 of methane (per mil) (65241)	delta H-2/H-1 of methane (per mil) (65245)	delta H-2/H-1 (per mil) (82082)	delta O-18/O-16 (per mil) (82085)	Tritium (pCi/L) (07000)	Carbon-14 (% modern) (49933)
Threshold type	na	na	na	na	na	na	SMCL-CA	na	na	na	na	na	SMCL-CA	na
Threshold level	na	na	na	na	na	na	[2]250 (500)	na	na	na	na	na	20,000	na
Alluvium														
MSBV #3	220 - 240	11/15/2023	2.64	0.0416	0.0453	30.4	12,900*	32,500	-38.8	-305	-39	-3.1	0.40	6.9
MSBV #3	220 - 240	11/12/2024	na	na	na	na	13,500*	28,600	na	na	-40	-3.1	na	na
Tulare Formation														
MSBV #2	440 - 460	11/14/2023	0.0042	<0.0001	<0.0001	na	391	4,480	na	na	-76	-9.9	-0.10	8.9
MSBV #2	440 - 460	11/13/2024	na	na	na	na	565*	4,510	na	na	-77	-9.9	na	na
MSBV #1	650 - 670	11/15/2023	0.0260	0.0439	0.0014	0.6	1,860*	16,200	na	na	-70	-8.1	-0.22	4.6
MSBV #1	650 - 670	11/12/2024	na	na	na	na	na	na	na	na	na	na	na	na

[1]The USGS site numbers associated with these common names are shown in table 6.

[2]This SMCL-CA has recommended lower and upper threshold values. The upper value is shown in parentheses.

SMCL-US from U.S. Environmental Protection Agency (2022). SMCL-CA from California State Water Resources Control Board (2022c).

Appendix 1. Dual Energy CT Scans of Cores

Dual Energy Computerized Tomography (DECT) rock types

[g/cc, grams per cubic centimeter; km/s, kilometers per second; Mpsi, mega pounds per square inch; PEF, photoelectric factor; PHI, porosity; PR, dynamic Poisson's ratio; UCS, unconfined compressive strength; Vp, compression wave sonic velocity; Vs, shear wave sonic velocity; YM, dynamic Young's modulus; Zeff, effective nuclear charge]

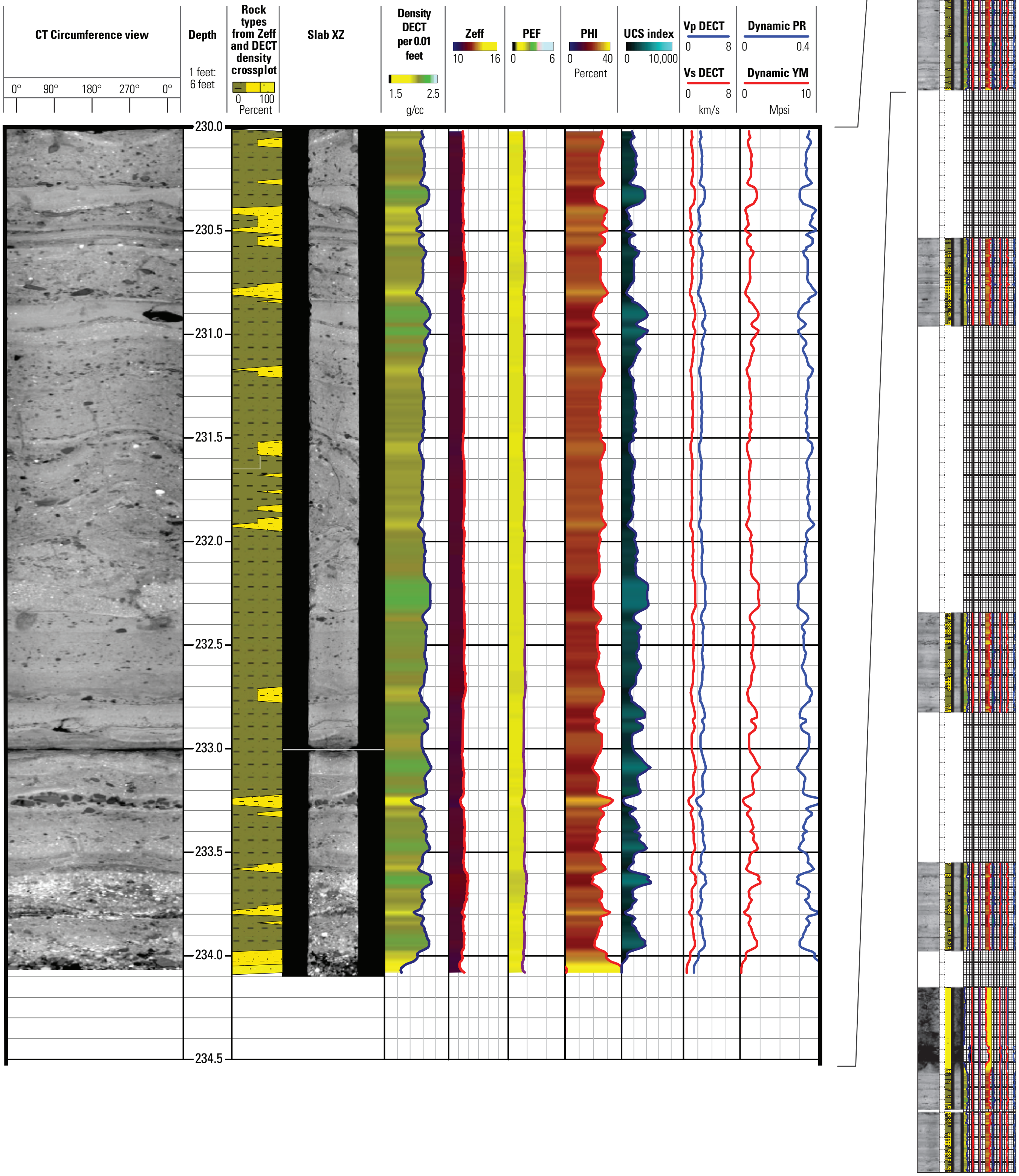

Appendix 1. Dual Energy CT Scans of Cores

Dual Energy Computerized Tomography (DECT) rock types

[g/cc, grams per cubic centimeter; km/s, kilometers per second; Mpsi, mega pounds per square inch; PEF, photoelectric factor; PHI, porosity; PR, dynamic Poisson's ratio; UCS, unconfined compressive strength; Vp, compression wave sonic velocity; Vs, shear wave sonic velocity; YM, dynamic Young's modulus; Zeff, effective nuclear charge]

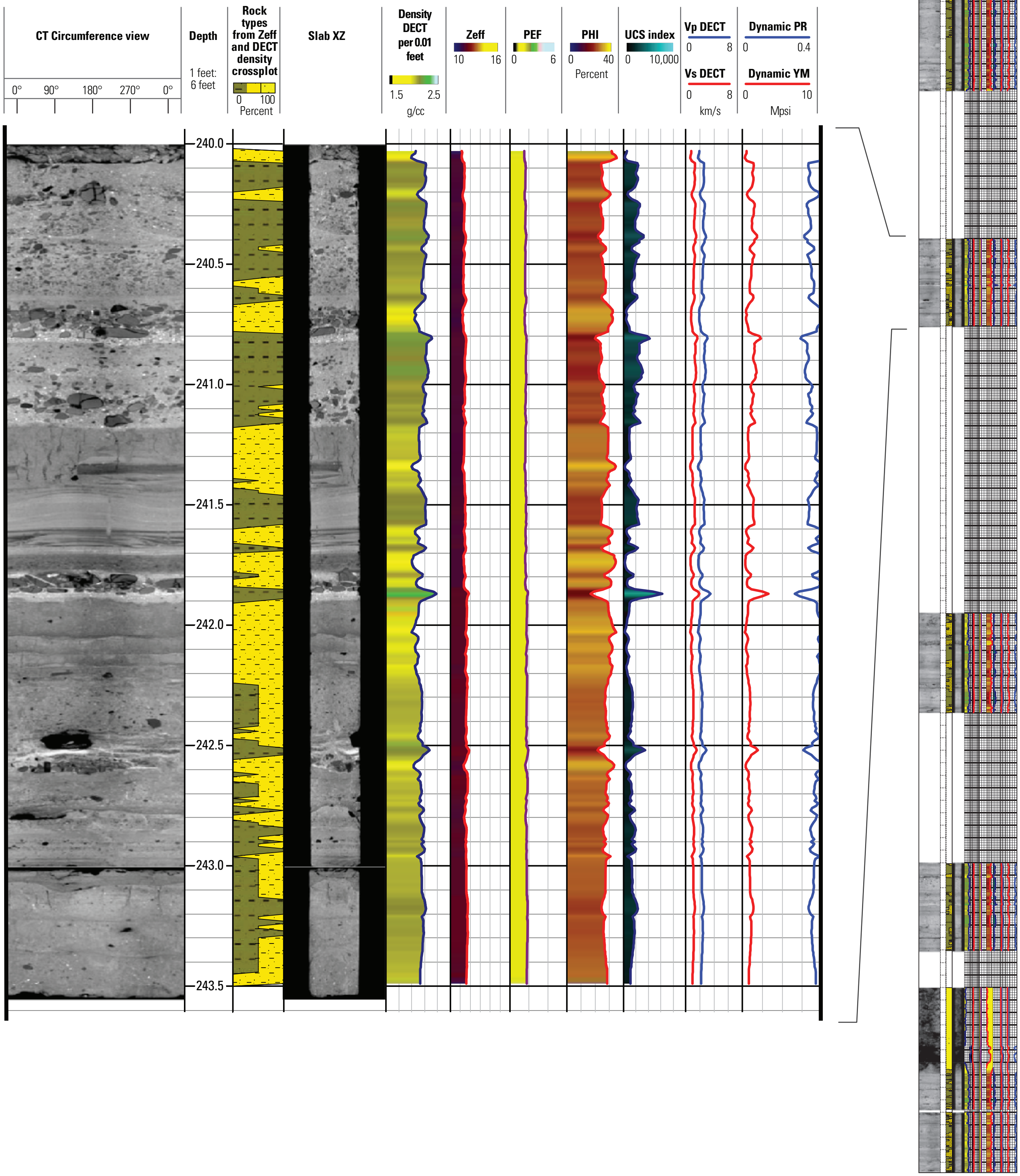

Appendix 1.—Continued

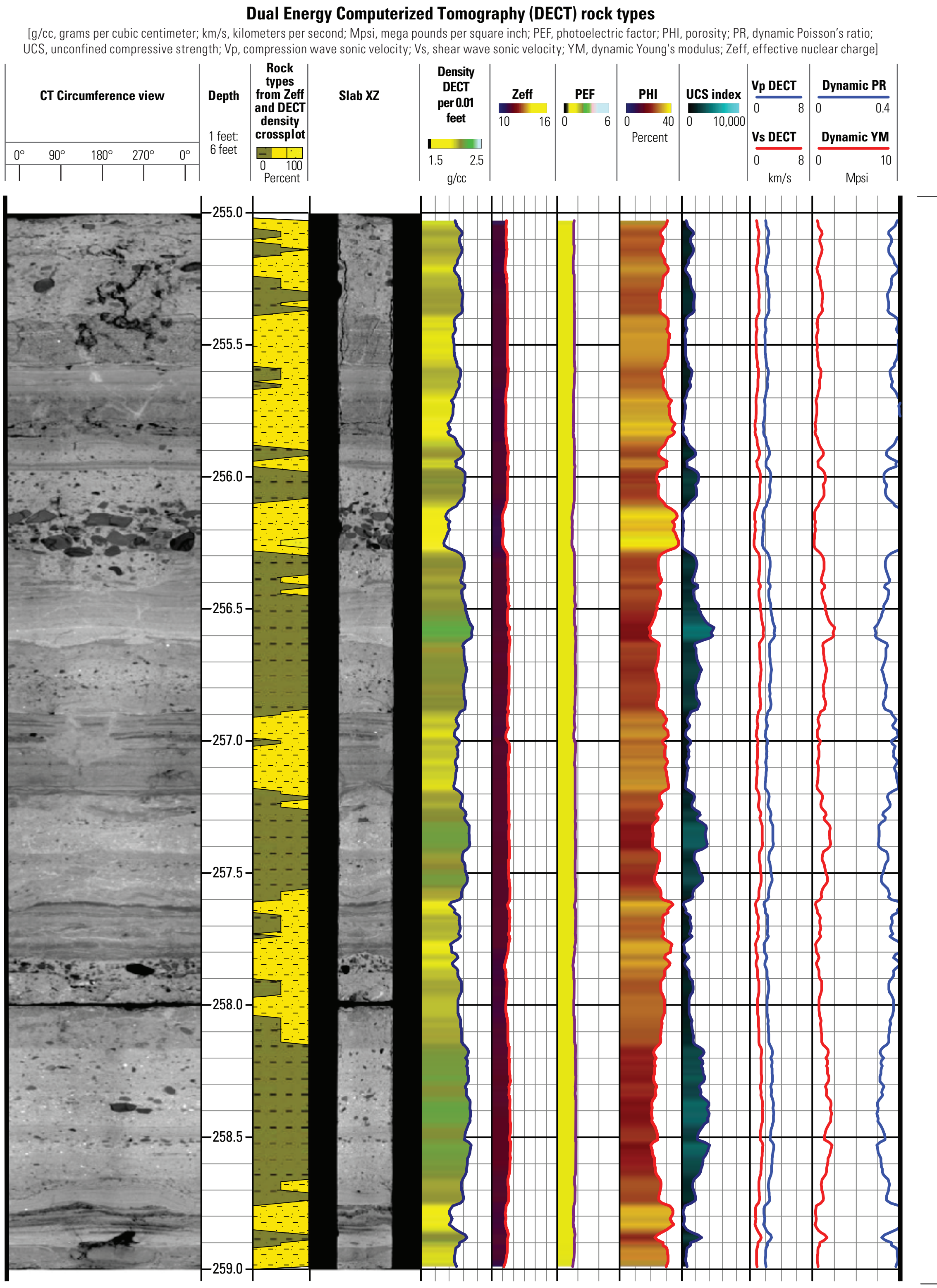

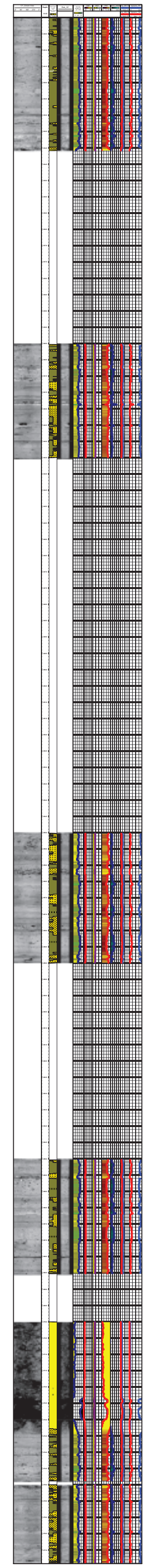

Appendix 1.—Continued

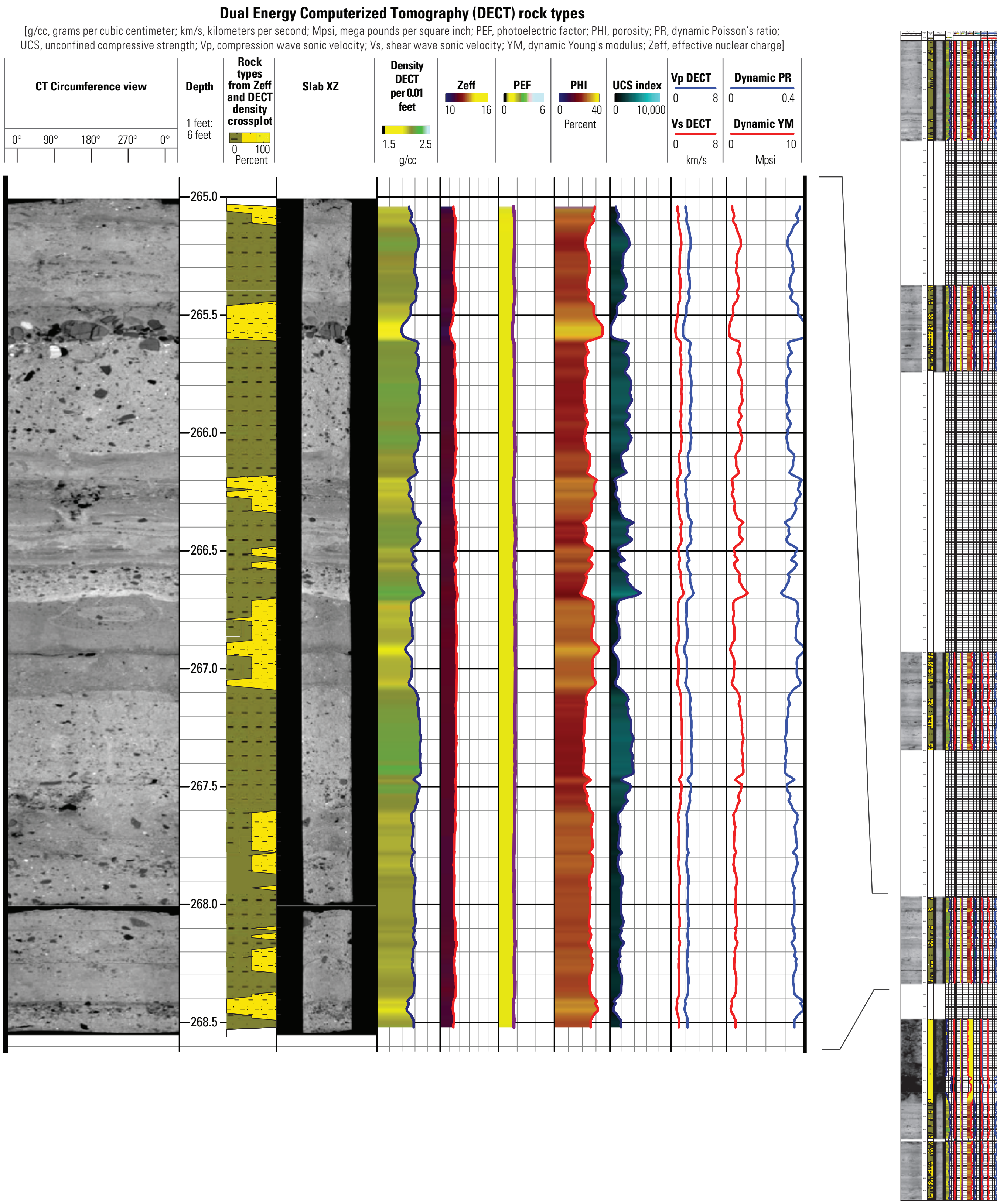

Appendix 1.—Continued

Dual Energy Computerized Tomography (DECT) rock types

[g/cc, grams per cubic centimeter; km/s, kilometers per second; Mpsi, mega pounds per square inch; PEF, photoelectric factor; PHI, porosity; PR, dynamic Poisson's ratio; UCS, unconfined compressive strength; Vp, compression wave sonic velocity; Vs, shear wave sonic velocity; YM, dynamic Young's modulus; Zeff, effective nuclear charge]

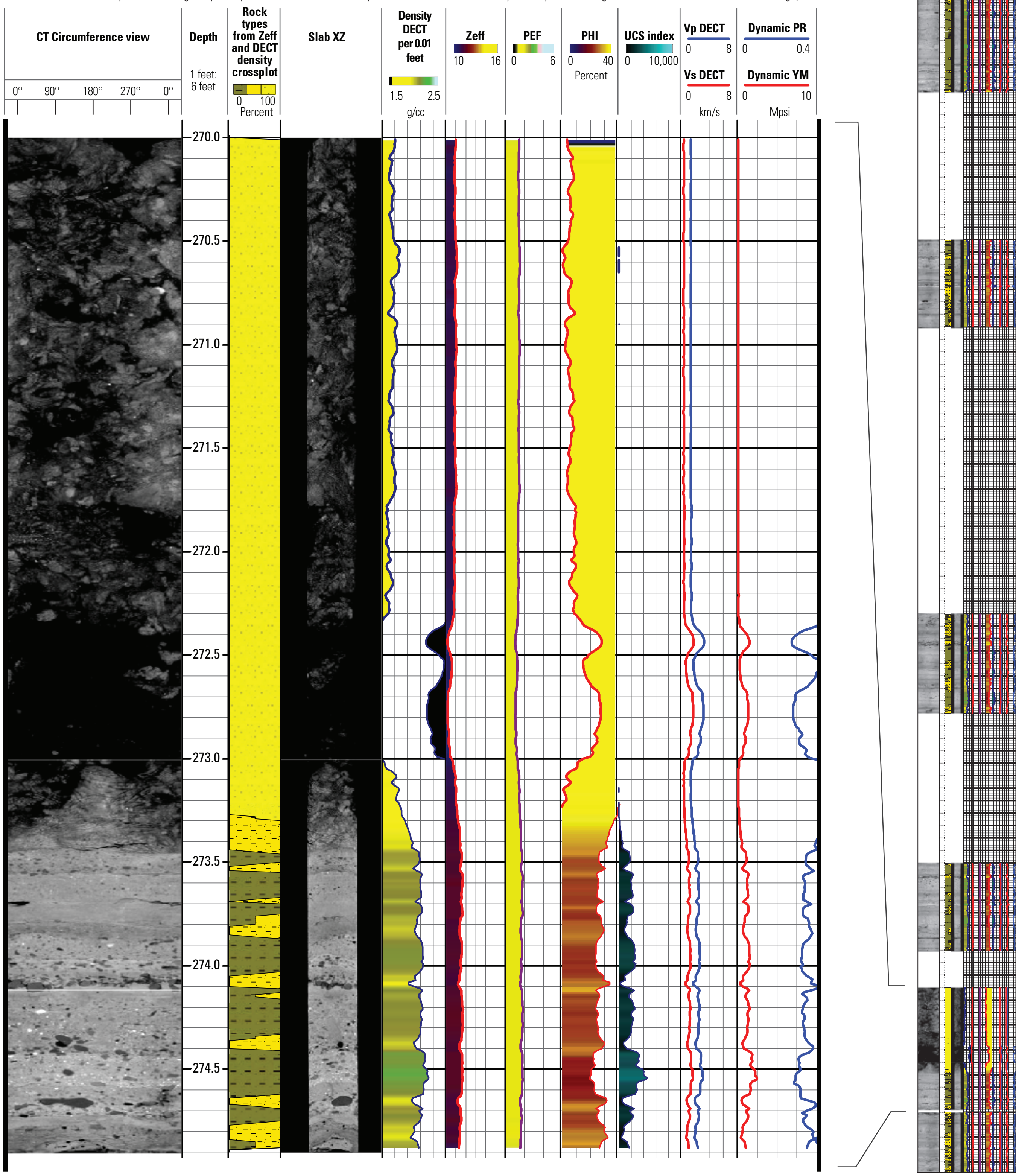

Appendix 1.—Continued

Dual Energy Computerized Tomography (DECT) rock types

[g/cc, grams per cubic centimeter; km/s, kilometers per second; Mpsi, mega pounds per square inch; PEF, photoelectric factor; PHI, porosity; PR, dynamic Poisson's ratio; UCS, unconfined compressive strength; Vp, compression wave sonic velocity; Vs, shear wave sonic velocity; YM, dynamic Young's modulus; Zeff, effective nuclear charge]

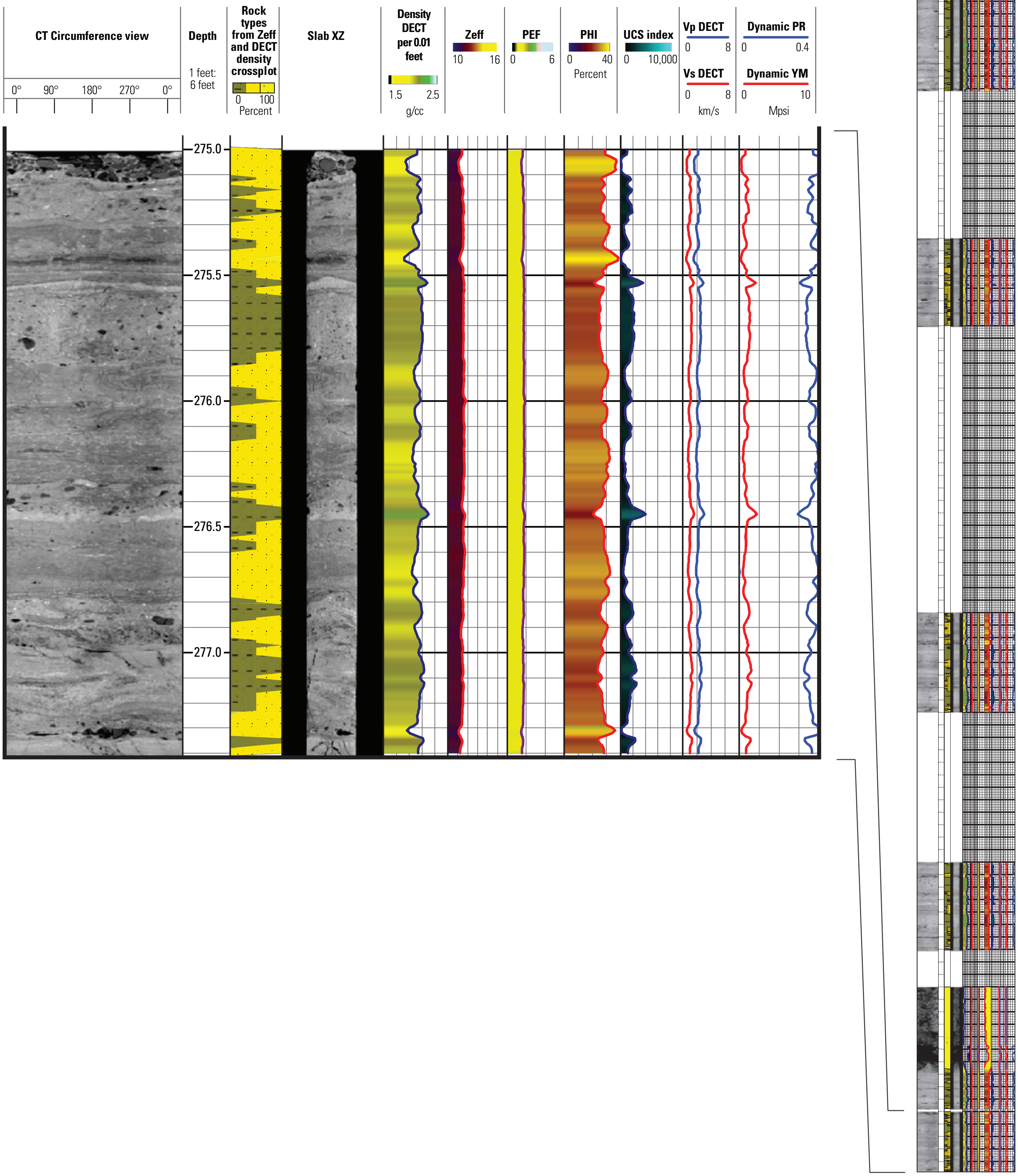

Appendix 1.—Continued

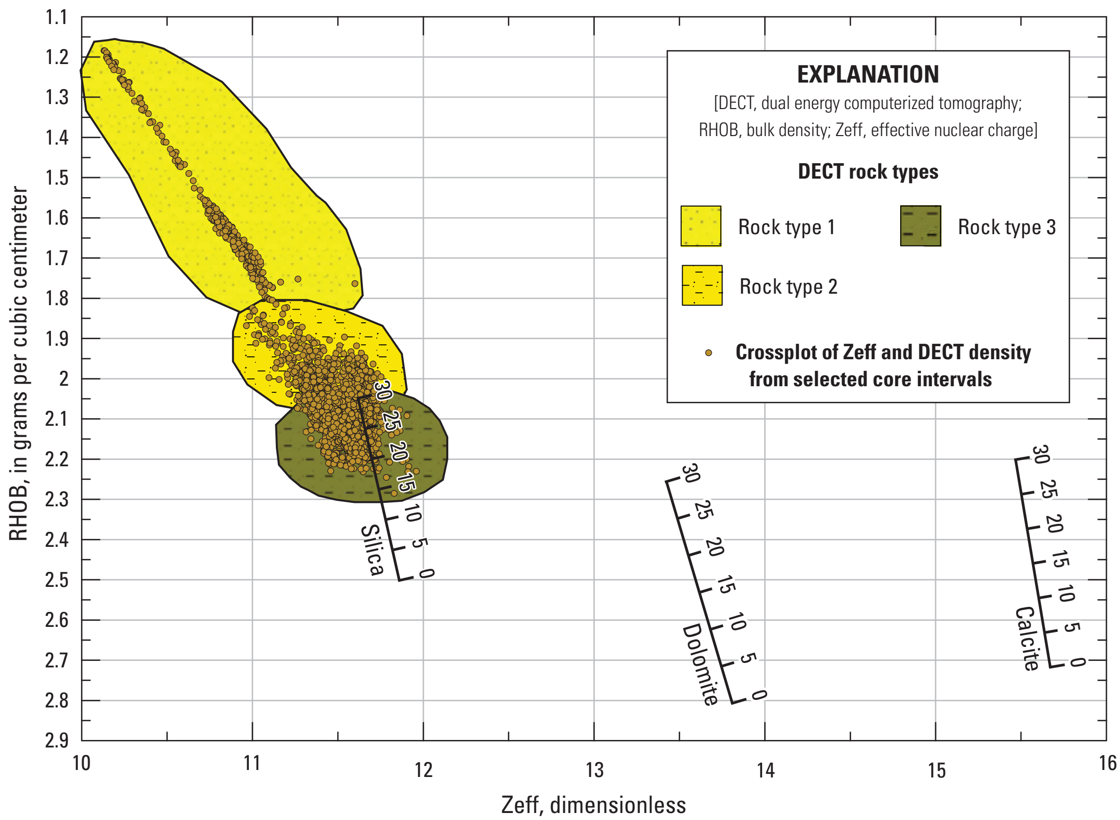

Appendix 1.—Continued

Appendix 2. Photos from Scanning Electron Microscope

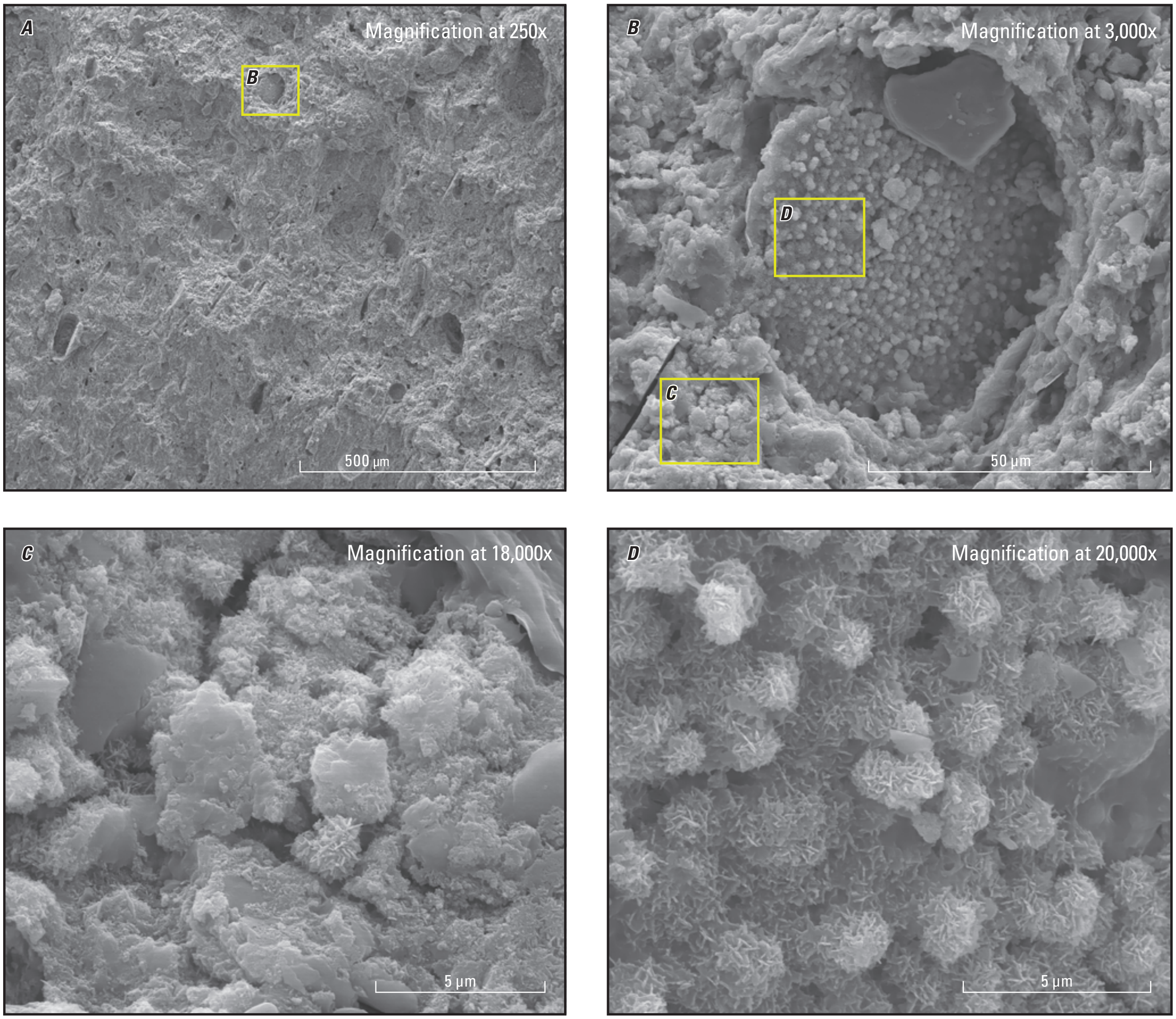

EXPLANATION

[µm, micrometer; x, times]

Area of detail shown in the next photo

Appendix 2. Photos from Scanning Electron Microscope.

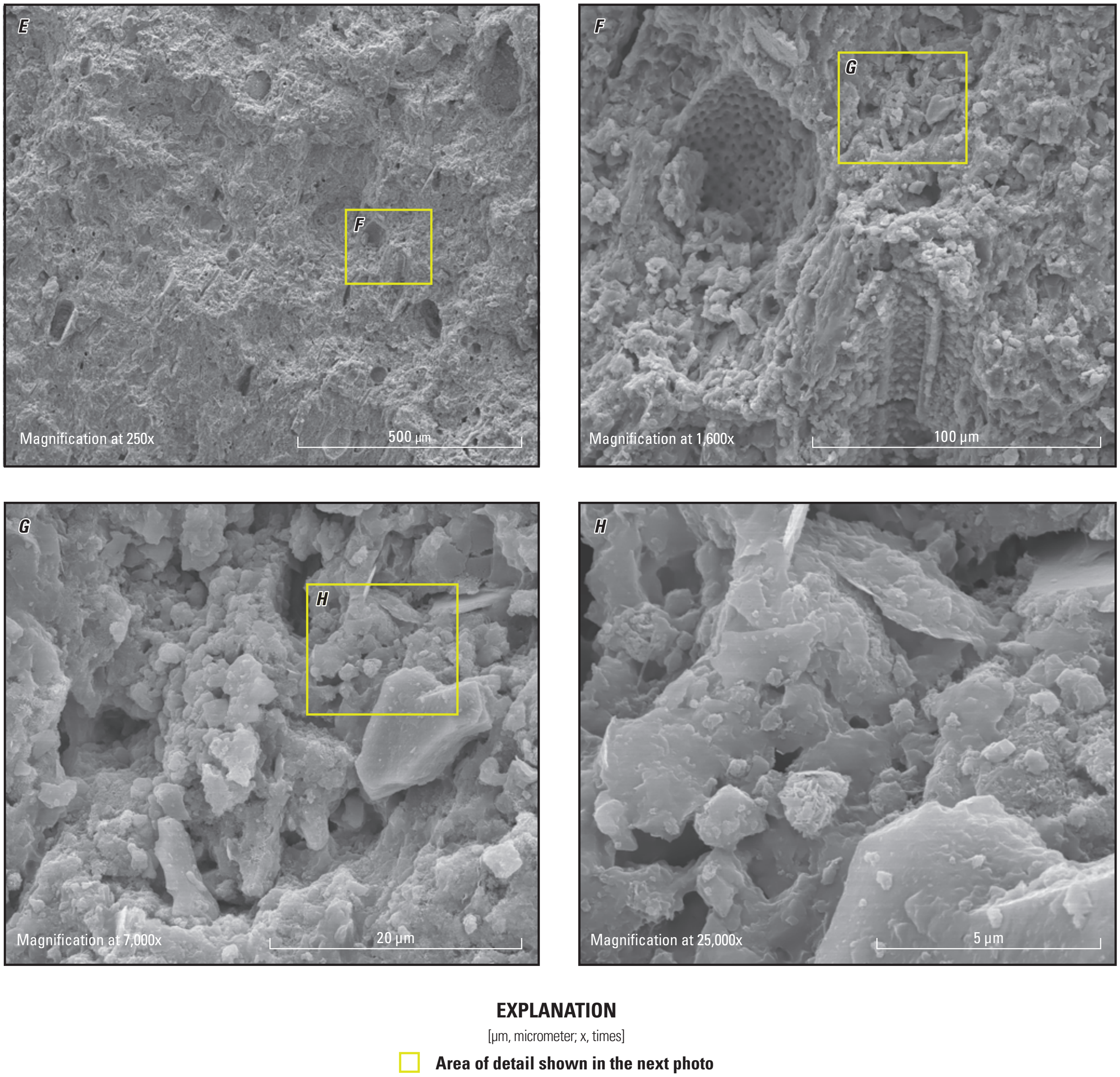

Appendix 2.—Continued

Appendix 3. Photos of Split Cores

[bls, below land surface; MSBV, Midway-Sunset Buena Vista multiple-well monitoring site]

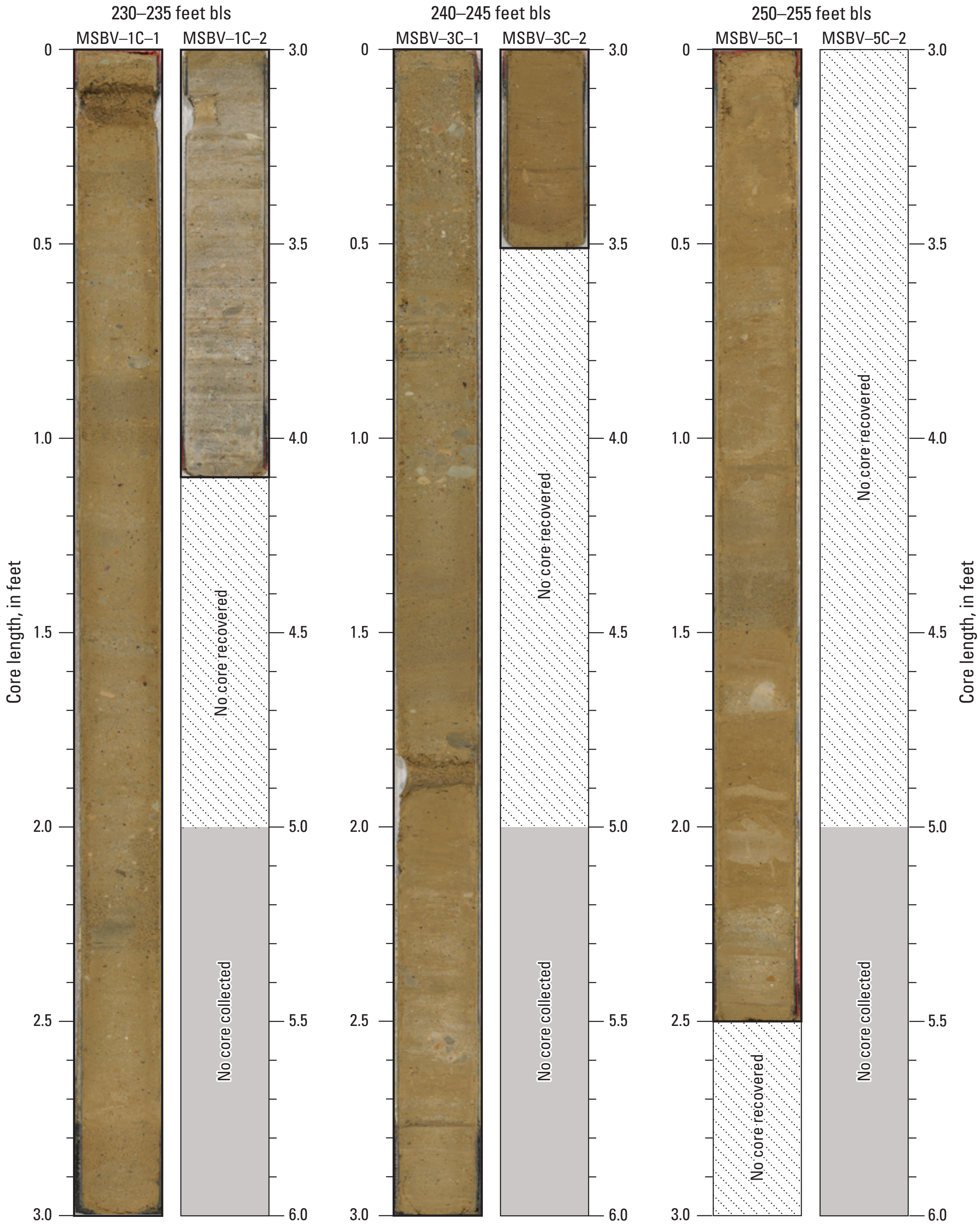

Appendix 3. Photos of Split Cores.

[bls, below land surface; MSBV, Midway-Sunset Buena Vista multiple-well monitoring site]

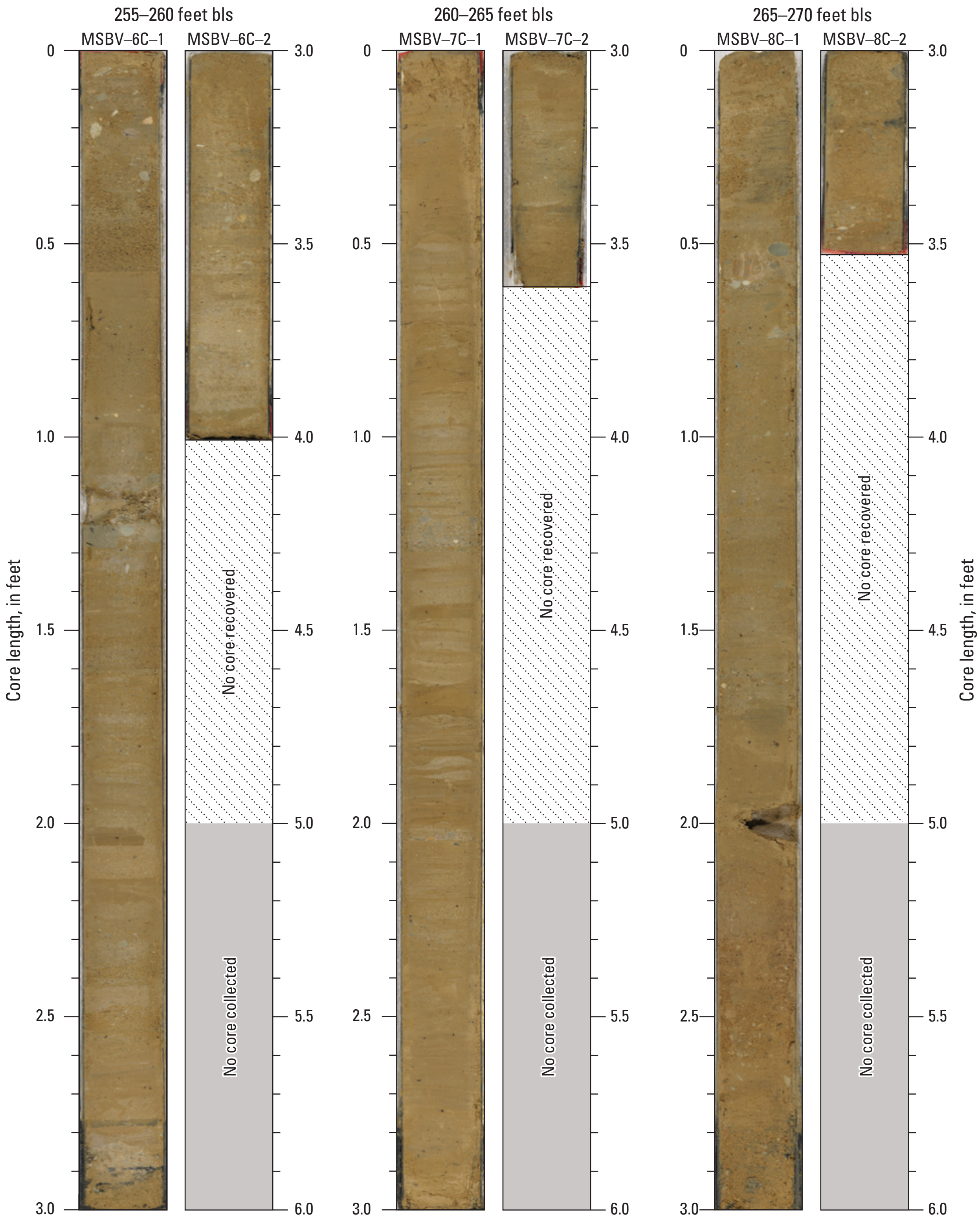

Appendix 3.—Continued

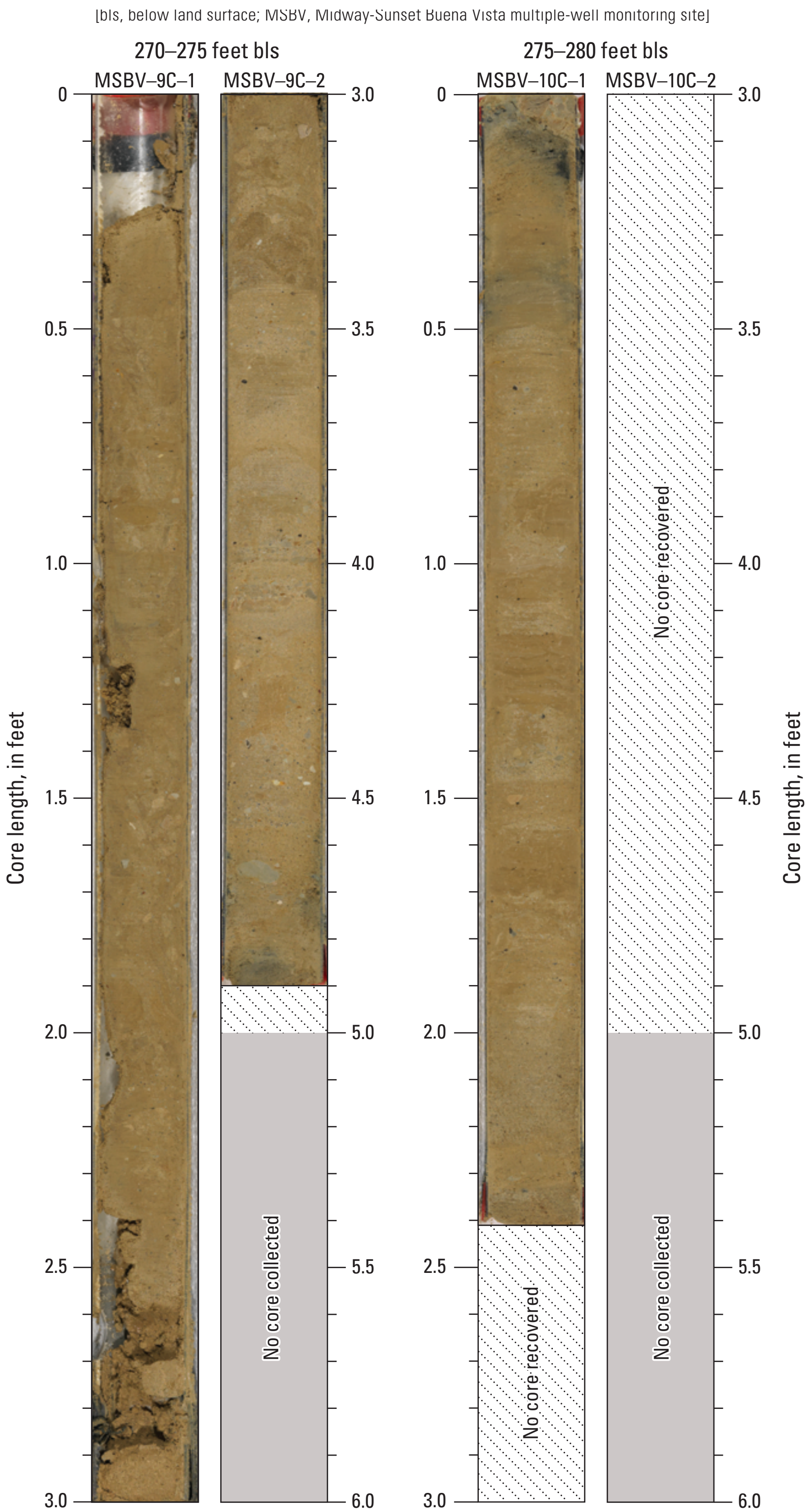

Appendix 3.—Continued